

# Atomic data for x-ray astrophysics

T. R. Kallman

*NASA Goddard Space Flight Center, Greenbelt, Maryland 20771, USA*

P. Palmeri

*Astrophysique et Spectroscopie, Université de Mons-Hainaut, 7000 Mons, Belgium*

(Published 5 January 2007)

The available atomic data used for interpreting and modeling x-ray observations are reviewed. The applications for these data can be divided into several levels of detail, ranging from compilations which can be used with direct inspection of raw data, such as line finding lists, to synthetic spectra which attempt to fit to an entire observed dataset simultaneously. This review covers cosmic sources driven by both electron ionization and photoionization and touches briefly on planetary surfaces and atmospheres. The applications to x-ray astronomy, the available data, and recommendations for astronomical users are all reviewed, and an attempt to point out the applications where the shortcomings are greatest is also given.

DOI: [10.1103/RevModPhys.79.79](https://doi.org/10.1103/RevModPhys.79.79)

PACS number(s): 95.30.Ky, 95.30.Dr, 32.80.-t

## CONTENTS

I. Introduction	79	3. Collisional excitation	110
II. On the Need for Atomic Data	81	a. Background	110
A. Atomic data accuracy requirements	83	b. Recent developments	111
III. Theoretical Techniques	86	4. Radiative transition probabilities	113
IV. Experimental Techniques	89	a. Background	113
V. Line Finding Lists and Related Tabulations	89	b. Recent developments	114
A. Coronal plasmas	89	B. Photoionized plasmas	114
1. Background	89	1. Photoionization	115
2. Recent developments	90	a. Background	115
B. Photoionized plasmas	91	b. Recent developments	115
1. Background	91	2. Radiative recombination	117
2. Recent developments	91	3. Dielectronic recombination	117
VI. Discrete Diagnostics	92	4. Charge transfer	118
A. Coronal plasmas	92	a. Background	118
1. He-like diagnostics	92	b. Recent developments	118
a. Background	92	C. Charge transfer in cometary and planetary	118
b. Recent developments	93	atmospheres	118
2. Dielectronic satellite lines	93	VIII. Discussion	119
3. Other diagnostics	95	Acknowledgments	121
4. Fe <sup>16+</sup>	96	Glossary	121
5. Optical depth diagnostics	96	References	121
6. Abundance diagnostics	96		
7. Nonequilibrium diagnostics	96		
8. Non-Maxwellian diagnostics	97		
B. Photoionized	97		
VII. Spectrum Synthesis and Global Fitting	98		
A. Coronal plasmas	98		
1. Electron impact ionization	98		
a. Background	98		
b. Experimental measurements	99		
c. Excitation autoionization	101		
2. Dielectronic recombination	102		
a. Background	102		
b. Experiment	104		
c. Theory	105		
d. Recent developments	108		

## I. INTRODUCTION

Essentially every observation in astronomy which involves spectra requires some aspect of atomic data for its interpretation. This can range from stellar colors as probes of age or abundance to high-resolution spectra of the Sun and the synthetic models which are used in their interpretation. The importance of atomic data to the field of x-ray astronomy comes from the fact that there are many atomic features in the x-ray band and the physical conditions in the sources are usually far from thermodynamic equilibrium, so that interpretation of line fluxes or ratios requires knowledge of collisional rate coefficients and radiative rates. Even the instruments with the greatest spectral resolving power are not capable of fully resolving many line blends, so that mod-

eling is of particular importance. Furthermore, the field has evolved rapidly, and many of the needs for new or accurate atomic data have only recently become apparent. In this paper we point out the motivation for accumulation of atomic data, and review available atomic data used for interpreting and modeling x-ray observations.

A review of atomic data for an application such as astronomy spans an audience including specialists with tools capable of providing new data, astronomers seeking to understand the accuracy and range of available data, and those who can use the data to synthesize spectra or other observables for comparison with observations. The subject differs from some other review topics since it is unified more by the application to a common problem or challenge than by a single physical process. In this paper we try to balance the needs of these communities as best we can.

For the physicist reader, we attempt to describe the capabilities of current x-ray astronomy instruments, some of the astrophysical science challenges, and the scope of existing work on the measurement and calculation of relevant atomic constants. It appears that much of the recent calculations and experimental work which is most useful to x-ray astrophysics has been done when there is a clear understanding of the astrophysical application. We also attempt to draw attention to those who have made important or extensive contributions in the past, even in cases where their work has been superseded. In doing this, it is not feasible to be comprehensive. A great deal of work has been done in this area, and we refer the reader to the many extensive bibliographies which provide a more complete set of references. For some physical processes we do provide relatively long lists of references to work which spans the many ions or atomic species of interest. These are cases where we think such lists are both relevant and useful, since they convey the volume or comprehensiveness of past work and also are of current interest.

For the astronomer reader, we attempt to describe the technical challenges of calculating or measuring relevant quantities. The goal is to provide an appreciation of the uncertainties imposed on astrophysics by an incomplete knowledge of atomic quantities. In addition, in many cases, the data cited or described here can be directly applied to observations.

For the reader interested in the synthesis of atomic data into model spectra or diagnostics which can be directly fit to astronomical observations, we attempt to provide pointers to data which are appropriate for a given application, the limitations in accuracy and comprehensiveness of existing data, and the prospects for future measurements or calculations. We also hope to foster cooperation between modelers or astronomers and the atomic physics community. This has proven to be an effective way to stimulate work on problems which are relevant to astrophysics, while also educating astronomers and modelers about the limitations and applicability of atomic structure and cross-section data.

We feel that the time is right for a review such as this, because the accuracy and quantity of atomic constants describing many processes has progressed significantly in the last 10–15 years. This is driven both by advances in observational data with the launch of the Chandra and XMM-Newton x-ray astronomy satellites, both statistical quality and spectral resolution, and by advances in the tools available to the physics community. There now exist values for rate coefficients and cross sections which will be accurate enough to allow interpretation of much of the available observational data for the near future, and current techniques will continue to improve the situation. In principle, the project of calculating or measuring atomic cross sections for any specific application has finite scope, and can at some point be considered complete. Although this is not imminent, we can estimate the quantity and accuracy of atomic data that will be needed for most applications to x-ray astronomy in the near future.

In addition, the advent of online databases has revolutionized the dissemination of atomic data. There is no longer a need for publication of rate coefficients or cross sections in obscure laboratory internal publications or conference proceedings, and results based on proprietary or fee-based databases or computational tools are receiving limited attention. The use of the web, faster computers, and essentially unlimited storage have made it practical to save and disseminate great quantities of data. So there is no technical limitation to the sharing of data. In this review we therefore intentionally omit reference to unpublished data, data which are part of a fee-based or proprietary database or code package, or which are published in obscure laboratory internal reports or conference proceedings which are not widely available. We feel strongly that scientific information of all types, to be truly useful, must be freely and easily available, and its provenance must be transparent to all.

Atomic data can be used in different ways according to the level of detail needed for a specific application. The levels of detail range from compilations used in direct inspection of raw data, such as line finding lists, to synthetic spectra which attempt to fit to an entire observed dataset simultaneously. The cosmic sources also differ, ranging from electron-ionized and photoionized plasmas to planetary surfaces and atmospheres. Although traditional x-ray astronomy is generally agreed to span the energy range 0.1–10 keV, modeling of x-ray data inevitably requires knowledge of cross sections which extend to the ionization potential of hydrogen. We adopt this broader definition, and include some discussion of cross sections and rate coefficients associated with photons emitted in the extreme ultraviolet (EUV) and UV bands. X-ray spectra thus far are only capable of detecting the 15 or so most cosmically abundant elements, including C, N, O, Ne, Na, Mg, Si, Al, S, Ar, Ca, Fe, and Ni, and we generally restrict our consideration to calculations and experiments relevant to these elements.

Much of the information relevant to this topic has already been reviewed by others. Recent advances in as-

trophysical x-ray spectroscopy have been reviewed by [Paerels and Kahn \(2003\)](#), [Kahn et al. \(2004\)](#), and some experimental results in atomic data by [Beiersdorfer \(2003\)](#). The subject of atomic data for x-ray astronomy has been discussed in specialized conference proceedings, including [Silver and Kahn \(1993\)](#), [Bautista, Kallman, and Pradhan \(2000\)](#), [Ferland and Savin \(2001\)](#), and [Smith \(2005\)](#). More specialized reviews pertaining to many of the subtopics discussed here will be mentioned in what follows.

This review is organized as follows: We begin with a discussion of some examples of the astronomical x-ray spectra, choosing from recent observations using Chandra and XMM-Newton, followed by a review of the techniques used to derive atomic data, both theoretical and experimental. We then discuss the atomic data currently available, classified according to the level of modeling needed in order to apply the data. These range from line finding lists which can be applied by inspection, to diagnostics of physical quantities involving a small number of measurable parameters such as line ratios or equivalent widths, to models which attempt to synthesize a large portion of the spectrum. These we divide into the likely excitation mechanism: coronal, for sources where the primary energy input is mechanical; photoionized, where photon excitation, heating, and ionization play a dominant role; and planetary, associated with neutral, molecular, or solid material. Then we further subdivide according to physical process.

We divide the discussion of each physical process or subtopic into sections: In the first section; we provide an overview of the work on the topic, dating from the early suggestions of the importance of the process and simple approaches to estimating rate coefficients and cross sections. In the second section we change tactics slightly, and provide an overview of the work which we consider to be the current state of the art, or which point the way to future developments or improvements in the state of the art. Inherent in this is the omission of some work in favor of that which we consider to be either of sufficient accuracy and comprehensiveness to be adequate for the needs of x-ray astronomy today or which we think points the way toward such data.

The study of x-ray spectra associated with planets, comets, and other primarily neutral or solid objects is newer than the study of other emission mechanisms. As a result, there is less work so far on interpretive tools for such spectra, and we do not give a separate discussion of line finding lists or discrete diagnostics for them. We also include a glossary in order to help keep track of the many acronyms and terms describing computational techniques, physical effects, and approximations. Throughout this paper we adopt chemical notation for ionic charge states, i.e., with a superscript denoting the ionic charge. This is in contrast to the spectroscopic notation used in much of the astrophysics literature, in which the charge state is denoted with a roman numeral: I=neutral, II=charge+1, etc. In the final section of the paper we discuss remaining needs for atomic data and prospects for future work.

## II. ON THE NEED FOR ATOMIC DATA

The recent impetus for atomic data applications to astronomy comes from developments in instrumentation. Evolution of instruments has been rapid in the field of space astronomy, which has arisen and grown to a level of sensitivity and spatial and spectral resolution which is comparable to that of ground-based optical instrumentation in approximately the last 40 years. The most recent developments are summarized in the review by [Paerels and Kahn \(2003\)](#) for the x-ray band. Much of the current work is motivated by the launch of the grating spectrographs on the Chandra and XMM-Newton satellites in 1999. These are described in detail by [Brinkman et al. \(2000\)](#) for the low-energy transmission grating (LETG), by [Canizares et al. \(2005\)](#) for the high-energy transmission grating (HETG) on the Chandra satellite, and by [Rasmussen et al. \(2001\)](#) for the reflection grating spectrograph (RGS) on XMM-Newton. The gratings provide spectra with resolving power  $\varepsilon/\Delta\varepsilon \sim 300-1000$  in the energy range between 0.2 and 8 keV, with effective areas  $\sim 10-100 \text{ cm}^2$ . In terms of wavelength, the resolution is  $\Delta\lambda = 0.01-0.05 \text{ \AA}$  depending on the instrument, and the wavelength range extends from  $\approx 1.8 \text{ \AA}$  for the Chandra HETG to  $170 \text{ \AA}$  for the Chandra LETGS. This is in contrast with the previous generation of instruments, exemplified by the ASCA satellite ([Tanaka, 1986](#)), which carried moderate resolution CCD (charge-coupled device) instruments and had a spectral resolving power  $\sim 20$ . The grating instruments have discovered line features in spectra previously thought to be featureless, and require a significantly more comprehensive and accurate database of atomic constants than had previously been in use. However, both Chandra and XMM-Newton also carry CCDs whose use is necessitated by cosmic sources which are too faint for adequate signal in the gratings, or which are spatially extended and hence cannot make use of the full grating spectral resolution.

The Chandra and XMM-Newton gratings represent a tremendous advance in resolution, but are not capable of unambiguously resolving thermal or natural line shapes from many sources. The nominal resolution ( $\sigma$ ) of the HETG at the energy of the O<sup>7+</sup> Ly $\alpha$  line corresponds to a Doppler velocity of  $170 \text{ km s}^{-1}$  ([Canizares et al., 2005](#)). In a thermal plasma this would be obtained at a temperature of  $10^{7.5} \text{ K}$ , which is significantly greater than the temperature where this ion is predicted to be abundant under most plausible conditions. The natural width of the line corresponds to  $0.008 \text{ eV}$  or an equivalent Doppler velocity of  $3.7 \text{ km s}^{-1}$ . Natural widths increase rapidly with the nuclear charge, and so for iron the corresponding velocity is  $550 \text{ km s}^{-1}$ . A typical dielectronic recombination (DR) satellite line to a hydrogenic resonance line (these terms are described in detail later in this review) is shifted by  $\Delta\varepsilon/\varepsilon \approx 0.002$  ([Boiko et al., 1977](#)). This is at the nominal resolution of the Chandra HETG. With good statistics, parameters describing line centroids or widths can be determined to precision better than the nominal resolution by factors of several.

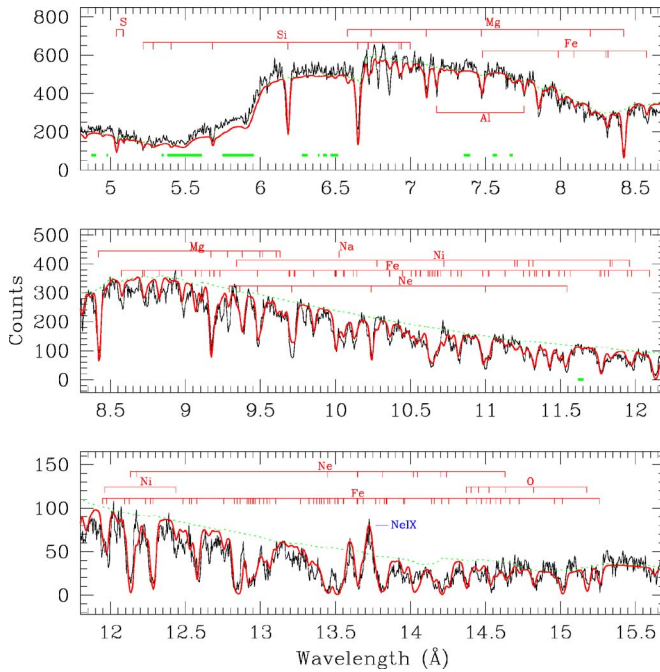


FIG. 1. (Color online) Chandra HETG spectrum of NGC 3783. From [Krongold et al., 2003](#).

Nonetheless, it is clear that the Chandra spectra are not capable of measuring thermal line shapes unambiguously, and the wavelength precision is not comparable to that obtainable in the laboratory or in solar observations with Bragg crystal spectrometers, for example. On the other hand, the HETG can resolve the important diagnostic lines discussed in this review, and it can detect the effects of supersonic turbulence or bulk motions at Mach numbers of  $\sim 2\text{--}3$  or more. This is of great astrophysical interest, since many x-ray plasmas are located in regions of strong gravity, or near shocks or other energetic sources.

As an illustration of the capabilities and limitations of the data obtained with Chandra and XMM-Newton we present spectra obtained using these instruments which test the available atomic data and synthetic spectra. These are not chosen because they are typical, but rather because they best show the capabilities of the instruments and the available atomic data. Figure 1 shows the spectrum of the Seyfert galaxy NGC 3783 obtained with the Chandra HETG. This object is an active galaxy, and the spectrum shows absorption from a large number of resonance lines from the  $K$  shells of highly ionized ions of medium- $Z$  elements, O–S, and also from the  $L$  shell of partially ionized iron. The smooth curve is a model fit, described by [Krongold et al. \(2003\)](#), showing general consistency but not perfect agreement for the majority of the strong lines. In this object the gas is likely to be photoionized, and all the lines are shifted to the blue from their rest wavelength by an amount corresponding to a velocity of  $\sim 500\text{--}1000 \text{ km s}^{-1}$ . This is interpreted as being a Doppler shift in an outflowing wind, and similar spectra have been observed from most of the other objects of this class. Discovery of such outflowing

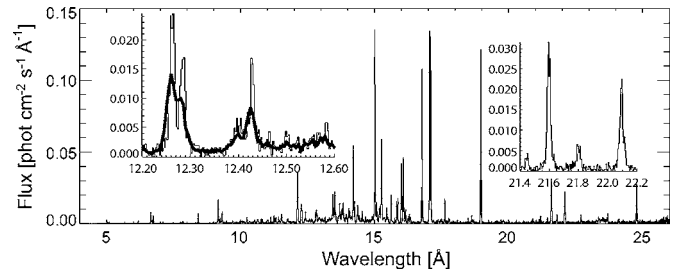


FIG. 2. HETG spectrum of Capella. Insets: The regions of the spectrum in the vicinity of the lines of He-like  $\text{Ne}^{8+}$  and  $\text{O}^{6+}$ . In the left inset panel the two curves are the data from the two arms of the dispersed image. The thin line is data from the higher energy arm (HEG) and the thick line is the data from the medium energy arm (MEG). From [Canizares et al., 2000](#).

gas is surprising, since active galaxies are strong sources of continuum x rays, and are thought to contain black holes which radiate as gas is pulled inward. This spectrum also illustrates the fact that the data from the gratings on Chandra and XMM-Newton can be used to constrain observed line wavelengths to within  $\sim 0.25\%$ . This exceeds the precision of most *ab initio* calculations and therefore requires laboratory measurements to provide wavelengths precise enough to allow reliable line identifications and to infer line shifts.

Figure 2 shows the spectrum of the nearby active star Capella obtained with the Chandra HETG ([Canizares et al., 2000](#)). This shows rich line emission, similar to the Sun, and which is typical for a coronal source. For the most part the lines in the  $10\text{--}18 \text{ \AA}$  range are due to emission from  $L$ -shell iron ions. The observed iron  $L$  spectrum can be reproduced almost entirely by assuming a single electron temperature of  $kT_e=600 \text{ eV}$  ([Behar, Cottam, et al., 2001](#)). This temperature is consistent both with the measured fractional ion abundances of iron and with the temperature derived from ratios of  $\text{Fe}^{16+}$  lines. However, there are some remaining discrepancies between single temperature models and data for the lines of  $\text{Fe}^{17+}$  near  $16 \text{ \AA}$  and also  $\text{Fe}^{16+}$  and  $\text{Fe}^{17+}$  at  $15.015$  and  $14.206 \text{ \AA}$  which are all overestimated by current models. The statistical quality of this spectrum is comparable to that obtained from the Sun, illustrating the power of x-ray spectroscopy to study nearby objects outside the solar system.

An illustration of the power of high-resolution x-ray spectroscopy to study distant objects is shown in Fig. 3, which shows the spectrum of a composite of galaxy clusters taken with the RGS on XMM-Newton ([Peterson et al., 2003](#)). The solid curve shows the data co-added for 13 clusters, which clearly exhibit coronal line emission from  $\text{Fe}^{22+}$ ,  $\text{Fe}^{23+}$ , and  $\text{O}^{7+}$  Ly $\alpha$ . This is consistent with emission from gas at an electron kinetic temperature of  $kT_e \approx 1.5 \text{ keV}$ . This temperature has also been derived from lower resolution observations of these and similar clusters. The gas densities can also be derived from the x-ray luminosities and sizes. Based on these quantities, the time for the gas to cool radiatively is predicted to be short compared with the probable cluster age, hence the

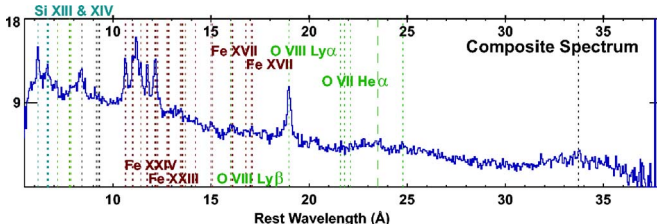


FIG. 3. (Color online) Composite spectrum of galaxy clusters where cooling gas is expected. Solid curve shows data from the RGS on XMM-Newton and dashed vertical lines show the predicted locations of various coronal emission lines. From Peterson *et al.*, 2003.

lines from lower ionization species are expected as the gas cools to  $\sim 1$  keV and below. The vertical dashed curves in the figure denote the positions of the lines which are predicted from such cooling flow models, such as O<sup>6+</sup> and Fe<sup>16+</sup>. Their absence requires a major reexamination of the prevalent model for cluster x-ray gas. One possibility is that the gas, rather than cooling steadily over cosmological time, is reheated by active galaxies in the cluster. If so, it would provide an additional example of the influence of black holes on their environments and on their likely influence on the growth of cosmic structures (Ruszkowski *et al.*, 2004).

Figure 4 shows the spectrum of a Seyfert galaxy NGC 1068 taken with the LETG on Chandra (Brinkman *et al.*, 2002). The extended long-wavelength coverage is a unique feature of this instrument. The black curve shows data taken from the nuclear region of the galaxy, and the solid jagged curve shows a model. The model consists of emission due to gas which is emitting primarily as a result of photoionization, photoexcitation, and scattering, as evidenced by the radiative recombination continuum (RRC) features due to O<sup>6+</sup> near 16.5 Å and C<sup>4+</sup> near 31.5 Å and their strengths relative to the resonance lines

from these ions. This is interpreted as being due to the fact that the galaxy contains a strong source of EUV and x-ray continuum radiation, likely a black hole, but that this source is hidden from our direct view by cold obscuring gas. This appears to be typical of type-2 Seyfert galaxies, which are likely intrinsically similar to the type-1 Seyfert galaxy NGC 3783 (Fig. 1). Both types contain a black hole partially surrounded by torus of nearly opaque cold gas, but their spectra reveal the fact that they are viewed at different orientations (Antonucci and Miller, 1985). Thus x-ray spectra such as these provide evidence for the presence of hidden black holes via their scattered radiation.

These examples illustrate the statistical quality of recent high-resolution x-ray spectra, and, crudely, the extent to which current synthetic spectra are able to match the observations. They also provide a glimpse of the astrophysical issues which can be addressed using x-ray spectra and the potential importance of atomic data to address these issues. They also illustrate the unique nature of the information provided by x-ray spectra; the scientific insights provided by these observations are not accessible to any other waveband, or to observations using lower resolution x-ray instruments.

### A. Atomic data accuracy requirements

Spectra such as the ones shown so far in this section can be used as a practical guide for x-ray atomic data accuracy requirements. Simple estimates can be obtained by examination of the spectra. The strongest emission line (the Ly $\alpha$  line of O $^{7+}$ ) in the spectrum of Capella, as shown in Fig. 2, for example, has flux of 0.02 photon cm $^{-2}$  s $^{-1}$ , corresponding to a total of  $\approx$ 1300 counts in a  $3 \times 10^4$  s observation. The dominant error for such an observation is counting statistics, and assuming Gaussian errors this corresponds to a statistical error on the line intensity of  $\approx$ 3%. This may be viewed as the implied accuracy requirement for a single atomic rate coefficient which affects the line flux linearly, if all other quantities which can affect the line flux are known or not of interest. Such rate coefficients, when they describe collisional processes, are derived by averaging the energy-dependent cross section for the process over the Maxwellian distribution of electron velocities. So an accuracy requirement on a rate coefficient translates approximately linearly into the requirement on the energy-dependent cross section if interpreted as applying uniformly over all energies. On the other hand, a greater uncertainty in the cross section can be tolerated if it applies over a narrow energy range. An observed line flux can be used to infer the total number of emitting ions if the excitation rate for the line is known. The accuracy of such a determination will be limited by the atomic data if the uncertainty in the excitation rate exceeds the statistical error in the observed spectrum.

On the other hand, inferring physical quantities such as gas temperature, density, or elemental abundance from a line or a spectrum in many cases requires comparison with models. Model results depend on various

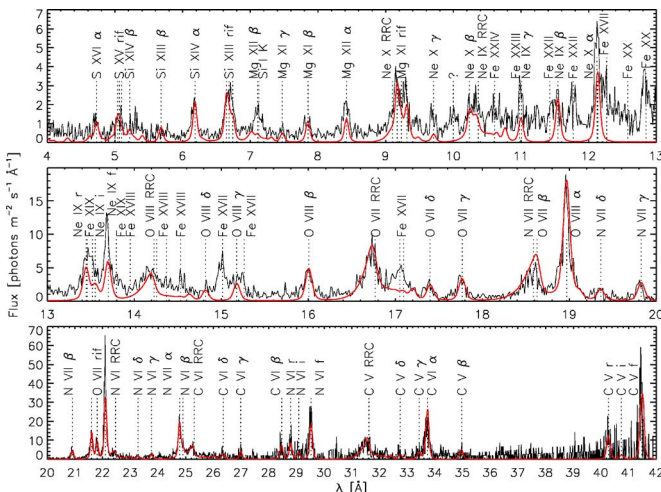


FIG. 4. (Color online) Spectrum of the Seyfert 2 galaxy NGC 1068, taken with the LETG on the Chandra satellite. The solid jagged curve shows the data taken of the nuclear region of the galaxy, and the smooth (red) curve shows a model (Kinkhabwala *et al.*, 2002). From Brinkman *et al.*, 2002.

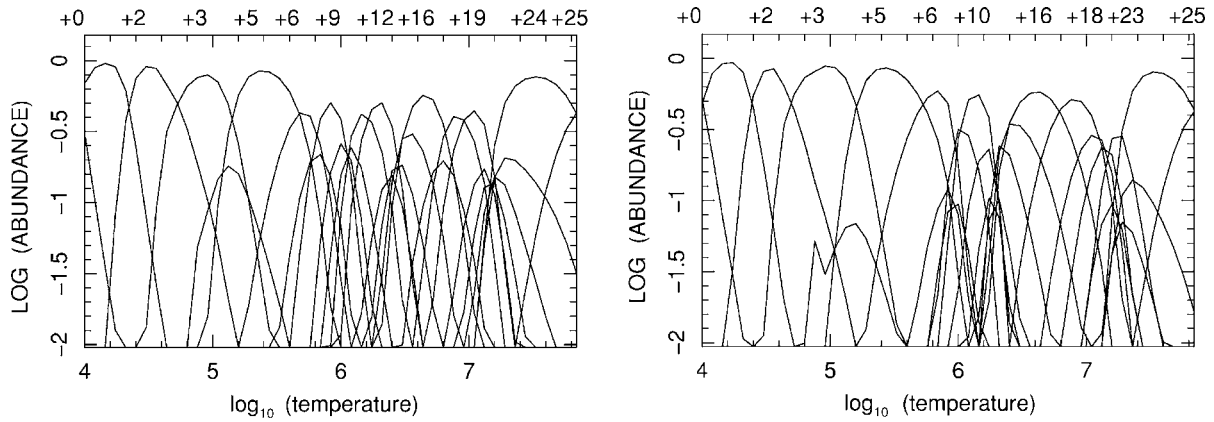


FIG. 5. Ionization balance comparison for coronal plasmas. Left panel: Ionization balance for iron in a coronal gas, calculated using rate coefficients described in the text. Right panel: Ionization balance calculated using perturbed rate coefficients as described in the text. Curves correspond to various ions of iron: in the left panel  $\text{Fe}^+$  dominates at  $\log(T)=4$ ,  $\text{Fe}^{+5}$  dominates at  $\log(T)=5.2$ ,  $\text{Fe}^{+8}$  dominates at  $\log(T)=5.9$ ,  $\text{Fe}^{+12}$  dominates at  $\log(T)=6.3$ ,  $\text{Fe}^{+16}$  dominates at  $\log(T)=6.6$ , and  $\text{Fe}^{+24}$  dominates at  $\log(T)=7.5$ . In the right panel, the temperature of maximum abundance of  $\text{Fe}^{+8}$ – $\text{Fe}^{+23}$  is displaced to lower temperature by  $\approx 0.1$  in  $\log(T)$ .

atomic rate coefficients: those affecting the ionization balance, those affecting excitation, and those affecting photon emission. The dependence of observables such as line strengths on rate coefficients affecting ionization balance or excitation can be nonlinear, and are not well suited to analytic estimates for atomic data accuracy requirements. Numerical experiments can illustrate the sensitivity of line strengths to the rate coefficients affecting ionization and excitation. As an illustration, Fig. 5 shows the ionization balance in coronal equilibrium for iron. Ion fractions are plotted as a function of temperature  $T$  in the range  $4 \leq \log(T) \leq 8$  and the dominant ionization stage ranges from  $\text{Fe}^+$  at low temperature to  $\text{Fe}^{26+}$  at the highest temperature. The left panel shows these quantities calculated using rate coefficients from Arnaud and Raymond (1992) for iron. We denote these as our baseline ionization balance [but note that the work by Bryans *et al.* (2006) represents a significant update]. The right panel has been calculated using the baseline rate coefficients, except that the rate coefficients for recombination for each ion have been perturbed, i.e., multiplied by a randomly chosen factor ranging between 0.79 and 1.28 (i.e.,  $\Delta \log[\text{rate coefficient}] = \pm 0.1$ ). This range is only slightly greater than the magnitude of the effect which is likely to be associated with plasma microfields, cf. Sec. VII.A.2 and Bandell *et al.* (2003), and so reflects a realistic limit to the level of accuracy needed from zero-external-field rate coefficients for this process. Within this range, the multiplicative factor affecting recombination is randomly chosen and evenly distributed. The recombination rate coefficients are stored as analytic functions of temperature and, for each ion, the same multiplicative factor is applied at all temperatures. Comparison of the two panels of Fig. 5 indicates the sensitivity of the ionization distribution to changes in the recombination rate of this magnitude: At a given temperature ion fractions can differ by factors  $\sim 2$ –4, although closed-shell ions

such as Ne-like and He-like ions are relatively unaffected. The temperature where the maximum fraction occurs can also change by  $\sim 0.1$ –0.2 in  $\log(T)$ .

The effects of the ionization balance change on the synthetic spectrum, and on the inferred distribution of gas temperatures in a real astrophysical source, are illustrated in Figs. 6 and 7. Figure 6 shows an observed spectrum from the active star Capella taken with the HETG grating on the Chandra satellite, the same source shown in Fig. 2. The observed spectrum is shown as data points with error bars. The solid (red) curve in Fig. 6 is a synthetic spectrum calculated using the baseline ionization balance shown in the left panel of Fig. 5. This spectrum is calculated using the ionization balance at two temperatures,  $\log(T)=6.9$  and 7.1. The element abundances and relative normalizations of the two components were allowed to vary in order to achieve a fit which has  $\chi^2=3267$  for the 1602 independent energy channels shown

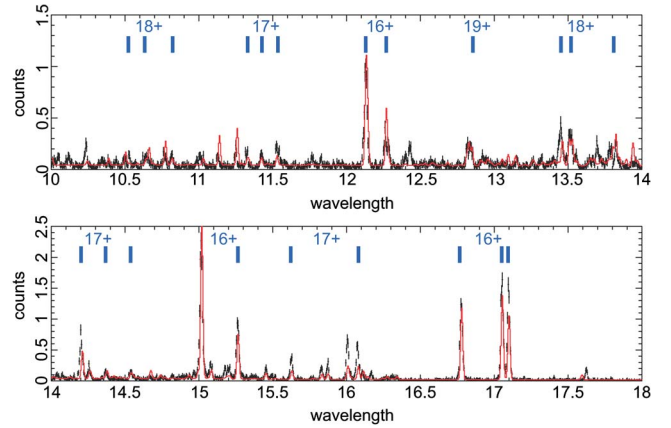


FIG. 6. (Color online) Fit to a  $3 \times 10^4$  s Chandra HETG observation of the active star Capella in the 10–18 Å region using the baseline ionization balance shown in the left panel of Fig. 5.

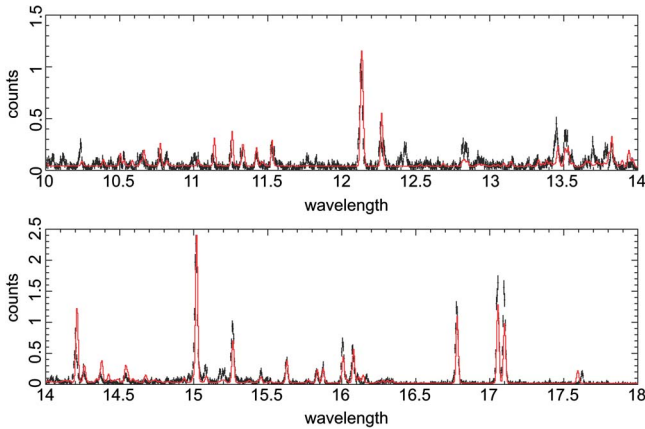


FIG. 7. (Color online) Same as Fig. 6 except using ionization balance shown in Fig. 5 derived from perturbed rate coefficients as described in the text and displayed in the right panel of Fig. 5.

in this figure. This is not in a range of  $\chi^2$  which permits application of traditional statistical measures of probability of random occurrence (Bevington, 1969), and is primarily of illustrative value. Similar values of  $\chi^2$  are found when these data are fit to two temperature component models calculated with other modeling packages which are in widespread use, such as APEC (Smith *et al.*, 2001) and MEKAL (Mewe, Kaastra, and Liedahl, 1995).

In the region of the spectrum shown most of the features are due to iron, the exception being the Lyman lines of  $\text{Ne}^{9+}$ . We find a best fit value of  $[\text{Ne}/\text{Fe}]$ , the abundance ratio relative to solar (Grevesse *et al.*, 1996), of 0.66. The strongest lines in this spectrum are indicated in Fig. 6:  $\text{Fe}^{16+}$  between 12 and 17 Å, and the  $\text{Ly}\alpha$  line of  $\text{Ne}^{9+}$  at 12.13 Å, which is blended with the corresponding  $\text{Fe}^{16+}$  line. Higher ionization lines include lines from  $\text{Fe}^{18+}$  at 10.5–10.8 Å,  $\text{Fe}^{17+}$  between 11 and 16 Å,  $\text{Fe}^{18+}$  at 13.5–13.8 Å, and  $\text{Fe}^{19+}$  at 12.85 Å. Lower ionization lines include  $\text{O}^{7+}$  at 16.00 Å,  $\text{Fe}^{17+}$  blended with  $\text{Ne}^{9+}$   $\text{Ly}\beta$  at 10.24 Å, and  $\text{Ne}^{8+}$  at 11.03 Å. The baseline model accounts for the strengths of many of the strongest lines, but underpredicts the  $\text{Fe}^{16+}$  15 and 17 Å lines; this is a manifestation of problems with rate coefficients affecting this ion which are in widespread use and which are discussed in Sec. VI.A.4.

The emission line spectrum radiated by the plasma is calculated using rate coefficients for electron impact collisional excitation culled from the references discussed later in this paper. These are enumerated in Baustista and Kallman (2001), with the addition of rate coefficients from the recent CHIANTI version 5 compilation (Landi *et al.*, 2005). It is well known that a source such as Capella is best fit using a broad distribution of temperatures, in the range  $\log(T)=6$ –7.4 (Canizares *et al.*, 2000), but we adopt the two-component model shown here for illustrative purposes.

The effects of perturbing the ionization balance on the fit to the spectrum can be seen in Fig. 7, in which the analogous procedure is carried out using the ionization balance shown in the right panel of Fig. 5. In making this

fit we have not attempted to reoptimize any of the parameters describing the fit, i.e., the normalization, temperatures, or elemental abundances in the two temperature components. Rather, we have left them the same as in Fig. 6 in order to illustrate the sensitivity to the ionization balance. Comparison with the fit shown in Fig. 6 shows that the fits to the strongest lines, i.e., those of  $\text{Fe}^{16+}$  and  $\text{Ne}^{9+}$ , are essentially identical. This is a reflection of the fact that the ionization balance of the closed-shell  $\text{Fe}^{16+}$  is little affected by the perturbation in recombination rate coefficients. However, significant differences are apparent in the fit to the ions in adjacent ionization stages, notably  $\text{Fe}^{17+}$  and  $\text{Fe}^{19+}$ . These show up in the lines near 14.2–14.5 Å for  $\text{Fe}^{17+}$  and 12.8 Å for  $\text{Fe}^{19+}$ , which are underpredicted by the model shown in Fig. 7. The lines of  $\text{Fe}^{18+}$  are not strongly affected by the perturbation in the recombination rate coefficients. The fit between data and model in Fig. 5 has  $\chi^2=3610$  for 1602 energy channels and is clearly worse than for the baseline model. However, when the perturbed model is iteratively fitted to the Chandra data a better fit is found when the high-temperature component increases to  $\log(T)=7.2$ . The resulting fit is improved, although still inferior to the baseline model:  $\chi^2=3522$  for 1602 energy channels as compared with  $\chi^2=3267$  for 1602 energy channels for the baseline model.

These experiments illustrate some of the effects of changes in the rate coefficients affecting ionization balance on fitting to observed astrophysical x-ray spectra and on the inferred temperature distribution. They indicate that changes of  $\sim 25\%$  in these rate coefficients can affect the model strengths of the lines of the more delicate ions by factors  $\sim 3$ –10, while the strong lines from stable ions are more robust. Such changes in model line strengths lead to changes in the inferred physical conditions derived by iterative model fitting which are significant. In this case we find changes of 0.1 in  $\log(T)$  from such a procedure, which is at the resolution of the grid of models used to calculate the spectra.

In a coronal plasma there is an exact symmetry between recombination and electron impact collisional ionization, so that perturbations to recombination rate coefficients can be interpreted as corresponding inverse perturbations to the ionization rate coefficients. The inferences from these numerical experiments are reciprocal between the two types of rates. At the same time, it is clear that the above model fits have been applied to only one spectrum, and only one numerical experiment at perturbing the rate coefficients has been performed. In order to adequately characterize the effects of perturbing various rate coefficients, this experiment should be repeated in order to truly randomize the perturbations, and experiments should be carried out with different amplitudes and with fits to other astrophysical x-ray spectra. More extensive experimentation of this type has been carried out with application to solar EUV and x-ray line emission by Gianetti, Landi, and Landini (2000) and Savin and Laming (2002). Masai (1997) examined the effects of uncertainties in rates affecting ioniza-

tion balance on the results of fitting to moderate resolution x-ray spectra obtained using CCD instruments.

### III. THEORETICAL TECHNIQUES

Theoretical calculation of atomic processes begins with the solution to the multielectronic Schrödinger or Dirac equation,

$$\left\{ \sum_i h_i + \sum_{i < j} V_{ij}^{e-e} \right\} \Psi = E \Psi, \quad (1)$$

where  $h_i$  are the one-electron Hamiltonians and  $V_{ij}^{e-e}$  the electron-electron interaction potentials. In the fully relativistic case,  $h_i$  are Dirac Hamiltonians,  $V_{ij}^{e-e}$  include the direct and exchange parts of the electrostatic interaction (the interaction energy due to the positional correlation of parallel-spin electrons according to the Pauli exclusion principle) and the Breit interaction (the two-body magnetic interaction), and  $\Psi$  is a four-component wave function. In the nonrelativistic case,  $h_i$  are Schrödinger Hamiltonians and  $V_{ij}^{e-e}$  include only the electrostatic interaction. In the Breit-Pauli (BP) relativistic approximation, the nonrelativistic multielectronic Hamiltonian is corrected by adding terms resulting from the reduction of the one-electron Dirac Hamiltonian and the Breit interaction to the Pauli form (Bethe and Salpeter, 1972). The relativistic correction terms are then the mass-correction, Darwin, and spin-orbit terms that are added to  $h_i$ , and the spin-other-orbit, spin-spin, orbit-orbit, spin-contact, and two-body Darwin terms that are added to  $V_{ij}^{e-e}$ . Higher-order relativistic interactions like QED have also to be treated in the case of highly ionized heavy atoms. The angular part of the Schrödinger equation solution is known exactly and is found using the Racah algebra (Racah, 1942, 1943; Fano and Racah, 1959; Edmonds, 1960). With regard to the radial part, the exact solution cannot be found due to the  $V_{ij}^{e-e}$  terms. One of the simplest approximations is the independent-particle or central-field model:

$$\sum_{j \neq i} V_{ij}^{e-e} \sim V_i(r), \quad (2)$$

where  $V_i(r)$  are local central potentials in which each electron moves independently. The atomic state function  $\Psi$  is then a product of the atomic orbitals  $\phi_i$  which are eigenstates of the monoelectronic Hamiltonians,

$$\{h_i + V_i(r)\} \phi_i = \epsilon_i \phi_i, \quad i = 1, \dots, N, \quad (3)$$

where  $N$  is the number of electrons. Different forms of the functions  $V_i(r)$  can be considered (Cowan, 1981). Forms that depend upon the orbitals themselves lead to the use of the self-consistent-field (SCF) iterative procedure (Cowan, 1981).

A more elaborate solution of Eq. (1) comes from the application of the variational principle. Using the trial atomic state function defined by

$$\Psi = (N!)^{-1/2} \det \phi_i(x_j), \quad (4)$$

where  $x_j$  are the electron space and spin coordinates and the determinant ensures the Pauli exclusion principle,  $\phi_i$  are obtained by requiring that the expectation value of the multielectronic Hamiltonian is minimum

$$\langle \delta \Psi | \sum_i h_i + \sum_{i < j} V_{ij}^{e-e} | \Psi \rangle = 0, \quad (5)$$

where the variation is taken with respect to the radial parts of the orbitals  $\phi_i$ . This leads to the Hartree-Fock equations (Hartree, 1957)

$$\begin{aligned} h_i \phi_i(x) + \sum_j \int dr' \phi_j(x') \frac{1}{|r - r'|} \phi_j(x') \phi_i(x) \\ = \epsilon_i \phi_i(x) + \sum_j \int dr' \phi_j(x') \frac{1}{|r - r'|} \phi_i(x') \phi_j(x), \\ i = 1, \dots, N. \end{aligned} \quad (6)$$

These nonhomogeneous coupled integro-differential equations are solved iteratively in a SCF procedure. An important property of the Hartree-Fock approximation follows from Brillouin's theorem which implies that the diagonal matrix elements of single-particle operators are given correctly to first order by Hartree-Fock atomic state functions. This approach essentially takes into account the part of the electron correlations within an electronic configuration.

Further improvement can be made using trial atomic state functions  $\Psi$  that are expansions of configuration state functions  $\Phi$ ,

$$\Psi = \sum_k c_k \Phi_k, \quad (7)$$

where  $\Phi_k$  are themselves expansions of Slater determinants [Eq. (4)] and  $c_k$  are the mixing coefficients. The summation in Eq. (7) can be systematically extended in principle to yield results of arbitrarily high accuracy or to achieve convergence. This approach is referred to as the configuration interaction (CI) approximation. When the variational principle [Eq. (5)] is applied to Eq. (7) varying  $c_k$  and the orbitals  $\phi_i$ , one talks about the multiconfiguration approach such as in the multiconfiguration Hartree-Fock (MCHF) (Fischer, 1996) and multi-configuration Dirac-Fock (MCDF) (Parpia *et al.*, 1996) methods. Otherwise one talks rather about the superposition of configurations approach where Eq. (3) or (6) is used to determine the orbitals  $\phi_i$  and the multielectronic Hamiltonian matrix is diagonalized afterward to obtain  $c_k$  and the eigenvalue  $E$  as, for example, in Cowan's code (Cowan, 1981). In practice, the CI expansion in Eq. (7) is limited and in order to include more correlation in  $\Psi$ , the multielectronic Hamiltonian matrix elements are corrected to reproduce the few available experimental energy levels. The approximation then becomes a semi-empirical one.

A different approximation which is also capable of systematic improvement of the atomic state function is based on the many-body perturbation theory (MBPT) of

Brueckner (1955) and Goldstone (1957). In this method, the multielectronic Hamiltonian is written as a sum of a zero-order Hamiltonian and a perturbation term

$$H = H_0 + H_{\text{pert}}, \quad (8)$$

where

$$H_0 = \sum_i \{h_i + V_i(r)\} \quad (9)$$

and

$$H_{\text{pert}} = \sum_{i < j} V_{ij}^{e-e} - \sum_i V_i(r). \quad (10)$$

A complete set of orbitals  $\phi_i$  are then obtained by solving Eq. (3) and used in the order-by-order Rayleigh-Schrödinger perturbation expansion of the atomic state energies  $E$  and other properties such as oscillator strengths. An example of the reduction of the perturbation expansion to MBPT formulas using Feynman diagrams and second-quantization method has been given by Avgoustoglou *et al.* (1992) for closed-shell atoms.

For processes involving the continuum, the continuum atomic state function  $\Psi(\varepsilon)$  for the  $(N+1)$ -electron system has to be evaluated,

$$\Psi(\varepsilon) = \sum_{\alpha} \chi_{\alpha} \phi_{\alpha}(\varepsilon), \quad (11)$$

where  $\varepsilon$  is the energy of the free electron,  $\phi_{\alpha}$  are free-electron orbitals, and  $\chi_{\alpha}$  are atomic state functions of the  $N$ -electron target Hamiltonian. The free-electron orbitals are solutions of the following Schrödinger equations:

$$\{h_{\alpha}^K + \varepsilon\} \phi_{\alpha} = \sum_{\alpha'} U_{\alpha\alpha'} \phi_{\alpha'}, \quad (12)$$

where  $h_{\alpha}^K$  are one-electron kinetic Hamiltonians and the matrix potential  $U_{\alpha\alpha'}$  is defined by

$$U_{\alpha\alpha'} = \int dx_1 \cdots dx_N \chi_{\alpha}(x_1 \cdots x_N) \times U(x_1 \cdots x_N x_{N+1}) \chi_{\alpha'}(x_1 \cdots x_N), \quad (13)$$

where  $U$  is the sum of the nuclear and electron-electron interaction potentials acting on all the  $N+1$  electrons of the target-plus-free-electron system.

The widely used distorted-wave (DW) approximation consists in neglecting the coupling between different channels or the interaction between continuum states, i.e.,

$$U_{\alpha\alpha'} = 0, \quad \alpha \neq \alpha', \quad (14)$$

by using the central-field model defined in Eq. (3). It becomes a good approximation for both the nonresonant background and resonance contributions. However, many DW excitation rate coefficients omit the resonance contribution entirely.

At sufficiently large ionization or free-electron energies, DW orbitals approximate closely to Coulomb orbitals calculated using

$$U_{\alpha\alpha} \sim -\frac{Z-N}{r}, \quad (15)$$

where  $Z$  is the atomic number. It is then called the Coulomb-Born (CB) approximation. The exchange part of the electrostatic interaction is neglected in the CB approximation but included in the Coulomb-Born-Oppenheimer (CBO) and Coulomb-Born-exchange (CBE) approximations.

The simplest approximation consists in considering plane waves to describe the continuum orbitals. It is equivalent to switching off the matrix potential, i.e.,  $U_{\alpha\alpha} \sim 0$ . This technique, called the Born approximation, is most likely to be accurate for energies far above threshold, and for an electron colliding with a neutral atom. It is a good approximation for the background cross section over a wide range of energies for positive ions, because the infinite energy limit for scattering of a positive ion is exactly the Born cross section and this limit controls the finite energy cross section over a wide range of energies due to the slowly varying behavior of the cross section with energy.

The three above-mentioned approximations make assumptions about the wave function of continuum electrons which are only appropriate when the energy of the projectile electron (or free electron) is much greater than the binding energy of target electrons (or bound electrons) of interest. In contrast, approximations such as the more elaborate and widely used  $R$ -matrix method (Burke and Berrington, 1993) can be invoked for free electrons at low energies and for low ionization charges up to negative ions where the coupling between channels is generally strong.

Moreover, the importance of resonant enhancement of rate coefficients for collisional excitation (see, e.g., Sec. VI.A.1) means that the  $R$ -matrix method is widely used for highly charged ions as well, as it is a very efficient way of determining the resonance contribution. Distorted-wave cross sections are traditionally nonresonant. There are two ways in which resonances can be taken account of subsequently. First (as exemplified by HULLAC), autoionizing states can be included in the collisional-radiative equations when calculating level populations and effective recombination and ionization rate coefficients. This can become very demanding computationally but it does allow for collisional redistribution of autoionizing states in dense plasmas. Second, the low-to-medium density approach, appropriate to the solar atmosphere, magnetic fusion plasmas, is to include the resonances in the excitation calculation, either via  $R$  matrix (always present) or perturbatively (as has been done for some ions using FAC) and so omit autoionizing states from the collisional-radiative population rate equations (otherwise they would be double counted). This hugely simplifies the collisional-radiative problem but means there is a density range below that for collisional equilibrium, where partial collisional redistribu-

tion of autoionizing states takes place, and where non-autoionizing level populations are not well described.<sup>1</sup>

The  $R$ -matrix method consists of dividing the space into internal and external regions. In the internal region where the interaction between the free electron and target electrons is strong, the ( $N+1$ )-system atomic state function  $\Psi(\varepsilon)$  is expanded in terms of target eigenfunctions  $\chi$ ,

$$\Psi(\varepsilon) = \mathcal{A} \sum_{\alpha} \bar{\chi}_{\alpha} \frac{u_{\varepsilon,\alpha}(r)}{r} + \sum_i c_i \Phi_i, \quad (16)$$

where  $\mathcal{A}$  is the antisymmetrization operator ensuring the Pauli exclusion principle, the bar over  $\chi$  indicates coupling with the angular and spin parts of the free-electron orbital  $\phi(\varepsilon)$ ,  $u_{\varepsilon}(r)/r$  represents the radial part of the latter, and  $\Phi_i$  are bound states of the  $N+1$  system that are constructed with target orbitals to ensure completeness of  $\Psi(\varepsilon)$  and improve short-range correlations. The functions  $u_{\varepsilon}(r)$  and coefficients  $c_i$  are obtained applying the Kohn variational principle to Eq. (16) giving rise to a set of coupled integro-differential equations.

These are solved by determining the  $R$  matrix which is a real, symmetric matrix whose rows and columns are labeled according to the possible channels of the scattering problem. At this point, one should notice by looking at Eq. (16) that resonances (quasibound states) are automatically included either in terms of closed channels in the first expansion or as linear combinations of bound states in the second expansion. In the external region,  $\Psi(\varepsilon)$  is represented by Eq. (11) and Eq. (12) is solved with the following long-range matrix potential:

$$U_{\alpha\alpha'}(r) = \sum_{\lambda} C_{\alpha\alpha'}^{(\lambda)} / r^{\lambda+1}. \quad (17)$$

The MBPT method described above is also a powerful technique to compute continuum processes. Here the perturbation expansion is reduced using Feynman diagrams involving, for instance, the photoelectron of the photoionization process.

We now describe some specific codes for computations of atomic structure and scattering. Codes employing similar assumptions and computational algorithms are grouped together.

**HULLAC:** The Hebrew University Lawrence Livermore Atomic Code (Bar-Shalom, Klapisch, and Oreg, 2001) is a full package for structure and scattering calculations. It solves the multielectronic Dirac equations and includes QED corrections. An analytical parametrized central-field potential is used to obtain the analytical Slater-type spin orbitals. The atomic states  $\Psi$  are constructed using CI expansions. The parameters appearing in both the central-field potential and spin orbitals are varied in a MC approach in order to minimize the energies of any set of levels or, in its semiempirical mode, to minimize the rms deviation between a set of experimen-

tal energy levels and their corresponding theoretical values. The continuum is treated in a DW approximation. Using interpolation techniques for the radial part of collision strengths, it can calculate large quantities of data.

**FAC:** The flexible atomic code (Gu, 2003a) is also a fully relativistic program computing both structure and scattering data. It uses a modified Dirac-Fock-Slater central-field potential which includes an approximate treatment of the exchange interaction. The orbitals are optimized in a SCF iterative procedure during which the average energy of a fictitious mean configuration with fractional orbital occupation numbers is minimized. This mean configuration represents the average electron cloud of the configurations retained in the CI expansion. This is an intermediate approach between MC and SC. The DW method is used to calculate continuum atomic state functions  $\Psi(\varepsilon)$ .

**MCDF/GRASP/GRASP92:** The Multiconfiguration Dirac-Fock structure code (Grant *et al.*, 1980) and its more recent versions, GRASP (Dyall *et al.*, 1989) and GRASP92 (Parpia *et al.*, 1996), use the elaborated fully relativistic Hartree-Fock MC variational principle to obtain the  $c_i$  and four-component  $\phi_i$  in the CI expansion defined by Eq. (7). One energy level or the average of a group or all energy levels is minimized in the orbital optimization. The QED interaction is treated as corrections to the energy levels.

**SUPERSTRUCTURE/AUTOSTRUCTURE/AUTOL SJ:** SUPERSTRUCTURE (Eissner *et al.*, 1974) solves the Breit-Pauli Schrödinger equation. CI atomic state functions are built using orbitals generated from the scaled Thomas-Fermi-Dirac central-field potential that is based on the free-electron gas with exchange approximation. The scaling factors for each orbital are optimized in a MC variational procedure minimizing a  $LS$  term energy or weighted average of  $LS$  term energies. Semiempirical corrections can be applied to the multielectronic Hamiltonian in which theoretical  $LS$  term energies are corrected in order to reproduce the centers of gravity of the available experimental multiplets. Other versions are AUTOSTRUCTURE (Badnell, 1986a, 1997) and AUTOL SJ (Dubau *et al.*, 1981). These include the treatment of the continuum in a DW approach. In AUTOSTRUCTURE, analytical Slater-type orbitals can be also used, and non-orthogonal orbital basis sets can be considered for the calculations of inner-shell processes.

**CIV3:** The configuration interaction version 3 code of Hibbert (1975) uses analytical Slater-type orbitals in CI expansions to represent atomic state functions and solves either the nonrelativistic or Breit-Pauli Schrödinger equations. The orbital parameters are varied in a MC optimization procedure to minimize one or several energy levels using an analytical central-field potential. The atomic state function can be improved in a semiempirical procedure called fine tuning in which the multielectronic Hamiltonian matrix elements are corrected in order to reproduce the available experimental energy levels.

**R-MATRIX/BPRM/DARC:** The BPRM scattering package described by Burke and Berrington (1993) implements

<sup>1</sup>The authors thank Dr. N. Badnell for pointing this out and providing the text for this paragraph.

the elaborated  $R$ -matrix method in the Breit-Pauli relativistic approximation. In the latter, only the one-body Darwin, mass-correction, and spin-orbit terms are considered. The scattering package can use either SUPERSTRUCTURE, AUTOSTRUCTURE, or CIV3 target orbitals. The radiation and Auger dampings which are important in processes involving inner shells have been included using an optical potential (Gorczyca and Badnell, 1996a, 2000). A fully relativistic implementation of the  $R$ -matrix approach using GRASP target spin orbitals is also available [DARC; Ait-Tahar *et al.* (1996)].

MCHF: In the multiconfiguration Hartree-Fock structure code (Fischer *et al.*, 1997), the nonrelativistic multi-electronic Schrödinger equation is solved using the elaborated Hartree-Fock MC variational principle to obtain the orbitals and mixing coefficients utilized in the CI expansion of the atomic state function. The relativistic corrections are included by diagonalizing afterward the Breit-Pauli multielectronic Hamiltonian.

HFR: The pseudorelativistic Hartree-Fock code of Cowan (1981) solves the Hartree-Fock equations for the spherically averaged atom for each electronic configuration. These equations are the result of applying the variational principle to the configuration average energy. Relativistic corrections are also included in this set of equations, i.e., the Blume-Watson spin-orbit, mass-variation, and one-body Darwin terms. The Blume-Watson spin-orbit term comprises the part of the Breit interaction that can be reduced to a one-body operator. CI is taken into account in an SC approach. The radial parts of the multielectronic Hamiltonian can be adjusted to reproduce the available energy levels in a least-squares fit procedure. These semiempirical corrections are used to allow inclusion of higher-order correlations in the atomic state functions. Continuum orbitals are calculated in a DW approach using HXR central-field potential which uses an approximate exchange part of the Hartree-Fock nonlocal potential.

MZ: This code is base on the  $Z$  expansion technique (Safronova and Urnov, 1980) in which a MBPT is applied using screened hydrogenic orbitals. The perturbation expansion then contains powers of  $Z$ , the atomic number. The Breit interaction and QED are also treated in this expansion. Convergence is best with this method for highly ionized ions, and all members of an isoelectronic sequence are treated simultaneously.

#### IV. EXPERIMENTAL TECHNIQUES

Experiments have the potential to directly simulate in the laboratory the same processes observed remotely using telescopes, and so can provide the most accurate and appropriate data for use in interpreting astronomical observations. This cannot always be achieved, owing to practical challenges of achieving the densities or radiation environments occurring in some sources, and also because the scope of the data needs exceeds the available experimental resources. So in many cases we rely on experimental results as crucial checks on computations, while for many other quantities of interest experi-

ments represent the only means to determine atomic quantities with sufficient accuracy for comparison with observations. This accuracy is needed in the case of line wavelengths or energy levels, where inaccurate values can lead to line misidentification or misleading redshifts or radial velocities. Experiments are also crucial for checks of the accuracy of DR rate coefficients at low temperature ( $\sim 10^4$  K), owing to the fact that this process requires energy levels which are accurate to  $\approx 1$  eV.

Experimental techniques have progressed at a rate comparable with the development of theoretical tools and computer platforms. Notable in their application to x-ray processes are the electron beam ion trap (EBIT), which has been described in detail by Beiersdorfer *et al.* (1990), and the storage rings described by Abrahamsson *et al.* (1993), Schippers *et al.* (1998), and Gwinner *et al.* (2001). These developments have been reviewed recently by Beiersdorfer (2003) and we will not repeat them here. In what follows we will describe, for each process, which experiments have contributed to the available database and what future developments might include.

#### V. LINE FINDING LISTS AND RELATED TABULATIONS

In order to organize the many different types and applications for atomic data, we divide them according to the level of computation required for their use. Atomic data which are simplest to use, in principle, include things like line finding lists, which can be utilized with a minimum of detailed fitting or model calculation. Such tabulations are crucial to interpretation of datasets taken at high resolution. They allow a crude determination of the likely conditions in the gas under study, and may be able to address simple questions about element abundances and the likely range of plasma conditions. In addition, they are needed for successful application of the tools described in the later sections. These differ according to the physical excitation mechanism, and we discuss them separately.

##### A. Coronal plasmas

###### 1. Background

Coronal plasmas are those in which the ionization balance is determined primarily by collisions between ions and thermal electrons. They are common to situations involving mechanical heating, such as supernova remnants, stellar coronae, and clusters of galaxies. For our purposes this includes objects such as supernova remnants which may not be in ionization equilibrium (Shklovsky, 1968). A feature of coronal plasmas which are in or near equilibrium is that the ionization balance adjusts so that the ionization potentials of the most abundant ions are comparable to the gas temperature. As a result, electrons have sufficient energy to excite many atomic bound states, and so the spectra are generally rich in line emission. For coronal plasmas, the most useful low level tools are likely to be finding lists for

emission lines. This typically includes resonance lines, lines which have the ionic ground term as the lowest level, since these are often the strongest and therefore most easily measured. It also includes satellite lines, which resemble resonance lines but with the addition of a spectator electron, since these can be used to infer temperature. Finally, it includes electric-dipole forbidden lines and lines connecting excited levels (subordinate lines) which are potential diagnostics of various plasma parameters such as electron density and the effects of cascades.

Prior to the launch of Chandra and XMM-Newton the need for accurate x-ray line wavelengths in astronomy was driven by the study of solar x rays. This led to the development of line lists in close cooperation with laboratory spectroscopists. Early work originated from data taken by rocket flights and the OSO satellites. These include rocket observations of first solar detection of O<sup>6+</sup> lines and others in the 14–22 Å range by [Freeman and Jones \(1970\)](#). [Walker and Rugge \(1970\)](#) presented observation of the forbidden lines in the He isosequence. [Meekins et al. \(1968\)](#) presented flare spectra from crystal spectrographs on OSO-4 in the wavelength ranges 0.5–3.9 and 1.0–8.5 Å. An analysis of the solar spectrum in the range 33–110 Å was presented by [Widing and Sandlin \(1968\)](#), and a rocket UV spectrum of the Sun from 60 to 385 Å was presented by [Behring et al. \(1972\)](#). These and other solar x-ray observations were reviewed by [Culhane and Acton \(1974\)](#). The launch of the second generation of solar instruments, the NRL spectroheliograph on Skylab, and SMM led to lists by [Widing et al. \(1982\)](#) of solar flare lines in the 170–345 Å range, and by [Phillips et al. \(1982\)](#) of the flare lines in the 5.7–19 Å range. [Lemen et al. \(1984\)](#) published a compilation of observations of the iron *K* line from solar flares. A compilation of solar spectra of the *K* line of Fe<sup>17+</sup>–Fe<sup>23+</sup> was performed by [Seely et al. \(1986\)](#), along with a comparison theoretical values calculated with the *Z* expansion technique. [Doschek and Cowan \(1984\)](#) compiled a line list based on observation of the Sun for the 10–200 Å range.

Motivated at least in part by solar observations, laboratory measurements of spectra using plasma machines or sparks provide spectra in the EUV and x ray for many ions. Examples include study of S, Ar, and Ca ions by [Deutschman and House \(1966, 1967\)](#). [Feldman and Cohen \(1968\)](#) published a list of lines from iron in the 10–18 Å range from both laboratory and solar flare spectra. [Kunze et al. \(1968\)](#) measured He-like line intensities from a theta pinch machine for C<sup>4+</sup> and O<sup>6+</sup> ions. [Connerade et al. \(1970\)](#) compared laboratory plasma measurements with Hartree-Fock structure calculations for Fe between 10 and 17 Å. [Fawcett \(1970\)](#) classified lines between 240 and 750 Å produced in a laser plasma, and [Fawcett \(1971\)](#) classified lines of Fe<sup>10+</sup>–Fe<sup>14+</sup> from a theta pinch machine. [Goldsmith et al. \(1972\)](#) classified Li-like spectra of *K* Mn in the EUV. [Fawcett and Hayes \(1972\)](#) identified Ni<sup>10+</sup>–Ni<sup>16+</sup> and Co<sup>9+</sup>–Co<sup>16+</sup> 3s-3p and 3p-3d lines from laboratory spectra. [Fawcett et al. \(1974\)](#)

made *ab initio* calculations of 2p-3d line wavelengths and oscillator strengths in Fe<sup>18+</sup>–Fe<sup>23+</sup>, and compared the results with experimental values. [Goldsmith et al. \(1973\)](#) classified 2s-2p transitions in laboratory spectra of Ca<sup>16+</sup> and Ti<sup>18+</sup>. [Feldman et al. \(1973\)](#) classified transitions of Fe<sup>17+</sup> and Fe<sup>18+</sup> observed in laser-produced plasmas. [Fawcett and Hayes \(1973\)](#) classified *n*=2–3 transitions from S<sup>9+</sup>–S<sup>13+</sup> and Ar<sup>11+</sup>–Ar<sup>15+</sup>. Other examples include the study of Fe by [Fawcett et al. \(1972\)](#) and [Boiko et al. \(1978\)](#). Comparison of theoretical and experimental *n*=2 energy levels for the C, N, Li, Be, O, and F isoelectronic sequences was carried out by [Edlen \(1983, 1984, 1985\)](#). Identifications of EUV lines of Fe<sup>9+</sup>–Fe<sup>23+</sup> based on solar and laboratory data were performed by [Jupen et al. \(1993\)](#).

## 2. Recent developments

A commonly accepted standard set of line lists for all applications have been compiled from laboratory spectra and energy levels for various elements by NIST. These include compilations for Mg ([Kaufman and Martin, 1991a](#)), Al ([Martin and Zalubas, 1979; Kaufman and Martin, 1991b](#)), Si ([Martin and Zalubas, 1983](#)), and S ([Martin et al., 1990; Kaufman and Martin, 1993](#)). Collections of energy levels and transition probabilities for iron were made by [Sugar and Corliss \(1979, 1985\)](#), [Corliss and Sugar \(1982\)](#), and [Shirai et al. \(1990\)](#). Energy levels for hydrogenic ions are taken from the calculations by [Erickson \(1977\)](#). The data are defined as NIST standard reference data, implying known or estimated accuracy. An exception is the energy-level data compiled by [Kelly \(1987\)](#) for some ions, which also includes some inner-shell energies. Together with older data on spectra of light ions ([Wiese et al., 1966, 1996](#)) this has been incorporated into the NIST spectroscopic database ([Fuhr et al., 1999](#)) at <http://physics.nist.gov/PhysRefData/ASD/index.html>. The accuracies of the transition strengths are evaluated according to the NIST convention: *A*=3%, *B*=10%, *C*=25%, *D*=50%, *E*=50%. Many of the lines in the x-ray band have ratings of *C* or below. A consequence of the restriction to critically evaluated data is that the data included in this database lag behind the production of data available for such a compilation. This does not greatly affect the selection or accuracy of data for strong lines in well-studied wavelength bands, but it does result in incompleteness of some line lists for use in x-ray astronomy.

Recent work using the EBIT instrument at Lawrence Livermore National Laboratory (LLNL) represent the beginning of an effort to fill the need for line wavelengths which are both comprehensive and sufficiently accurate to be used in fitting high-resolution space astronomy data. [Brown et al. \(2001\)](#) have measured the spectrum of ions of Fe<sup>16+</sup>–Fe<sup>23+</sup> in the 10–20 Å wavelength range. [Lepson et al. \(2003\)](#) have measured the spectra of ions of Ar in the range 20–50 Å, and [Lepson et al. \(2005a, 2005b\)](#) summarize measurements for Ne-like through Li-like Ar, S, and Si.

Using many-body perturbation theory approaches, Gu (2005) has calculated the level energies of excited  $L$ -shell complexes in iron and nickel ions. Comparison with experimental results shows that the line wavelengths are generally in agreement to within  $\leq 10$  mÅ. Energy levels with comparable accuracy have been obtained by Kotchigova *et al.* (2005) also using a many-body perturbation method. This is a significant improvement over that obtainable with *ab initio* calculations using standard configuration interaction methods, and is adequate for many purposes for fitting to observed spectra using Chandra and XMM-Newton.

Attempts to update and extend the NIST database for use in analyzing Chandra data include the lists for Ne, Mg, Si, S in the 10–30 Å wavelength range by Podobedova *et al.* (2003). Lists specific to the x-ray band are given as part of the CHIANTI database (Dere *et al.*, 1997; Landi *et al.*, 1999; Landi and Bhatia, 2005a). Other compilations widely used in analyzing x-ray and EUV spectra are APEC (Smith *et al.*, 2001) and MEKAL (Mewe, Kaastra, and Liedahl, 1995). These generally represent compilations from diverse sources, including both experimental and theoretical work, in order to be sufficiently comprehensive to be used in analyzing Chandra and XMM-Newton data. Effort has been devoted to updating these to the accuracy required for interpreting high-resolution observations, since most of these compilations were begun before the launch of these instruments. These updates are available as part of the corresponding data analysis packages in widespread use for analyzing x-ray spectral data (cf. <http://heasarc.gsfc.nasa.gov/docs/software/lheasoft/>, <http://cxc.harvard.edu/ciao/>).

## B. Photoionized plasmas

### 1. Background

In astrophysical sources containing a strong source of ionizing continuum radiation and where mechanical heating is negligible, the ionization balance in the gas will be determined by photoionization. Electron-ion collisions play a role in recombination and cooling the gas, and in equilibrium the temperature is determined by balancing the heating by photoelectrons with collisional cooling (Tarter *et al.*, 1969). A key distinction between photoionized and coronal plasmas is that the electron temperature in a photoionized plasma is  $\sim 5\text{--}10\%$  of the ionization potential of the dominant ions. Line emission is due to recombination, inner-shell fluorescence, or collisional excitation of low-lying levels. Emission line equivalent widths are defined as the ratio of the line flux to the average continuum level in the vicinity of the line. These are generally smaller in photoionized plasmas than for coronal plasmas, owing partly to the contribution from the continuum source and also because of the reduced energy available from electron collisions.

The interpretation of photoionized plasmas shares with coronal plasmas the need for line lists. Photoioniza-

tion by a radiation field which is nonthermal can lead to a situation where there is a substantial flux of ionizing photons with energies far above the first ionization potential of the abundant ions. This is in contrast to the typical situation in coronal plasmas. It greatly increases the importance of inner shells in opacity and ionization. As a result, spectra can have strong fluorescence line emission and inner-shell lines seen in absorption as the source of photoionization is viewed through the transmitted spectrum of intervening gas. Fluorescence emission and inner-shell absorption are unique x-ray signatures which can be observed from gas under a wide range of conditions, including neutral or near-neutral gas. Few inner-shell transitions, other than satellite lines excited by DR, are included in the compilations of lines for coronal plasmas. Theoretical wavelengths for  $K$  lines were calculated by House (1969) using a single configuration Hartree-Fock method. Kaastra and Mewe (1993) compiled wavelengths and branching ratios for many inner-shell lines based on energy levels of Lotz (1967). A compilation of solar spectra of the  $K$  lines of  $\text{Fe}^{17+}\text{--}\text{Fe}^{23+}$  was performed by Seely *et al.* (1986), along with a comparison with theoretical values calculated with the  $Z$  expansion technique. Shirai *et al.* (2000) compiled experimental energy levels for Fe ions.

## 2. Recent developments

Wavelengths and oscillator strengths of inner-shell  $n=2$  to  $n=3$  transitions in iron ions ( $\text{Fe}^0\text{--}\text{Fe}^{15+}$ ) have been calculated by Behar, Sako, and Kahn (2001) using HULLAC. These features form a broad unresolved transition array (UTA) near 16–17 Å. Calculations of transition probabilities for a subset of these lines, using CIV3 and an extensive selection of configurations in the CI expansion, were carried out by Kisielius *et al.* (2003). Extensive calculations of the UTA transitions, including transitions to  $n=4$  states, have been carried out by Dubau *et al.* (2003) using AUTOL SJ. Wavelengths,  $A$  values, and Auger rate coefficients for  $K$  lines of all ions of iron have been published by Palmeri *et al.* (2002), Bautista *et al.* (2003), Palmeri, Mendoza, Kallman, and Bautista (2003), and Palmeri, Mendoza, Kallman, Bautista, and Meléndez (2003). These represent a compilation of experimental results where available, supplemented by calculations using AUTOSTRUCTURE and HFR for the lower ionization states.

An additional observable which is associated primarily with photoionized gases is the photon spectrum due to radiative recombination (RR). The continuum radiation associated with radiative recombination (RRC) is emitted as a feature at the threshold energy which has an exponential shape, i.e.,  $j(\varepsilon) \propto \exp[-(\varepsilon - \varepsilon_{Th})/kT_e]$ , above threshold  $\varepsilon_{th}$ , with a width proportional to the electron temperature  $T_e$ . RRC features in coronal plasmas are broadened by the higher characteristic temperature and therefore are not easily observable. There is no published database of experimental RRC threshold

energies as such, although energy-level databases such as the NIST database can be used to derive them.

Lists of resonance lines, which can be applied to spectra seen in absorption in front of a strong continuum source, were compiled by [Verner, Barthel, and Tytler \(1994\)](#). This includes lines from all wavelengths longward of the  $\text{He}^+$  Lyman limit at 227.838 Å and all the ion states of all elements from hydrogen to bismuth ( $Z = 83$ ) and includes experimental and critically evaluated wavelengths. At shorter wavelengths, [Verner, Verner, and Ferland \(1996\)](#) compiled experimental and critically evaluated energy level and derived wavelengths for lines originating from ground-term multiplets in the spectral region 1–200 Å.

*Ab initio* wavelengths for some  $K$  lines of medium- $Z$  elements have been calculated by [Behar and Netzer \(2002\)](#) using HULLAC. Comparison with Chandra spectra suggests a likely accuracy of  $\geq 20$  mÅ. Wavelengths for the  $K$  lines of oxygen have been calculated by [Pradhan \(2000\)](#) and [Pradhan et al. \(2003\)](#) using BPRM. Using a multiplatform approach (AUTOSTRUCTURE, HFR, and BPRM), [Garcia et al. \(2005\)](#) calculated the atomic data relevant to the photoabsorption near the  $K$  edge of all oxygen ions. The accuracy of the  $K$  line wavelengths was estimated to be better than 20 mÅ by comparison to the available experimental data. Experimental measurements of inner-shell lines include  $K$  lines of  $\text{Fe}^{16+}$ – $\text{Fe}^{23+}$  measured from tokamak plasmas by [Beiersdorfer et al. \(1993\)](#), measurements of  $K$  lines of  $\text{Fe}^{9+}$ – $\text{Fe}^{15+}$  by [Decaux et al. \(1997\)](#) using EBIT, and the EBIT measurements of the  $K$  lines from  $\text{O}^{4+}$  and  $\text{O}^{5+}$  by [Schmidt et al. \(2004\)](#). [Gu et al. \(2005\)](#) combined EBIT measurements of the  $K$  lines of oxygen ions with FAC calculations of population kinetics to provide line wavelengths and identifications with accuracies ranging from 5 to 20 mÅ. Wavelengths of  $n=1$ –2 inner-shell transitions in the Be-like up to F-like ions of magnesium, aluminum, silicon, phosphorus, and sulfur were measured in a laser-produced plasma and were interpreted using the  $Z$  expansion technique ([Feanov et al., 1994](#)). [Biemont et al. \(2000\)](#) observed the  $K\alpha$  lines of  $\text{Ar}^{9+}$ – $\text{Ar}^{16+}$  in a plasma focus discharge and modeled the spectra using HFR and MCDF.  $K$ -shell binding energies and line wavelengths can also be derived from Auger electron spectroscopy. Examples of this are given by [Bruch et al. \(1979, 1987, 1992\)](#) and [Lin et al. \(2001a, 2001b\)](#). Experimental techniques and results have been reviewed by [Stolterfoht \(1987\)](#).

## VI. DISCRETE DIAGNOSTICS

Beyond the detection and identification of spectral features, physical parameters of the gas can be derived from the shapes and strengths of the features. Line ratios can be used to infer density or temperature. These require the accurate measurement of a subset of lines or spectral features, and can only be applied in situations where the measurement is clean enough to make these features unambiguous. If so, they serve to allow accurate

determination of some physical quantities describing the gas under study often without requiring extensive numerical calculation or use of spectral deconvolution.

### A. Coronal plasmas

Use of line ratios has been extensively applied to coronal plasmas, where they have been used to infer density, temperature, elemental abundance, departures from ionization equilibrium, and non-Maxwellian electron velocity distribution. Density diagnostics rely on the competition between collisions and radiative transitions for two or more lines with greatly differing radiative decay rates. Ratios of lines with differing excitation energies provide temperature diagnostics. Examples of the use of these diagnostics in the context of classical nebulae such as H II regions and planetary nebulae have been discussed in detail by [Osterbrock and Ferland \(2006\)](#). In the Sun the conditions in x-ray gas vary both in time and with position, and the use of discrete diagnostics provides a means to study a limited spatial region, corresponding to the atmospheric zone where a given set of lines is emitted most efficiently. This may provide insight which is easier to interpret for objects which are clearly inhomogeneous, than global modeling, which involves modeling the entire atmosphere at once ([Zirin, 1988; Mariska, 1993](#)). Use of such diagnostics must be applied with care, however, since there may be neighboring regions which may have lower emissivity but larger emission measure and which can thereby contaminate the diagnostic line measurements.

#### 1. He-like diagnostics

##### a. Background

He-like ions are stable against ionization over a comparatively wide range of conditions, and they emit strong  $n=1$ –2 lines which are relatively free from confusion with other lines. The three characteristic lines are the resonance  $r$  ( $1s^2 \ ^1S_0 - 1s2p \ ^1P_1$ ), intercombination  $i$  ( $1s^2 \ ^1S_0 - 1s2p \ ^3P_{2,1}$ ), and forbidden  $f$  ( $1s^2 \ ^1S_0 - 1s2s \ ^3S_1$ ), forming the triplet lines. The  $i$  line actually consists of two components corresponding to the two different total angular momentum states in the upper level, but these are blended at the resolution of all available astronomical x-ray observations. The relative strengths of these lines are studied through conventional line ratios  $R = f/i$  and  $G = (f+i)/r$ . The ratio  $R$  is sensitive to gas density via collisions or the effects of a strong UV radiation field driving the transition  $1s2s \ ^3S_1 - 1s2p \ ^3P_{2,1}$ . The ratio  $G$  is sensitive to temperature owing to the fact that the excitation energies for the  $^3P$  and  $^3S$  levels are lower than for the  $^1P$  levels. The  $G$  ratio is also affected strongly by recombination, which increases the populations of the  $^3S$  and  $^3P$  upper levels relative to the  $^1P$  level. Radiative excitation of the  $^1P$  from ground can have the opposite effect on  $G$ .

The importance of the He-like lines as diagnostics was pointed out by [Gabriel and Jordan \(1969\)](#), who discussed

the density dependence of  $R$  and made a density determination for the solar corona. Blumenthal *et al.* (1972) discussed the processes populating the upper levels of these lines and showed that  $R$  is also temperature dependent. The dependence of  $G$  and  $R$  on temperature and density for many elements, including the effects of satellite lines from DR into the Li-like ion, resonances and inner-shell ionization for coronal equilibrium conditions were calculated by Pradhan and Shull (1981). Mewe and Schrijver (1975) calculated population densities of all levels with principal quantum number  $n=2$  in several He-like ions with  $Z$  ranging from 6 to 20. Calculation of level populations including the effects of photoexcitation within the  $n=2$  manifold were performed by Mewe and Schrijver (1978a). Mewe and Schrijver (1978b) examined the effects of time-dependent ionization appropriate to solar flares. Pradhan (1985) showed that recombination drives up the value of  $G$  in a plasma which is recombination dominated, i.e., photoionized, owing to the fact that RR preferentially populates the triplet states.

#### b. Recent developments

Diagnostic use of He-like line ratios depends on rate coefficients and cross sections populating the  $n=2$  levels, and on the line wavelengths needed for accurate identifications. Other rate coefficients needed for complete modeling of He-like diagnostics include radiative rate coefficients for non-dipole-allowed transitions, which have been calculated by Lin *et al.* (1977), and DR satellite line intensities, which have been calculated by Safronova, Vasilyev, and Smith (2001) and others as discussed in Sec. VII.A.2. Theoretical wavelengths for He-like ions up to  $Z=100$  using nonrelativistic variational calculations were calculated by Drake (1988). Rate coefficients for two-photon decay of metastable He-like ions were calculated by Derevianko and Johnson (1997).  $R$ -matrix calculations of transition probabilities for He-like ions were presented by Fernley, Taylor, and Seaton (1987) and have been incorporated into TOPbase (Cunto and Mendoza, 1992). Wavelengths for the He-like lines in solar flares have been measured for the  $1s2s\ ^3S_1-1s2p\ ^3P_{0,2}$  lines in He-like Ne, Mg, Na, and Si to within 20–30 mÅ using the SOHO SUMER instrument (Curdt *et al.*, 2000). Lifetime measurements have been carried out for the excited states of many ions, not just for the He-like isosequence, and many of these are reviewed by Träbert (2002). Experiments using ion traps can measure lifetimes for forbidden and intercombination transitions, and these provide an important check on transition probabilities for use in modeling He-like lines.

The rate coefficients for collisional excitation of He-like ions were reviewed by Dubau (1994) and Kato and Nakazaki (1989), who showed the importance of resonances in the  $1s2s$  manifold for high- $Z$  elements, i.e., Ca and Fe. These have been taken into account in the modified relativistic DW calculations of Zhang and Sampson (1987). Adoption of these rate coefficients is

recommended for high  $Z$  elements, and  $R$ -matrix calculations for low- $Z$  elements. These rate coefficients, together with radiative recombination coefficients from Pequignot *et al.* (1991), calculations of  $f$  values and energy levels from Fernley, Taylor, and Seaton (1987), and DR satellite calculations of Bely-Dubau, Faucher, Dubau, and Gabriel (1982) and Bely-Dubau *et al.* (1982) were used by Porquet and Dubau (2000) to model He-like line ratios, including a discussion of recombining plasma compared with coronal plasma. Bautista and Kallman (2000) calculated the line emissivities and level populations using similar collisional rate coefficients plus a recombination cascade treatment, including the effects of three-body recombination and suppression of DR at high density. The calculations by Bautista and Kallman (2000) and Porquet and Dubau (2000) provided consistent physically reasonable values for density when applied to Chandra spectra from both recombination and collision-dominated objects. Harra-Murnion *et al.* (1996) calculated rate coefficients for the emission of lines from  $S^{14+}$ , benchmarked these against observations of tokamaks, and then used them to set limits on the density in solar flares.

## 2. Dielectronic satellite lines

Lines emitted during dielectronic recombination (DR) are in principle sensitive temperature diagnostics because the emission process involves collisional excitation of a recombining ion, so the rate depends on the fraction of electrons capable of surmounting the core excitation energy barrier. DR is a two-step recombination process that begins when a free electron approaches an ion, collisionally excites a bound electron of the ion, and is simultaneously captured. This process is discussed in more detail in Sec. VII.A.2; here we limit ourselves to discussion of satellite emission. Satellite lines are emitted during the stabilization of the doubly excited state, when core electrons relax to their ground level in the presence of the additional recombined electron. This spectator electron is responsible for shifting the line wavelength away from the wavelength of the resonance line in the parent ion. Detection of satellite lines requires a spectral resolution of  $\epsilon/\Delta\epsilon \geq 500$ . Interpretation of satellite intensities is simplified by the lack of ambiguity on the excitation mechanism, although satellites can also be emitted following inner-shell collisional or radiative excitation. Even if they are not resolved, satellites can contribute significantly to the intensity of the adjacent resonance line. Thus they can affect the use of discrete diagnostics, such as the H-like diagnostics, and must be taken into account for accurate treatment of discrete diagnostics.

A basic description of the calculation of intensities of DR satellites and their diagnostic value was first presented by Gabriel (1972) and Gabriel and Paget (1972). Most DR proceeds through high  $n$  ( $n > 50$ ) for ions in isoelectronic sequences beyond H and He, and satellites from this are indistinguishable from resonance lines. For satellites, only states with  $n < 4$  produce lines which can

be resolved from the adjacent resonance line. The low- $n$  satellites require different assumptions to calculate compared with the high- $n$  states, and the importance of low- $n$  states increases with  $Z$ . [Gabriel \(1972\)](#) showed that satellites are temperature diagnostics, largely independent of ionization balance. The satellite intensity depends on  $Z^4$ , and so they are relatively unimportant for  $Z < 10$ . The formalism for treating satellite intensities makes the assumption of LTE between satellite upper level and the relevant autoionizing continuum. The satellite intensity then depends on energy separation and branching ratio for line emission. The resonance line intensity must also be corrected for unresolved satellites, and satellite intensities must include the effects of direct excitation of inner shells in the adjacent ion. Enhancement of resonance line intensities by unresolved satellites has been treated by [Ansari and Alam \(1975\)](#). [Gabriel and Phillips \(1979\)](#) showed that satellites can be a diagnostic of non-Maxwellian electron energy distributions. This is because of the relative importance of inner-shell excitation to DR. The resonance line can be excited by all electrons with energies greater than threshold, while DR is a resonant process, selectively excited by electrons at an energy corresponding to the particular resonance. Thus, with two or more measured satellites plus the resonance line it is possible to determine if the excitation rate is consistent with a Maxwellian electron velocity distribution, and to constrain the form of the distribution if not.

Calculations of satellite intensities using nonrelativistic Hartree-Fock orbitals were reported in a series of papers by Karim and Bhalla. [Bhalla et al. \(1975\)](#) calculated intensity factors for DR satellite spectra for highly charged He-like ions. This includes more accurate calculations of autoionization rate coefficients and more accurate calculations of inner shell collisional excitation rate coefficients than the previous work by [Gabriel \(1972\)](#). This results in smaller emissivities for lines arising from  $1s2p(^1P)2s^2P$  levels. These calculations used nonrelativistic Hartree-Fock-Slater orbitals in  $LS$  coupling with CI and exchange. [Bhalla and Karim \(1986\)](#) and [Karim and Bhalla \(1986\)](#) used this technique to calculate intensity factors for the satellite to the Ly $\alpha$  line of  $\text{Ne}^{9+}$ . [Karim and Bhalla \(1988b\)](#) calculated DR for selected hydrogenlike ions ( $Z=10, 14, 18, 20, 22, 26$ , and  $28$ ) using the Hartree-Fock-Slater orbitals. The effects of configuration interaction and spin-orbit coupling were included for  $n \leq 4$ . Configuration average rate coefficients were used to calculate DR rate coefficients for  $n = 5$ , and  $1/n^3$  scaling was assumed for all higher states. This shows that the maximum DR rate decreases with  $Z$  and the position of maximum shifts to higher temperature with increasing  $Z$ . At lower temperatures DR rate coefficients for light elements are greater than those for heavy elements while at higher temperature the trend is reversed. Satellite line intensities were compared with calculations using Thomas-Fermi ([Dubau et al., 1981](#)) and  $Z$  expansion ([Bitter et al., 1984](#)), and  $\sim 10\%$  difference is found. [Karim and Bhalla \(1988b\)](#) found an

$\sim 40\%$  difference in the maximum DR rate for Fe compared with [Dubau et al. \(1981\)](#), possibly due to neglect of some high- $nl$  states ( $2lnl'$ ,  $n > 4$ ). [Karim and Bhalla \(1988c\)](#) calculated x-ray and Auger transition rate coefficients from doubly excited states of He-like ions for  $Z=10, 14, 18, 20, 22, 24, 26$ , and  $28$ , along with intensity factors of satellites originating from DR of ground-state hydrogenic ions via the autoionizing states. [Bhalla and Karim \(1988\)](#) calculated satellite intensity factors for H-like  $\text{Fe}^{25+}$ , showing good agreement with Thomas-Fermi calculations for  $n=2$ , but discrepancies for  $n > 2$ . DR satellite spectra for high-lying resonance states of H-like Fe and Ni were calculated by [Karim and Bhalla \(1995\)](#), and for H-like Si, Ca, and Fe ([Karim et al., 1992](#)). DR rate coefficients for some selected ions in the He isoelectronic sequence were calculated by [Karim and Bhalla \(1989a, 1989b\)](#). These authors presented a comparison with other calculations, including that of [Nilsen \(1986\)](#) which employs relativistic wave functions but which uses rate coefficients which are extrapolated for levels above  $n=4$ . They argued that accurate treatment of the high- $n$  levels is important for ions with  $Z < 20$ . Effects of radiative cascades on H-like DR satellite spectra were studied by [Karim and Bhalla \(1988a\)](#), in an attempt to address conflicting claims by [Gau et al. \(1980\)](#) and [Dubau et al. \(1981\)](#). Possible systematic discrepancies are discussed between results obtained using Hartree-Slater, Thomas-Fermi, and  $Z$  expansion techniques. Calculations of DR satellites arising from levels with  $n > 4$  for He-like Cr and Ni were presented by [Karim and Bhalla \(1990\)](#). The validity of the commonly used  $1/n^3$  scaling for high- $n$  satellites was discussed, and it was pointed out that high- $n$  satellites are likely to be unresolvable, but can appreciably affect total line intensity and should be taken into account. The dependence of DR satellite intensity factors on  $n$  for  $1s\epsilon l \rightarrow 2l'n''l'' \rightarrow 1snl''$  in selected hydrogenlike ions was studied by [Karim et al. \(1991\)](#), and for  $1s^2\epsilon l \rightarrow 1s2pn \rightarrow 1s^2nl$  in He-like ions by [Karim and Bhalla \(1991\)](#).

Calculations of satellite intensities using wave functions based on a Thomas-Fermi potential were carried out by Dubau and co-workers. [Dubau et al. \(1980\)](#) calculated the emission from DR satellites to the  $\text{Mg}^{11+}$  resonance lines including CI, intermediate coupling, and wave functions calculated with SUPERSTRUCTURE. They showed that the relative importance of satellites increases up to  $n=4$ , and decreases for higher  $n$ . Also included were the cascade contribution to the lower  $n$  satellites. The results are consistent with previous work of [Vainshtein and Safranova \(1978\)](#) for wavelengths and radiative transition probabilities, but differ systematically for the autoionization probabilities. [Dubau and Volonte \(1980\)](#) reviewed calculations and solar observations of satellite line intensities. [Volonte et al. \(1987\)](#) calculated DR satellites to  $\text{Ca}^{19+}$  Ly $\alpha$ . This resolved a problem dating from the work of [Dubau et al. \(1981\)](#) and [Blanchet et al. \(1985\)](#) in which the extrapolation of the contribution of low- $n$  satellites does not properly converge to the resonance line for  $n > 4$ , and may explain why the calcu-

lated intensity for Ly $\alpha$  was lower than observed from solar flares by Dubau *et al.* (1981). Bely-Dubau *et al.* (1982) calculated rate coefficients for production of satellite lines by DR and inner-shell excitation in Ca, as well as the production of He-like spectra by excitation, radiative, and DR and through cascades. Bely-Dubau, Faucher, Dubau, and Gabriel (1982) calculated  $n=1-2$  spectra of Fe $^{23+}$  and Fe $^{24+}$  due to inner-shell direct excitation, cascade, RR, and DR. The results were compared with solar spectra. Bely-Dubau (1983) compared results of these calculations with spectra from the PLT tokamak. The Fe $^{24+}$  DR rate coefficient associated with the 1s-2p core excitation was measured for temperatures in the range 0.9–3 keV and good agreement was obtained with contemporaneous calculations.

The use of DR satellites as temperature diagnostics in the solar corona was discussed for iron by Bely-Dubau *et al.* (1979a, 1979b) and for Ca by Bely-Dubau *et al.* (1982). Doschek and Feldman (1987) discussed temperature determinations from solar flares. These authors presented model temperature distributions and studied their effect on the satellite line strengths and on the temperatures which would be inferred from them based on available calculations. A review of the x-ray emission from solar flares was provided by Doschek (1972), who also discussed temperature determinations using H/He-like ratios for S, Si, Mg, and satellites due to DR onto He-like ions. The He-like rate coefficients for Mg $^{10+}$  were calculated by Keenan *et al.* (1986), who showed that the 1s-3p line, when compared with the  $n=1-2$  lines, can be used as a temperature diagnostic in solar flares and active regions.

Phillips *et al.* (1983) used HFR to calculate inner-shell spectra of Fe $^{18+}$ –Fe $^{21+}$  under conditions of solar flares. The excitation was found to be primarily due to DR rather than direct excitation. M. S. Chen (1986) and Nilsen (1987, 1988) also carried out calculations of satellite spectra of H- and He-like ions using relativistic multiconfiguration wave functions. Calculations of DR coefficients and satellite spectra for He-like ions were carried out by Vainshtein and Safranova (1978) and Safranova *et al.* (2000), using the Z expansion technique and including Breit-Pauli operators. The systematic dependence with Z is examined and compared with previous work. An extensive discussion and comparison of different computational methods for satellite spectra for iron was presented by Kato *et al.* (1997).

Calculations of satellite line wavelengths and of the cross section for satellite emission by DR have been benchmarked by the EBIT experiment. Beiersdorfer *et al.* (1992) measured the satellite spectrum of Fe $^{24+}$  and Fe $^{23+}$  in order to measure the cross section for DR capture and stabilization. They find reasonably close agreement with the theoretical calculations of Vainshtein and Safranova (1978) and Bely-Dubau *et al.* (1979a, 1982). Gu *et al.* (2001) measured the EBIT spectra for the other ions of iron Fe $^{20+}$ –Fe $^{23+}$  over a wide range of incident electron energies, and showed that unresolved DR satellites can contribute as much as 15% to the intensities

of strong resonance lines. Satellite spectra of He-like Fe and Ni obtained from a tokamak plasma were studied by Smith *et al.* (1993). Experimental measurements of satellite lines from He-like ions of Ne and heavier elements using EBIT were carried out by Smith *et al.* (1996), Smith, Beiersdorfer, *et al.* (2000), and Wargelin *et al.* (2001).

### 3. Other diagnostics

Ions in the Be–Ne isoelectronic sequences have ground terms with many levels which can be mixed collisionally at high density. When this occurs it opens channels for emission in x-ray lines whose strength is therefore a density diagnostic. This occurs for densities greater than  $\sim 10^{13}$  cm $^{-3}$  for lines in the  $2s^22p^k$ - $2s2p^{k+1}$  transition array of the ions of iron Fe $^{17+}$ –Fe $^{20+}$  in the 80–140 Å range (Stratton *et al.*, 1984). Mauche (2005) has modeled the effect of the ground term mixing on lines in the 10–20 Å wavelength range from these ions. The lines from the ions Fe $^{15+}$ , Fe $^{16+}$ , and Fe $^{17+}$  in the 14–19 Å range have been modeled by Cornille *et al.* (1994). They calculated the structure, radiative, and collisional rate coefficients using AUTOL SJ. These can be used to identify lines in the spectrum of solar active regions. The intensities of the Fe $^{15+}$  DR satellites to Fe $^{16+}$  at 15 Å and of the lines of Fe $^{17+}$  at 14.2 and 16 Å are shown to be sensitive to temperature.

Calculations of level populations affecting emission in strong UV, EUV, and x-ray lines, demonstrating the density dependence due to the collisional mixing of levels in the ground configuration, have been carried out in a series of papers by Bhatia and co-workers: Si $^{6+}$  (Bhatia and Landi, 2003a), Si $^{7+}$  (Bhatia and Landi, 2003d), S $^{8+}$  (Bhatia and Landi, 2003c), S $^{9+}$  (Bhatia and Landi, 2003b), S $^{10+}$  (Bhatia *et al.*, 1987), Ca $^{14+}$  (Bhatia and Mason, 1986b), Ca $^{16+}$  (Bhatia and Mason, 1983), Fe $^{9+}$  (Bhatia and Doschek, 1995), Fe $^{10+}$  (Bhatia and Doschek, 1996; Bhatia *et al.*, 2002), Fe $^{13+}$  (Bhatia and Doschek, 1993; Bhatia *et al.*, 1994), Fe $^{14+}$  (Bhatia and Kastner, 1980; Bhatia and Mason, 1997), Fe $^{16+}$  (Bhatia and Doschek, 2003), Fe $^{18+}$  (Bhatia, Fawcett, *et al.*, 1989), Fe $^{19+}$  (Bhatia and Mason, 1980; Mason and Bhatia, 1983), Fe $^{20+}$  (Mason *et al.*, 1979), Fe $^{21+}$  (Mason and Storey, 1980), Fe $^{22+}$  (Bhatia and Mason, 1981, 1986a), Ni $^{12+}$  (Bhatia and Doschek, 1998), Ni $^{15+}$  (Bhatia and Doschek, 1999), Ni $^{16+}$  (Bhatia and Kastner, 1980), and Ni $^{20+}$  (Bhatia *et al.*, 2003). These include energy levels based on CI calculations using SUPERSTRUCTURE, transition probabilities, and collision strengths in the DW approximation with the addition of a correction calculated in the Coulomb-Bethe approximation (Burgess and Sheorey, 1974) to take into account high partial waves. These references are only a representative sample of available work on such density diagnostics. Other references can be found in the extensive bibliographic tabulations contained in the AMBDAS (<http://www-amdis.iaea.org/AMBDAS/>) and ORNL (<http://www-cfadc.phy.ornl.gov/bibliography/search.html>) databases. Other relevant data for application to fusion plasmas is collected in the

ALADDIN (<http://www-amdis.iaea.org/ALADDIN/>) database.

#### 4. Fe<sup>16+</sup>

The strong lines of Fe<sup>16+</sup> near 15 and 17 Å are among the most prominent in the x-ray spectra of many coronal sources. The relative strengths of the  $2p^6$ - $2p^53s$  lines near 17 Å, the  $2p^6$ - $2p^53d$  lines near 15 Å, and the  $2p^6$ - $2p^54d$  lines near 12 Å are temperature sensitive owing to the differing rate coefficients for electron impact ionization (EII) (Raymond and Smith, 1986). The ratio of the  $2p^6$ - $2p^53d$  lines near 15 Å and the  $2p^6$ - $2p^53s$  lines at 17 Å can also be an indicator of recombination (Liedahl *et al.*, 1995).

Calculations of transition probabilities in intermediate coupling with CI have been carried out by Loulougue (1971). The wavelengths of the  $3s$ - $3p$  subordinate lines for several Ne-like ions have been calculated by Kastner (1983). Bhatia and Kastner (1985) discussed the use of the  $2p^6$  $^1S_0$ - $2p^53s$  $^3P_2$  forbidden line as a density diagnostic. They also presented observability diagrams which serve as a convenient overview of the known and unobserved lines, both for Fe<sup>16+</sup> and for other ions in the neon isoelectronic sequence. Cross sections for excitation of the Fe<sup>16+</sup> lines have been calculated by Mann (1983), Hagelstein and Jung (1987), Zhang and Sampson (1989), and for Fe<sup>15+</sup> by Zhang *et al.* (1989). The lines have been modeled by Loulougue and Nussbaumer (1973, 1975), Smith *et al.* (1985), Bhatia and Doschek (1992), Cornille, Dubau, *et al.* (1992, 1994) and Phillips *et al.* (1997). Calculations of excitation for Fe<sup>14+</sup>-Fe<sup>16+</sup> were reviewed by Badnell and Moores (1994). Cross sections for excitation of the Fe<sup>16+</sup> lines have been calculated by Gupta, Deb, and Msezane (2000) and Chen, Pradhan, and Eissner (2003).

It has long been known that the ratios of the  $2p^6$ - $2p^53d$  components observed from the Sun (Parkinson, 1973, 1975) differ from calculations. This was emphasized by Beiersdorfer *et al.* (2004), who pointed out that calculations of Fe<sup>16+</sup> excitation cross sections differ systematically from the ensemble of laboratory and astrophysical data. Earlier suggested explanations for this discrepancy include the effects of cascades (Goldstein *et al.*, 1989), inner-shell ionization of Fe<sup>15+</sup> (Bautista, 2000), and optical depth effects (Bhatia and Kastner, 1985). The effects of cascades were further explored by Loch *et al.* (2006), who pointed out the importance of correcting experimental measurements for polarization. Smith *et al.* (1985) have shown that the Fe<sup>15+</sup> DR satellites, such as the 15.226-Å satellite to the Fe<sup>16+</sup>  $2p^6$  $^1S_0$ - $2p^53d$  $^3D_1$  line at 15.261 Å, can be comparable to the intensity of the Fe<sup>16+</sup>  $\lambda$  15.01 Å lines.

The strongest lines from Fe<sup>16+</sup> under coronal conditions are the  $2p^6$  $^1S_0$ - $2p^53d$  $^1P_1$  resonance and  $2p^6$  $^1S_0$ - $2p^53d$  $^3D_1$  intercombination lines at 15.01 and 15.26 Å. The relative strengths are not highly sensitive to temperature or density (Loulougue and Nussbaumer, 1973), and they have been observed and mod-

eled extensively (Fawcett *et al.*, 1979). The ratio of strengths of these two features, as measured in the laboratory (Brown *et al.*, 1998), is found to be independent of conditions and excitation process, including radiative cascades, resonance excitation, and blends with unresolved DR satellites. The laboratory ratio is measured to be 3.04, and is greater than that measured in many astrophysical sources. EBIT measurements and modeling of the lines of Ni<sup>19+</sup> (Gu *et al.*, 2004) confirm the results for Fe<sup>17+</sup>.

#### 5. Optical depth diagnostics

Multiple resonance scatterings will affect measured ratios of lines with differing thermalization properties. Thermalization depends on the line optical depth and on the probabilities of destruction or conversion per scattering. Such ratios, whose excitation is relatively insensitive to other conditions, include the relative strengths of the Fe<sup>16+</sup> 15 Å lines. The effects of optical depth on the ratios of x-ray and EUV lines of this ion have been studied by Bhatia and Kastner (1999). Although optical depths have been suggested as the origin of ratios of the 15 Å lines which are discrepant with calculations, the discrepancy now appears to be affected by blending and possibly with omission of important physical effects in the calculations (Beiersdorfer *et al.*, 2004). Other line ratios which are affected by optical depth include the Lyman series of hydrogenic ions, and the *G* ratio of He-like  $n=1$ - $2$  lines. In both of these cases the ratio in question also depends on other factors such as density or temperature, and this complicates diagnostic measurement of optical depth using these lines.

#### 6. Abundance diagnostics

Elemental abundances cannot be directly derived from line intensity ratios, owing to the dependence of emissivities on temperature and density. Line equivalent widths have been used to derive abundances in coronal plasmas, since the continuum in many spectral regions is dominated by electron-proton bremsstrahlung, and so is only weakly dependent on abundances of metals (Sylvester *et al.*, 1998). This requires that the temperature be derived from measurement of the continuum shape, for example, since both the line and continuum emissivities depend on temperature. Abundances can also be derived through full spectral fitting, as described in the next section.

#### 7. Nonequilibrium diagnostics

Departure from ionization equilibrium shifts the ionization balance, at a given electron temperature, away from the equilibrium value. This has the effect of increasing the importance of processes associated with adjacent ions in emitting lines from a given species, such as inner-shell ionization (excitation autoionization or direct ionization) when the ionization balance shifts to the low side, or recombination (DR or RR) when the balance shifts to the high side. An example was studied by Mewe

and Schrijver (1978b) for He-like lines, who showed that nonequilibrium effects can enhance the inner-shell contribution from ionization of Li-like species, if the temperature is high and the ionization is low, or the recombination from H-like species if the temperature is low and the ionization is high. Oelgoetz and Pradhan (2004) studied time-dependent recombination-dominated plasmas. Oelgoetz and Pradhan (2001) showed that the DR satellites dominate the emission of the  $\text{Fe}^{24+}$  at temperatures below that of maximum abundance in collisional ionization equilibrium. Owing to their extreme temperature sensitivity, the satellites are excellent spectral diagnostics for such temperatures in photoionized, collisional, or hybrid plasmas, whereas the forbidden, intercombination, and resonance lines of  $\text{Fe}^{24+}$  are not. Similar effects occur with  $\text{Fe}^{16+}$  (Bautista, 2000) and other ions. The importance of iron  $K$  lines as diagnostics of nonequilibrium, and detailed modeling of the excitation and emission of these lines, was discussed by Decaux *et al.* (2003).

## 8. Non-Maxwellian diagnostics

Gabriel and Phillips (1979) first suggested the use of DR satellites as indicators of nonthermal electron velocities. They showed that the intensities of two satellite lines  $1s^2nl-1s2pnl$  with  $n=2,3$  relative to the  $\text{Fe}^{24+}$  resonance line  $1s^2-1s2p$  can be described by a single temperature only if the emitting plasma has a Maxwellian distribution of electrons. This effect was detected in the laboratory by Bartiromo *et al.* (1985) and in solar flares by Seely *et al.* (1987). The effects of non-Maxwellian velocity distributions on the coronal ionization balance have been examined by Dzifcakova (1992, 1998), following on work by Owocki and Scudder (1983), who showed that the oxygen ionization balance in the solar corona is more sensitive to nonthermal effects than is iron, and that these effects can cause apparent differences in temperatures inferred from the two elements. The effects of non-Maxwellian velocity distributions on the He-like line ratios have been examined by Dzifcakova and Kulikova (2002). They parametrize the electron velocity distribution according to the formulation of Owocki and Scudder (1983), and show that at large departures from Maxwellian the value of  $G$  can greatly exceed that of an equilibrium coronal plasma at the same value of  $R$ . This corresponds to the appearance of greater temperature in the  $G$  ratio, for a given value of  $R$ .

## B. Photoionized

RRCs have an exponential shape with characteristic width equal to the electron temperature, and only in photoionized plasmas are they likely to be narrow enough to be clearly detected. This was pointed out by Liedahl *et al.* (1995), and has been used to infer the temperature in x-ray binaries (Wojdowski *et al.*, 2001) and in Seyfert 2 galaxies (Sako *et al.*, 2000; Brinkman *et al.*, 2002; Kinkhabwala *et al.*, 2002). This procedure relies on the determination of the background continuum level,

and so is subject in principle to blending and confusion with other features. The influence of bremsstrahlung continuum emission cannot be ignored (Mewe *et al.*, 1986). Blending with lines of iron complicates use of the features from Ne, for example, but is less important for the RRCs from Si and S. Use of relative strengths of RRCs to determine abundances requires atomic data for the photoionization cross section. The atomic data needed for this are discussed in the next section.

Metastable levels in ions of the Be isoelectronic sequence can provide diagnostics of the combined effects of gas density and UV photoexcitation. These can be applied to gases which are photoionized via their effect on the absorption spectrum. As shown by Kaastra *et al.* (2004), the absorption from metastable  $2s2p^3P$  in the  $\text{O}^{4+}$  ion provides a constraint on density in the range  $10^8-10^{13} \text{ cm}^{-3}$ . They showed a marginal detection of lines arising from this level from an active galaxy observed with the LETG on Chandra.

Owing to the presence of a strong continuum source, spectra of photoionized sources in the x-ray band can be viewed in transmission, and if so exhibit primarily absorption due to bound-free continuum and resonance lines. Line strengths, as measured by the line equivalent width, are therefore diagnostic of the gas column density and the line intrinsic width. Curve of growth analysis, familiar from the analysis of stellar spectra (Mihalas, 1978), has been applied to analysis of Chandra spectra of active galaxies by, e.g., Lee *et al.* (2001). An important difference between the optical/UV and x-ray case is that the damping parameter  $a$ , which is typically  $\leq 10^{-8}$  for a line such as  $\text{Ly}\alpha$  of hydrogen, can be as great as  $\sim 1$  for x-ray lines such as Fe  $K\alpha$  lines owing to the typically very short lifetimes of line upper levels (Liedahl, 2003; Masai and Ishida, 2004).

Broadening of bound-free absorption features is dominated by the intrinsic properties of the transition, i.e., level or resonance structure near the threshold and the phase space above the threshold. So such features serve as diagnostics of the presence of certain ions or atomic species. Examples include the resonance structure and edge position in ions of oxygen. These have been calculated for  $\text{O}^{5+}$  (Pradhan, 2000), neutral oxygen,  $\text{O}^+$  and  $\text{O}^{2+}$  (Pradhan *et al.*, 2003), and for all ions of oxygen by Garcia *et al.* (2005). The position and shape of the neutral oxygen edge, and the resonance structure, have been calculated by Gorczyca *et al.* (2003) using the *R*-matrix code package. Comparison with experimental measurements (Schmidt *et al.*, 2004) using the EBIT device at Lawrence Livermore National Laboratory shows that the calculations of Garcia *et al.* (2005) are accurate to within  $\sim 10 \text{ m}\text{\AA}$  for  $\text{O}^{4+}$  and  $\text{O}^{5+}$ .  $\text{O}^{2+}-\text{O}^{5+}$   $K$ -line wavelengths were measured with an accuracy ranging from 5 to  $20 \text{ m}\text{\AA}$  in an EBIT experiment and were interpreted in a collisional-radiative model using the FAC code (Gu *et al.*, 2005). These lines were observed by Paerels *et al.* (2001), and have been used by Juett *et al.* (2004) to infer the mean ionization balance in the interstellar gas along the lines of sight to several x-ray binaries.

## VII. SPECTRUM SYNTHESIS AND GLOBAL FITTING

In many situations the most detailed information about the conditions in astrophysical plasmas can be gained by modeling the microphysical processes affecting the excitation/decay, and ionization/recombination, in sufficient detail to synthesize the effects on the spectrum from many ions and elements simultaneously. This entails calculating the ion fractions and level populations and also the emitted spectrum, opacity, or both. This procedure, sometimes described as spectrum synthesis or global modeling, is necessary in cases where the observed spectral resolution or signal-to-noise ratio is not sufficient to cleanly resolve individual spectral features to be used as discrete diagnostics. This is the realm of data analysis in x-ray astronomy prior to the gratings on Chandra and XMM-Newton, when the instrumental resolution was capable of resolving only the strongest lines in uncrowded spectral regions, such as the Lyman- $\alpha$  line from O<sup>7+</sup> in coronal sources. Much of the data obtained by Chandra and XMM-Newton still are obtained with the CCD instruments alone, for sources which are too faint for gratings or which are spatially extended, and even grating spectra or bright sources are unable to resolve or unambiguously detect weak lines in crowded spectral regions. Global modeling is also useful when there is strong coupling expected between the ions responsible for spectral formation. An example is in a photoionized gas, where in equilibrium the temperature will couple the emission and absorption properties of all ions in the gas.

### A. Coronal plasmas

Early work on coronal ionization balance was carried out by [Jordan \(1969, 1970\)](#), who first included a treatment of DR and autoionization and the suppression of these processes at high densities. Early work on the cooling function of coronal plasma was presented by [Cox and Tucker \(1969\)](#) and [Cox and Daltabuit \(1971\)](#). Other calculations of coronal ionization and emission include [Allen and Dupree \(1969\)](#), [Tucker and Koren \(1971\)](#), [Landini and Fossi \(1972\)](#), and [Jain and Narain \(1978\)](#). The work of Mewe and co-workers served to better characterize many of the rate coefficients needed for coronal emissivity calculations. These began with calculations of x-ray ([Mewe, 1972a, 1972b](#); [Mewe et al., 1985](#)) and EUV ([Mewe, 1975](#)) lines from the solar corona, He-like lines ([Mewe and Schrijver, 1978a](#)), exploration of abundance dependences on lines ([Mewe and Gronenschild, 1981](#)) and continuum ([Gronenschild and Mewe, 1978](#)), and nonequilibrium ionization ([Gronenschild and Mewe, 1982](#)). Many of these rate coefficients and cross sections were incorporated into the MEKAL code ([Mewe et al., 1985, 1986; Kaastra, 1992; Mewe, Kaastra, and Liedahl, 1995; Mewe, Kaastra, Schrijver, et al., 1995](#)), and updated to the SPEX code ([Kaastra, Mewe, and Nieuwenhuijzen, 1996](#)), a unified plasma model/analysis environment.

Current ionization balance calculations in widespread use are those of [Arnaud and Rothenflug \(1985\)](#) who calculated the ionization balance for most elements of interest to x-ray astrophysics, and [Arnaud and Raymond \(1992\)](#) who evaluated and compiled recombination and collisional ionization rate coefficients for all ions of iron, and the ionization balance of [Mazzotta et al. \(1998\)](#). Both [Arnaud and Rothenflug \(1985\)](#) and [Mazzotta et al. \(1998\)](#) make use of many of the rate coefficients of [Shull and van Steenberg \(1982a, 1982b\)](#), which in turn use the DR rate coefficients of [Jacobs et al. \(1977a\)](#). As pointed out in Sec. VII.A.2, the rate coefficients of [Jacobs et al. \(1977a\)](#) have been shown to overestimate the effect of cascades to autoionizing levels. [Bryans et al. \(2006\)](#) have published ionization balance calculations which make use of the most recent rate coefficients (summarized later in this section) and which have now been extensively benchmarked and fitted to experiments. The CHIANTI database ([Derevianko and Johnson, 1997; Dere et al., 2001](#)) contains evaluated collisional excitation and radiative data, augmented to include wavelengths shorter than 50 Å ([Landi et al., 1999](#)) and excitation by protons ([Young et al., 2003](#)), and including much of the data appropriate to coronal plasmas reported in this review. The most recent update to CHIANTI version 5 ([Landi and Bhatia, 2005a](#)) also includes transitions to the  $n \geq 4$  levels of iron ions based on calculations using FAC, new UV lines from C-, N-, and O-like isosequences, and updated level energies from [Landi and Phillips \(2005\)](#).

Other calculations of coronal ionization balance and spectra include studies of time-dependent ionization ([Shapiro and Moore, 1975; Sutherland and Dopita, 1993](#)), exploration of the effects of ionization balance on plasma diagnostics ([Gianetti, Landi, and Landini, 2000](#)), calculation of nonequilibrium ionization in supernova remnants ([Hamilton, Chevalier, and Sarazin, 1983](#)), and spectra of supernova remnants in the adiabatic phase ([Itoh, 1979](#)). Comprehensive calculations of coronal emission spectra for the x-ray band including both ionization balance and spectrum synthesis by [Raymond and Smith \(1977\)](#) remain in widespread use. These have recently been updated and greatly expanded by [Brickhouse, Raymond, and Smith \(1995\)](#) and [Smith et al. \(2001\)](#) to form the core of the APEC code, which is in use in analyzing high-resolution astrophysical x-ray spectra.

### 1. Electron impact ionization

#### a. Background

Electron impact ionization (EII) is of fundamental importance to coronal plasmas, in which electrons are energized by some mechanical agent such as shocks, acoustic waves, or MHD dissipation. It can be divided into direct ionization (DI), which we discuss in this subsection, and other processes involving an intermediate state which are addressed in the succeeding subsections. It is challenging to compute owing to the fact that it requires a treatment of two continuum electrons in the final state. Therefore experimental cross sections play a key role in the determination of accurate rates. Measurement tech-

niques include crossed beams, merged beams, traps, plasmas, or indirect methods. Of these, crossed beam measurements have been most widely applied. Storage ring methods have the potential to eliminate the greatest systematic uncertainty, namely, the metastable states in the target beam.

A convenient point for comparison comes from the classical treatment of electron scattering (Seaton, 1962). In a collision between two free electrons, one initially at rest, the energy transferred is  $\epsilon = E/[1+(RE/e^2)^2]$ , where  $E$  is the kinetic energy of the incident electron and  $R$  is the impact parameter. If this energy transfer is instead interpreted as the energy available for ionization of a bound electron, then the cross section is determined by the maximum impact parameter such that the transferred energy is the ionization potential  $I$ :

$$\sigma_{\text{classical}}(E) = 4 \left( \frac{I_H}{I} \right)^2 \left( \frac{I}{E} \right) \left( 1 - \frac{I}{E} \right) \pi a_0^2. \quad (18)$$

Equation (18) is not accurate enough for quantitative work; at low energies it overestimates the cross section and at large energies measured cross sections decrease  $\propto \log(E)/E$ . The functional behavior derived from Eq. (18), with modifications, has been used to parametrize the cross section in many tabulations of cross sections and collision strengths derived from both experiment and theory.

The semiempirical formula of Lotz (1967) was developed at a time when few accurate experimental measurements were available. Selected experimental rate coefficients and isoelectronic interpolation, based on the compilation of experimental rate coefficients by Kieffer and Dunn (1966), were fitted by hand for each subshell to

$$\sigma(E) = \zeta \frac{a \log(E/\chi)}{\chi E}, \quad (19)$$

where  $\chi$  is the ionization potential of the subshell. Equation (19) captures the correct behavior in the asymptotic (Born) limit, while allowing semiempirical adjustment of the cross section near threshold. It was found that a good fit to the available experimental data was obtained if  $a$  is approximately constant and  $\zeta$  is the average number of electrons per subshell. This was done for the lowest two charge states of H, He, Li, N, Ne, Na, K and for neutral Ar, Kr, Rb, Xe, Cs, and Hg. Based on this, Lotz (1968) derived the energy-dependent cross section and ionization rate coefficients for all ions of elements up to Ca, estimated to be accurate to  $\pm 40\%$ .

Summers (1974) developed calculations for direct ionization using the semiclassical exchange classical impact parameter (ECIP) method. This combines a classical binary treatment of close collisions, which gives accurate cross sections at low energies, with a treatment which has the proper asymptotic behavior (Burgess and Summers, 1976). This method was applied by Summers (1972, 1974) to calculations of ionization rate coefficients. Burgess *et al.* (1977) evaluated these rates by comparison with experiment, and found better agree-

ment than other calculations available at the time for most ions. Calculations using the CBO approximation, were carried out by Golden and Sampson (1977, 1980), Golden *et al.* (1978), and Moores *et al.* (1980). Born approximation cross sections were computed for ions of Al and Na (McGuire, 1977, 1982). The importance of excitation autoionization and direct ionization of Na-like ions was pointed out by Sampson (1982). Shevelko *et al.* (1983) used the CBE approximation to calculate the rate coefficients for EII for ions belonging to the isoelectronic sequences from H to Ca. DW calculations in  $LS$  coupling were carried out for the isosequences: H and Li (Younger, 1980a), He (Younger, 1980b), Ne (Younger, 1981a), Na (Younger, 1981b), Cl (Younger, 1982a), and Ar (Younger, 1982b). These remain in widespread use for astrophysical modeling.

DW calculations are likely to be accurate for ions with charge greater than 1, but in order to provide calculations for less ionized species techniques such close coupling must be used. Close-coupling calculations for the electron-impact ionization include the time-dependent close-coupling method, which was applied by Pindzola and Robicheaux (2000) and Pindzola *et al.* (2000) to calculations of ionization of He, C, and Ne. With this technique the time-dependent Schrödinger equation is solved for radial wave functions. These calculations used a configuration-averaged potential due to core electrons and resulted in poor agreement with experiment for Ne, suggesting the need for a full Hartree-Fock treatment of the interaction with core electrons. Comparison of time-independent and time-dependent close-coupling methods was carried out by Badnell *et al.* (1998) for Na-like Mg, Al, and Si. The time-independent methods were  $R$ -matrix and convergent close-coupling solutions, based on a total wave function constructed using antisymmetrized products of Laguerre pseudo-orbitals and physical bound orbitals. General agreement was found between the results of the methods and with the experiment of Peart *et al.* (1991) at the 10% level. Calculation of ionization from metastable Ne was carried out by Ballance *et al.* (2004), and for  $C^{2+}$  by Loch *et al.* (2005), using the  $R$  matrix with pseudostates method. Relativistic methods have not been extensively applied to calculations of collisional ionization. The use of MCDF methods has been demonstrated by Pindzola *et al.* (1989) and Moores and Pindzola (1990).

### b. Experimental measurements

Experimental measurements of collisional ionization have been carried out for many ions of interest to astrophysics, and these are summarized in Table I. Measurements using crossed beams include those of Brook *et al.* (1978) for He, C, N, and O, Crandall *et al.* (1982) for Na-like ions of Mg, Al, and Si, Diserens *et al.* (1984) for  $Ne^+$ , Gregory *et al.* (1983) for  $Ne^{3+}$  and  $Ar^{3+}$ , Gregory *et al.* (1986) for  $Fe^{5+}$ ,  $Fe^{6+}$ ,  $Fe^{9+}$ , Gregory *et al.* (1987) for  $Fe^{11+}$ ,  $Fe^{13+}$ , and  $Fe^{15+}$ , Montague *et al.* (1984) for  $Fe^+$ . Measurements of single and multiple ionization of sulfur atoms by EII were made by Ziegler *et al.* (1982).

TABLE I. Experimental measurements of collisional ionization cross sections.

Ion	Reference	Compilation
H <sup>0</sup>	McGowan and Clarke (1968)	Bely
H <sup>0</sup>	Rothe <i>et al.</i> (1962)	Bely
H <sup>0</sup>	Fite and Brackmann (1959)	Bely
H <sup>-</sup>	McDowell and Williamson (1963)	Bely
H <sup>-</sup>	Inokuti and Kim (1968)	Bely
H <sup>-</sup>	Dance <i>et al.</i> (1967)	Bely
H <sup>-</sup>	Tisone and Branscomb (1968)	Bely
He <sup>0</sup>	Montague <i>et al.</i> (1984)	Belfast
He <sup>0</sup>	Dolder <i>et al.</i> (1961)	Bely
He <sup>0</sup>	Brook <i>et al.</i> (1978)	Belfast
C <sup>0</sup>	Brook <i>et al.</i> (1978)	Belfast
C <sup>+</sup>	Hamdan <i>et al.</i> (1978)	Belfast
C <sup>+</sup>	Aitken <i>et al.</i> (1971)	Burgess
C <sup>2+</sup>	Falk <i>et al.</i> (1983)	ORNL
C <sup>2+</sup>	Woodruff, Hublet, and Harrison (1978)	Burgess
C <sup>3+</sup>	Gregory <i>et al.</i> (1985)	ORNL
C <sup>3+</sup>	Crandall, Phaneuf, Hasselquist, <i>et al.</i> (1979)	ORNL
C <sup>4+</sup>	Crandall, Phaneuf, Hasselquist, <i>et al.</i> (1979)	ORNL
C <sup>5+</sup>	Aichele <i>et al.</i> (1998)	
N <sup>0</sup>	Brook <i>et al.</i> (1978)	Belfast
N <sup>2+</sup>	Gregory <i>et al.</i> (1985)	ORNL
N <sup>2+</sup>	Aitken <i>et al.</i> (1971)	Burgess
N <sup>3+</sup>	Falk <i>et al.</i> (1983)	ORNL
N <sup>3+</sup>	Gregory <i>et al.</i> (1985)	ORNL
N <sup>4+</sup>	Crandall, Phaneuf, Hasselquist, <i>et al.</i> (1979)	ORNL
N <sup>4+</sup>	Defrance <i>et al.</i> (1990)	
N <sup>5+</sup>	Crandall, Phaneuf, and Gregory (1979)	ORNL
N <sup>6+</sup>	Aichele <i>et al.</i> (1998)	
O <sup>-</sup>	Tisone and Branscomb (1968)	Bely
O <sup>0</sup>	Rothe <i>et al.</i> (1962)	Bely
O <sup>0</sup>	Brook <i>et al.</i> (1978)	Belfast
O <sup>0</sup>	Fite <i>et al.</i> (1968)	Bely
O <sup>+</sup>	Aitken and Harrison (1971)	Burgess
O <sup>+</sup>	Loch <i>et al.</i> (2003)	
O <sup>2+</sup>	Gregory <i>et al.</i> (1985)	ORNL
O <sup>2+</sup>	Aitken and Harrison (1971)	Burgess
O <sup>2+</sup>	Loch <i>et al.</i> (2003)	
O <sup>3+</sup>	Crandall, Phaneuf, and Gregory (1979)	ORNL
O <sup>3+</sup>	Loch <i>et al.</i> (2003)	
O <sup>4+</sup>	Falk <i>et al.</i> (1983)	ORNL
O <sup>4+</sup>	Loch <i>et al.</i> (2003)	
O <sup>5+</sup>	Defrance <i>et al.</i> (1990)	
O <sup>5+</sup>	Trefftz (1963)	Bely
O <sup>5+</sup>	Crandall <i>et al.</i> (1986)	ORNL
O <sup>5+</sup>	Crandall, Phaneuf, and Gregory (1979)	ORNL
O <sup>5+</sup>	Crandall, Phaneuf, Hasselquist, <i>et al.</i> (1979)	ORNL
O <sup>5+</sup>	Rinn <i>et al.</i> (1987)	ORNL
O <sup>7+</sup>	Aichele <i>et al.</i> (1998)	
Ne <sup>0</sup>	Nagy <i>et al.</i> (1980)	Belfast

TABLE I. (Continued.)

Ion	Reference	Compilation
Ne <sup>0</sup>	Banister <i>et al.</i> (1996)	ORNL
Ne <sup>+</sup>	Dolder <i>et al.</i> (1963)	Bely
Ne <sup>+</sup>	Diserens <i>et al.</i> (1984)	Belfast
Ne <sup>2+</sup>	Mastsumoto <i>et al.</i> (1990)	
Ne <sup>2+</sup>	Danjo <i>et al.</i> (1984)	Belfast
Ne <sup>2+</sup>	Banister <i>et al.</i> (1996)	ORNL
Ne <sup>3+</sup>	Gregory <i>et al.</i> (1983)	ORNL
Ne <sup>4+</sup>	Banister <i>et al.</i> (1996)	ORNL
Ne <sup>4+</sup>	Duponchelle <i>et al.</i> (1997)	
Ne <sup>5+</sup>	Duponchelle <i>et al.</i> (1997)	
Ne <sup>6+</sup>	Bannister <i>et al.</i> (1996)	ORNL
Ne <sup>6+</sup>	Duponchelle <i>et al.</i> (1997)	
Ne <sup>7+</sup>	Defrance <i>et al.</i> (1990)	
Ne <sup>7+</sup>	Duponchelle <i>et al.</i> (1997)	
Ne <sup>8+</sup>	Duponchelle <i>et al.</i> (1997)	
Mg <sup>0</sup>	Karstensen and Schneider (1978)	Belfast
Mg <sup>+</sup>	Becker <i>et al.</i> (2004)	
Mg <sup>+</sup>	Peart <i>et al.</i> (1991)	
Mg <sup>+</sup>	Martin <i>et al.</i> (1968)	Bely
Al <sup>+</sup>	Hayton and Peart (1994)	
Al <sup>2+</sup>	Crandall <i>et al.</i> (1982)	ORNL
Al <sup>3+</sup>	Aichelle, Steidl, <i>et al.</i> (2001)	
Al <sup>4+</sup>	Aichelle, Steidl, <i>et al.</i> (2001)	
Al <sup>5+</sup>	Aichelle, Steidl, <i>et al.</i> (2001)	
Al <sup>6+</sup>	Aichelle, Steidl, <i>et al.</i> (2001)	
Al <sup>7+</sup>	Aichelle, Steidl, <i>et al.</i> (2001)	
Si <sup>+</sup>	Djuric <i>et al.</i> (1993)	ORNL
Si <sup>2+</sup>	Djuric <i>et al.</i> (1993)	ORNL
Si <sup>3+</sup>	Crandall <i>et al.</i> (1982)	ORNL
Si <sup>4+</sup>	Thompson and Gregory (1994)	ORNL
Si <sup>5+</sup>	Thompson and Gregory (1994)	ORNL
Si <sup>6+</sup>	Zeijlmans <i>et al.</i> (1993)	ORNL
Si <sup>7+</sup>	Zeijlmans <i>et al.</i> (1993)	ORNL
S <sup>4+</sup>	Howald <i>et al.</i> (1986)	ORNL
Ar <sup>0</sup>	Wetzel <i>et al.</i> (1987)	Belfast
Ar <sup>0</sup>	Stephen <i>et al.</i> (1980)	Belfast
Ar <sup>+</sup>	Woodruff, Hublet, and Harrison (1978)	Burgess
Ar <sup>+</sup>	Diserens <i>et al.</i> (1988)	Belfast
Ar <sup>+</sup>	Man <i>et al.</i> (1987)	Belfast
Ar <sup>+</sup>	Müller, Huber, <i>et al.</i> (1985)	
Ar <sup>2+</sup>	Man <i>et al.</i> (1993)	
Ar <sup>2+</sup>	Matsumoto <i>et al.</i> (1990)	
Ar <sup>2+</sup>	Mueller, Morgan, <i>et al.</i> (1985)	ORNL
Ar <sup>3+</sup>	Gregory <i>et al.</i> (1983)	ORNL
Ar <sup>4+</sup>	Crandall, Phaneuf, and Gregory (1979)	ORNL
Ar <sup>4+</sup>	Pindzola <i>et al.</i> (1984)	ORNL
Ar <sup>5+</sup>	Gregory <i>et al.</i> (1985)	ORNL
Ar <sup>6+</sup>	Howald <i>et al.</i> (1986)	ORNL
Ar <sup>7+</sup>	Zhang and Sampson (1992)	ORNL

TABLE I. (*Continued.*)

Ion	Reference	Compilation
Ar <sup>7+</sup>	Rachafi <i>et al.</i> (1991)	
Ar <sup>8+</sup>	Zhang <i>et al.</i> (1991)	ORNL
Fe <sup>2+</sup>	Mueller, Morgan, (1985)	ORNL
Fe <sup>5+</sup>	Gregory <i>et al.</i> (1986)	ORNL
Fe <sup>6+</sup>	Gregory <i>et al.</i> (1986)	ORNL
Fe <sup>9+</sup>	Gregory <i>et al.</i> (1986)	ORNL
Fe <sup>9+</sup>	Stenke, Aichele, <i>et al.</i> (1995)	
Fe <sup>11+</sup>	Gregory <i>et al.</i> (1987)	ORNL
Fe <sup>13+</sup>	Gregory <i>et al.</i> (1987)	ORNL
Fe <sup>15+</sup>	Gregory <i>et al.</i> (1987)	ORNL
Fe <sup>15+</sup>	Linkemann <i>et al.</i> (1995)	
Fe <sup>23+</sup>	Wong <i>et al.</i> (1993)	
Ni <sup>2+</sup>	Stenke, Hathiramani, <i>et al.</i> (1995)	
Ni <sup>3+</sup>	Strenke, Hathiramani, <i>et al.</i> (1995)	
Ni <sup>3+</sup>	Gregory and Howald (1986)	ORNL
Ni <sup>4+</sup>	Stenke, Hathiramani, <i>et al.</i> (1995)	
Ni <sup>5+</sup>	Wang <i>et al.</i> (1988)	ORNL
Ni <sup>5+</sup>	Strenke, Hathiramani, <i>et al.</i> (1995)	
Ni <sup>6+</sup>	Wang <i>et al.</i> (1988)	ORNL
Ni <sup>7+</sup>	Wang <i>et al.</i> (1988)	ORNL
Ni <sup>8+</sup>	Wang <i>et al.</i> (1988)	ORNL
Ni <sup>12+</sup>	Wang <i>et al.</i> (1988)	ORNL
Ni <sup>14+</sup>	Wang <i>et al.</i> (1988)	ORNL

Experiments by Linkemann *et al.* (1995) and Stenke (1999) illustrated the complications inherent in the measurement of collisional ionization. These include the effects of metastable levels in the initial-state ions, which can have greater cross section for collisional ionization than the ground state, and excitation autoionization (EA) in which an ion is collisionally excited to a level which autoionizes. Stenke (1999) made crossed beam measurements of ionization of iron ions, Fe<sup>+</sup>–Fe<sup>9+</sup>, showing the influence of metastables as evidenced by ionization at energies below the ground-state threshold, and also excitation autoionization on the total cross section. Metastables are not likely to be present in lowest density astrophysical plasmas, and so must be separated from the total cross section for use in astrophysics. However, their inclusion in a self-consistent way is a goal for the realistic simulation of finite-density astrophysical plasmas. Falk *et al.* (1983) used crossed beams to measure the influence of metastables on the EII for Be-like ions of B, C, N, and O by varying the metastable fraction in the target beam, demonstrating that metastable levels can dominate the collisional ionization in this iso-electronic sequence.

Experimental and theoretical data have been reviewed by several groups. Early reviews include those of Kieffer and Dunn (1966) and Bely and van Regemorter (1970). A review by the Belfast group includes Bell *et al.* (1983) for elements lighter than fluorine, and Lennon *et*

*al.* (1988) for elements from fluorine to Ni. These result in a set of recommended data utilizing the scaling formula of Lotz (1968), normalized to the distorted-wave calculations of Younger (1980a, 1980b, 1981a, 1981b, 1982a, 1982b) and where available experimental measurements. These rate coefficients have been further evaluated by Kato, Masai, and Arnaud (1991), who found the rate coefficients too low for neutral and near-neutral species, and also for Na-like ions due to neglect of excitation autoionization. Voronov (1997) has compiled rate coefficients based on the Belfast compilation, but which attempts to correct these problems by adopting the rate coefficients of Lotz (1968) for many of the species in question. An extensive review of the physical principles and many experimental and theoretical results has been given by Müller (1991). In addition, rate coefficients for collisional ionization have also been reviewed in the previously mentioned ionization balance calculations: Arnaud and Rothenflug (1985), Arnaud and Raymond (1992), and Mazzotta *et al.* (1998). Sources include Kato, Masai, and Arnaud (1991) and corrections to errors in the Belfast collections in <http://dpc.nifs.ac.jp/aladdin/>. Bibliographies of measurements and calculations of collisional ionization are given by Burgess and Chidichimo (1983), Itikawa *et al.* (1984), and Itikawa (1991, 1996). Both theoretical cross sections and extensive bibliographic data have been collected at the ORNL collisional database website <http://cfadc.phy.ornl.gov/astro/ps/data/home.html>.

The extent of available experimental data is illustrated in Table I, which lists the ion stage and reference for various experimental papers appropriate to astrophysically abundant elements, along with the referring compilation in cases where these have been adopted by a compilation such as Belfast, ORNL (<http://cfadc.phy.ornl.gov/astro/ps/data/home.html>), or Bely and van Regemorter (1970). It is apparent that there are multiple measurements for many ionic species, and that there is little overlap between the adopted datasets used by various compilations. This is a manifestation of the fact that the ionization database needs to be thoroughly reexamined because different databases give different rate coefficients (Savin, 2005). There is no consensus among the widely used calculations of ionization balance as to which is most accurate. In fact, Arnaud and Rothenflug (1985) and Mazzotta *et al.* (1998) primarily make use of distorted-wave calculations, such as those by Younger (1980a), rather than experimental results directly. This is due to the remaining uncertainties with regard to the applicability of experimental results to low density environments, as well as convenience. Experimental results such as those of Bannister (1996) and Stenke (1999), in which the beam composition can be thoroughly characterized, provide a hopeful step in this direction.

### c. Excitation autoionization

Excitation autoionization (EA) is a process in which an ion is collisionally excited to a multiply excited level which then autoionizes. This process can dominate the

total collisional ionization cross section for many ions at energies above the threshold for direct ionization. Its importance was pointed out by [Goldberg et al. \(1965\)](#) and [Bely \(1968\)](#). An experimental demonstration of the importance of EA was performed by [Martin et al. \(1968\)](#).

Calculations of the effect in  $\text{Fe}^{15+}$  were carried out by [Cowan and Mann \(1979\)](#). [Burgess and Chidichimo \(1983\)](#) performed functional fitting similar to that of Lotz for EA. DW calculations include rate coefficients from ground and excited levels of Ar  $L$ -shell ions by [Griffin, Bottcher, and Pindzola \(1982\)](#), [Griffin, Pindzola, and Bottcher \(1987\)](#), and [Cohen et al. \(1998\)](#). Also in this category are the calculations for Na-like and Mg-like ions and  $\text{Fe}^{5+}$ – $\text{Fe}^{13+}$  by [Pindzola et al. \(1986a, 1986b, 1998\)](#) and [Mitnik, Shaw, et al. \(1998\)](#), for  $\text{Fe}^{0+}$  by [Pindzola et al. \(1995\)](#), and for all ions of Ni by [Griffin and Pindzola \(1988\)](#) and [Pindzola et al. \(1991\)](#). CBE calculations of EII with inclusion of EA in the H-C isoelectronic sequences were performed by [Sampson and Golden \(1979, 1981\)](#), and [Sampson \(1982\)](#) made similar calculations for Na-like ions.

Close-coupling calculations including inner-shell excitation and EA were made for Li-like ions of C, N, and O ([Henry, 1979](#)), Na-like ions of Al and Si ([Henry and Msezane, 1982](#)), and for  $\text{Fe}^{23+}$  using  $R$  matrix ([Butler and Moores, 1985](#)).  $R$  matrix with pseudostates calculations include pseudo-orbitals in order to allow for an accurate treatment of the bound and continuum wave functions. Ions which have been treated in this way include H ([Bartschat and Bray, 1996](#)), He ([Hudson et al., 1996](#)),  $\text{Li}^+$  ([Brown et al., 1999](#)),  $\text{Be}^+$  ([Bartschat and Bray, 1997; Pindzola et al., 1997](#)), B ([Marchalant and Bartschat, 1997](#)),  $\text{B}^{2+}$  ([Marchalant et al., 1997; Woitke et al., 1998](#)),  $\text{C}^{3+}$  ([Mitnik et al., 1999](#)), Na-like Mg, Al, and Si ([Badnell et al., 1998](#)), and  $\text{Al}^{2+}$  ([Teng, 2000](#)).

An additional process which affects EII is resonance excitation double autoionization (REDA), which is the first stage of dielectronic recombination, dielectronic capture (cf. Sec. VII.A.2), followed by double autoionization. A related process is resonant excitation auto-double-ionization (READI), in which the autoionization occurs as a single event resulting in the ejection of two Auger electrons. The net result is an effective ionization event. [Linkemann et al. \(1995\)](#) have studied the effects of EA and REDA in  $\text{Fe}^{15+}$  using the Heidelberg storage ring, and compared their results with distorted-wave calculations by [Chen et al. \(1990\)](#) and [Badnell and Pindzola \(1993\)](#). EA dominates the cross section by a factor  $\sim 5$  above 800 eV for this ion, and REDA can contribute  $\sim 20$ –30 % to the total ionization rate. Theoretical cross sections reproduce the magnitude of the experimental cross section, but they do not accurately reproduce the complex resonance structure. Possible reasons for this are the isolated resonance approximation which omits interacting resonance effects. Experimental measurements of multiple ionization have been carried out by [Müller, Tischert, et al. \(1985\)](#) for  $\text{Ar}^+$  and  $\text{Ar}^{4+}$ , [Teng et al. \(2000\)](#) and [Knopp et al. \(2001\)](#) for  $\text{C}^{3+}$ , and [Aichele, Shi, et al. \(2001\)](#) for  $\text{Ne}^{7+}$ . Semiempirical formulas for

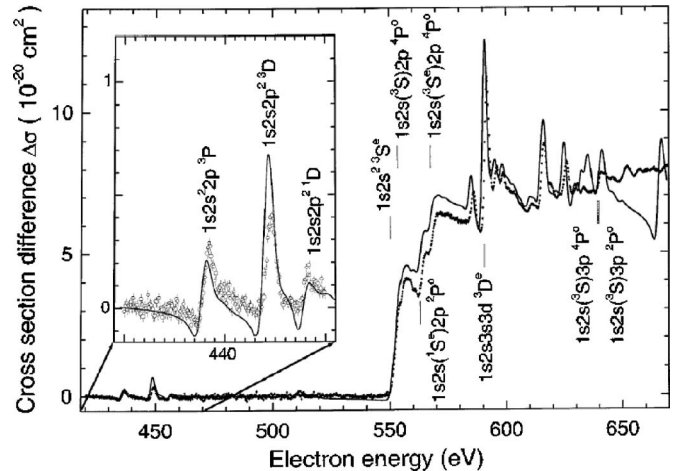


FIG. 8. Cross section for electron-impact ionization of  $\text{O}^{5+}$  in the vicinity of the  $1s2s2\ 3S^0$  EA threshold. The DI contribution has been subtracted off. Data points are crossed beam measurements ([Müller et al., 2000](#)); the solid curve is the  $R$ -matrix calculation.

electron-impact double-ionization cross sections were presented by [Shevelko et al. \(2005, 2006\)](#).  $R$ -matrix calculations can reproduce the fine structure in the EA/REDA/READI cross section for some ions, as evidenced by the comparison shown in Fig. 8. This shows the  $R$ -matrix calculation and crossed beam measurements of excitation autoionization for the K shell of  $\text{O}^{5+}$  ([Müller et al., 2000](#)).

## 2. Dielectronic recombination

### a. Background

In coronal equilibrium ionization balance is determined by the relative rates of collisional ionization and recombination, where the most important recombination processes at low density are radiative recombination (RR), discussed in the next section, and dielectronic recombination (DR), which we discuss in this section. We offer first a note about terminology. It is most common to refer to recombination of ion  $j$  when discussing recombination from ion with charge state  $j$  to charge state  $j-1$ , and adopt this convention in most of our discussion of DR. In the less common case where DR is discussed in terms of the final state ion  $j-1$ , we will refer to it as recombination into ion  $j-1$ .

DR dominates over RR in coronal equilibrium for many ions and at a wide range of temperature, but not universally. The H- and He-like ions are an exception, in which RR dominates at temperatures characteristic of equilibrium. Accurate ionization balance calculations require that both processes be included. A description of the process has been provided by [Savin et al. \(2003\)](#), which we quote with minor modification: “DR is a two-step recombination process that begins when a free electron approaches an ion, collisionally excites a bound electron of the ion, and is simultaneously captured. The electron excitation can be labeled  $nl_j \rightarrow n'l'_j$ , where  $n$  is

the principal quantum number of the core electron,  $l$  is its orbital angular momentum, and  $j$  is its total angular momentum. This intermediate state, formed by the simultaneous excitation and capture, may autoionize. The DR process is complete when the intermediate state emits a photon which reduces the total energy of the recombined ion to below its ionization limit. Conservation of energy requires that for DR to go forward  $E_k = \Delta E - E_b$ . Here  $E_k$  is the kinetic energy of the incident electron,  $\Delta E$  is the excitation energy of the initially bound electron, and  $E_b$  is the binding energy released when the incident electron is captured onto the excited ion. Because  $\Delta E$  and  $E_b$  are quantized, DR is a resonant process."

For the purposes of computation, DR is generally treated as an independent process from RR (although a unified approach is discussed later in this section). The calculation of rate coefficients divides into two basic parts: determination of the energy structure of the doubly excited levels which mediate the process, and the rate coefficients or branching ratios for the stabilizing decays. The first discussion of the importance of this process is that of [Massey and Bates \(1942\)](#). A more detailed summary on the history of the importance of DR has been given by [Seaton and Storey \(1976\)](#). Historically, the understanding of this process has progressed at a rate determined primarily by atomic structure calculations and measurements. This is particularly true for DR at low temperatures, where the excitation energy of the initially bound core electron in the presence of the captured electron (i.e., the quantity  $\Delta E$  defined above) is very small for each of the resonances which contribute to the rate coefficient. This increases the need for accurate calculations of these resonance energies, since the Maxwellian distribution of the recombining electron kinetic energies will be sharply peaked at low energy if the temperature is low. An accurate calculation of the extent to which a given resonance overlaps with this distribution requires values for  $\Delta E$  which are accurate to  $\ll kT_e$ , or  $\ll 1$  eV at  $T_e \sim 10^4$  K.

An outline of the rate calculation was provided by [Bates and Dalgarno \(1962\)](#), which we reproduce here. If the autoionization of the capture state is much more probable than stabilization, then the capture state can be regarded as being in LTE with the continuum to a good approximation. Then the DR rate is simply the equilibrium abundance of the capture state, given by the Saha-Boltzmann equation, times a (small) branching ratio expressing the fraction of ions which stabilize. That is, the capture and autoionization reactions will maintain a quasiequilibrium between the forward and reverse reactions of



State  $d$  is an excited state of the recombined ion  $X_d^{(q-1)+}$  that lies above the ionization potential of ion  $X_b^{(q-1)+}$ , and  $i$  is the ground state of the recombining ion  $X_i^{q+}$ . The population of state  $d$  can be derived from the local balance between dielectronic capture and autoionization.

The DR rate coefficient is then the density of the capture state times the stabilization rate:

$$\alpha_i^{\text{dr}}(T) = \frac{n(X_d^{(q-1)+})}{n_e n(X_i^{q+}) b(X_d^{(q-1)+})} \Gamma_s, \quad (21)$$

where  $n(X_d^{(q-1)+})$ ,  $n(X_i^{q+})$  are, respectively, the number densities of state  $d$  and state  $i$ ,  $n_e$  is the electronic density, and  $\Gamma_s$  is the damping constant for radiative stabilization. The factor  $b(X_d^{(q-1)+})$  is a departure coefficient which reflects the fact that the true number in state  $d$  will be reduced from the Saha value by the branching ratio for autoionization, which is very close to unity:

$$b(X_d^{(q-1)+}) = \frac{\Gamma_a}{\Gamma_a + \Gamma_s}. \quad (22)$$

Here  $\Gamma_a$  is the damping constant for the autoionizing transition and  $n(X_d^{(q-1)+})$  is given by the Saha equation:

$$\frac{n(X_d^{(q-1)+})}{n_e n(X_i^{q+})} = \frac{\omega_d}{2\omega_i} \frac{h^3}{(2\pi mkT)^{3/2}} e^{-\varepsilon_i/kT}, \quad (23)$$

where  $\omega_d$  and  $\omega_i$  are, respectively, the statistical weights of states  $d$  and  $i$ , and  $\varepsilon_i$  is the energy difference between states  $d$  and  $i$ . So the rate coefficient may be written

$$\alpha_i^{\text{dr}}(T) = \frac{\Gamma_a \Gamma_s}{\Gamma_a + \Gamma_s} \frac{\omega_d}{2\omega_i} \frac{h^3}{(2\pi mkT)^{3/2}} e^{-\varepsilon_i/kT} \quad (24)$$

$$= \frac{1}{\tau_s + \tau_a} \frac{\omega_d}{2\omega_i} \frac{h^3}{(2\pi mkT)^{3/2}} e^{-\varepsilon_i/kT}, \quad (25)$$

where  $\tau_s = \Gamma_s^{-1}$  and  $\tau_a = \Gamma_a^{-1}$  are, respectively, the lifetimes for radiative stabilization and autoionization. Since the lifetime for stabilization is generally much longer, this can be written

$$\alpha_i^{\text{dr}}(T) = \Gamma_s \frac{\omega_d}{2\omega_i} \frac{h^3}{(2\pi mkT)^{3/2}} e^{-\varepsilon_i/kT} \quad (26)$$

(note that present day calculations do not need to use this approximation).  $\Gamma_s$  can be expressed in terms of the absorption oscillator strength  $f_{bd}$  for the transition  $b \rightarrow d$ ,  $b$  is an excited state (or the ground state) of the recombined ion  $X_b^{(q-1)+}$  that cannot further autoionize and to which the autoionizing state  $d$  can decay,

$$\alpha_i^{\text{dr}} = CT^{-3/2} \frac{\omega_b}{\omega_i} \nu_{bd}^2 f_{bd} e^{-\varepsilon_i/kT}, \quad (27)$$

where

$$C = \frac{(2\pi)^{1/2} e^2 h^3}{ck^{3/2} m^{5/2}} \quad (28)$$

and  $\nu_{bd}$  is the wave number of the emitted radiation.

The DR rate for an ion is obtained by summing over all levels  $b$  and  $d$ . [Burgess \(1946\)](#) pointed out that the summation over statistical weights and Boltzmann factors can diverge formally, or can be very large if many states participate in the DR process. This is reduced because the approximation used to derive Eq. (26) breaks

down for large  $n$ , i.e., that the autoionization no longer dominates over stabilization. [Burgess \(1964\)](#) calculated the rate coefficient for recombination onto  $\text{He}^+$  using values for  $\Gamma_s$  calculated by extrapolating the collisional excitation cross section to below threshold. A prescription for calculating DR rate coefficients was presented by [Burgess \(1965\)](#), in which he demonstrated by numerical experiment that when the sum over  $b$  and  $d$  is performed on Eq. (27) the dependence on the nuclear charge and level energy separate, and the rate can be written as a sum over the oscillator strengths of the stabilizing radiative transitions and a polynomial in the energies of the same stabilizing transitions. These polynomials, known together as the Burgess general formula (GF), allow the rate coefficient for DR to be calculated using an analytic function of nuclear charge, atomic number, and temperature. This remains the standard set of rate coefficients against which others are compared, and which are in widespread use in various calculations of ionization balance.

The GF is meant to be used for DR where the channels which dominate the total rate are into high- $n$  levels near the DR series limit. This allows all these high- $n$  levels to be treated approximately as a single resonance at the energy of the series limit. It is most accurate when the temperature is comparable to the dominant core excitation, i.e.,  $\varepsilon_i/kT \sim 1$ . It is not meant to be used where the dominant recombination channels are those at low energies far away from the series limit. The GF models DR as a dipole core excitation followed by the inverse decay. It does not allow for autoionization into excited states, nondipole core excitation, or alternative radiative stabilization pathways by either the core or Rydberg electron. Comparison with experiment ([Savin, 1999](#)) shows the GF, and modifications by Merts and by [Burgess and Tworkowski \(1976\)](#), to be reliable to approximately a factor of 2.

The importance of using accurate term energies rather than configuration-average energies in the calculation of DR rate coefficients was pointed out by [Shore \(1969\)](#). This is because of the Boltzmann factor in Eq. (27), and also because of the effect on the overlap of the resonance energies. [Shore \(1969\)](#) calculated DR rate coefficients for various ions of the H-like, Li-like, Na-like iso-electronic sequences, in addition to  $\text{C}^+$  and  $\text{Ca}^+$  ions using mono-configurational screened hydrogenic wave functions including the effect of finite stabilization. These results demonstrate a qualitative difference between recombination onto ions where  $\Delta n = 0$  transitions are allowed in core excitation, such as Li- or Be-like ions, and those in which they are not, such as H-like ions. In the former case, capture states are those with  $n > 100$ , while in the latter case capture occurs primarily to states with  $n < 50$ . The [Burgess \(1965\)](#) formula provides results which are most accurate for ions dominated by the high- $n$  capture states. Larger errors can result for ions where the low- $n$  states dominate. For high  $Z$  dielectronic capture and stabilization can occur predominantly through states with  $n \leq 4$ . The stabilization transition

therefore can correspond to a spectroscopically resolvable emission line, although with an energy which is shifted from the corresponding line in the parent ion due to the partial screening provided by the recombining electron. These satellite lines have diagnostic value and are discussed in Sec. VI.A.2.

The calculations of [Shore \(1969\)](#) neglected exchange effects and channel coupling, both of which are expected to reduce the autoionization rates. The effects of stabilization and resonance overlap, in addition to exchange and channel coupling, were examined by [Burgess and Tworkowski \(1976\)](#) using the Coulomb-Born approximation for recombination onto H-like ions with  $1 \leq Z \leq 40$ . Comparison with the GF shows agreement to within 30% or better. Compilations of DR recombination rate coefficients calculated using the GF have been made by [Aldrovandi and Pequignot \(1973, 1976\)](#), and remain in widespread use.

### *b. Experiment*

Experimental treatments of DR divide into those involving plasma measurement and those involving direct measurement of reaction yield using a beam or trap. In plasma measurements ion fractions are measured or inferred from spectra and then the recombination rate is derived under assumptions about the ionization rate. This procedure was carried out by [Breton et al. \(1978\)](#), who observed time variability of spectra from a tokamak in which the time variability comes from sawtooth heating due to an MHD instability. By measuring the spectra of two ions simultaneously (Mg-like and Na-like  $\text{Mo}^{30+}$  and  $\text{Mo}^{31+}$ ), whose abundances peak near 2 keV in equilibrium, the ionization and DR rate coefficients could be disentangled. [Brook et al. \(1978\)](#) measured DR at  $kT = 100$  eV for  $\text{Fe}^{8+}-\text{Fe}^{10+}$  by adding Fe to a theta pinch plasma. The measured rate coefficients are approximately 50% of those calculated by [Jacobs et al. \(1977a\)](#), and are much less than those predicted by the [Burgess \(1965\)](#) GF. [Isler, Crume, and Arnurius \(1982\)](#) measured relative abundances of iron ions in a tokamak where coronal equilibrium is achieved. DR rate coefficients were inferred by assuming collisional ionization rates. The results lead to inferred DR rate coefficients which are approximately  $\sim 10\%$  of those predicted by the [Burgess \(1965\)](#) GF.

A related technique is the observation of DR satellites from plasma experiments. Such a measurement was carried out by [Bitter et al. \(1979\)](#) for He-like Fe in tokamak. These were found to agree with calculations of [Jordan \(1969\)](#) and [Summers \(1974\)](#). [Decaux et al. \(1991\)](#) measured satellite spectra of  $\text{Fe}^{25+}$  and compared with various available calculations, showing agreement in the satellite intensity factors to within  $\approx 10\%$ . [Decaux, Bitter, et al. \(1991\)](#) compared experiment with HF calculations using the technique of [Karim and Balla \(1991\)](#) for  $n=3-8$  DR satellites of the Fe XXV  $K\alpha$  resonance line, and discussed the diagnostic use of the DR satellites for deriving the plasma temperature.

Measurements using traps and related techniques include those of [Briand et al. \(1984\)](#), who studied the energies of the  $K$ -shell resonance in  $\text{Ar}^{12+}$ – $\text{Ar}^{15+}$  using an electron-beam ion source (EBIS). Rates for DR onto He-like argon were measured by [Ali et al. \(1990\)](#) also using an EBIS. [Knapp et al. \(1989\)](#) measured DR satellites from recombination into  $\text{Ni}^{27+}$  using an electron-beam ion trap (EBIT), and inferred cross sections at the resonance energies. [Beiersdorfer et al. \(1992\)](#) measured DR satellites for He-like iron using an EBIT, along with extensive comparison with theoretical predictions for the strengths of these features. Good agreement was found between experiment and theory for the strongest lines, within the 20% experimental error, although for weak lines much greater discrepancies were found.

Beam experiments divide into those performed at high energy, using highly stripped ions, and those performed at energies similar to those expected in thermal equilibrium. An example of the former is the measurement of [Tanis et al. \(1981\)](#), who measured the  $K\alpha$  radiation produced following electron capture by highly stripped  $\text{S}^{13+}$ – $\text{S}^{16+}$  with neutral argon at 13 MeV. This fluorescence process is the high-energy analog of DR. Similar techniques were used by [Clark et al. \(1985\)](#) in a study of  $K$ -shell excitation in  $\text{Si}^{11+}$ –He at 95 MeV, and by [Schultz et al. \(1987\)](#) who measured cross sections for the correlated emission of two  $K$  x rays following the collision of  $\text{S}^{15+}$  ions with  $\text{H}_2$  in the energy range between 70 and 160 MeV.

Merged beam experiments allow reactions to be measured at low energies, close to what is expected for thermal equilibrium. Key to merged beam measurements is reduction of background ions in the interaction region, which can be an important contaminant at low beam energies. Experimental measurements of DR were carried out for  $\text{C}^+$  recombining to C using merged beams by [Mitchell et al. \(1983\)](#). This resulted in a lower limit which exceeds that calculated by [Lagattuta and Hahn \(1982a\)](#). Also experimental measurement of DR for  $\text{Mg}^+$  using merged beams was carried out by [Belic et al. \(1983\)](#), with measured cross sections found to slightly exceed those calculated by [Lagattuta and Hahn \(1982a\)](#). [Dittner et al. \(1983\)](#) carried out measurement of DR in Li-like C and B with merged beams, with a high energy ion beam from a tandem Van de Graaff accelerator. This has the advantage of low background due to the high beam energy, and showed good agreement with [Lagattuta and Hahn \(1982a\)](#) in the region of the  $2s$ - $2p$  resonance for B. In  $\text{C}^{2+}$  a discrepancy with theory was found near threshold, in which the measurement is lower, possibly due to errors in the theoretical calculation of the  $2p4d$  and  $2p4f$  levels. Merged beam experimental measurements of DR in boron-like N, O, F were carried out by [Dittner et al. \(1988\)](#) which resolved the  $^2D$ ,  $^2P$ ,  $^2S$  states of the  $2s2p^2$  electrons.

### c. Theory

As mentioned above, the GF provides DR rate coefficients which are easily applied and accurate to within a

factor of  $\sim 2$  for temperatures  $kT \sim \epsilon_i$ . Improvements to these rates divide into several categories: improved term energies and bound-state wave functions, associated with more accurate structure calculations; inclusion of other types of transitions such as autoionization into excited states, nondipole core excitation, and stabilization by decay to excited levels; and examination of the computational formalism, such as the isolated resonance approximation and the use of perturbation theory to calculate matrix elements. Improvements to the structure initially made use of single configuration nonrelativistic Hartree-Fock wave functions in  $LS$  coupling, in order to study the systematic behavior of DR and related processes for many ions.

Study of processes which affect DR rate coefficients, including Auger and radiative transition probabilities, and inner-shell excitation, were carried out by Hahn and co-workers. For example, inner-shell excitation in electron-ion collisions in which the incident electron energy exceeds the first ionization threshold is the high-energy analog of DR. The relation between this process and DR was explored by [Hahn \(1977\)](#), who pointed out the importance of inner-shell excitation followed by autoionization. The importance of Auger ionization to the total ionization cross section for highly charged ions was also pointed out by [Hahn \(1978\)](#). Excitation probabilities, to both discrete and continuum states, were calculated for inner- and outer-shell electrons, using an improvement to the Bethe approximation. The result showed a decrease in the relative transition strength to the continuum as the degree of ionization  $Z_I$  increases. The branching ratios for Auger ionization and fluorescence decay were fitted as functions of  $Z_I$  for ionized targets. The Auger ionization and electron fluorescence cross sections were compared with the corresponding direct processes. Calculations of a related process, excitation followed by double autoionization of the ion  $\text{Fe}^{15+}$ , were carried out by [Lagattuta and Hahn \(1981a\)](#) using single configuration bound-state and distorted-wave continuum orbitals. [McLaughlin and Hahn \(1982\)](#) calculated cross sections for the resonant excitation of  $1s$  electrons accompanied by the capture of an incident electron for the target ions  $\text{Si}^{11+}$  and  $\text{S}^{13+}$ . A systematic study of the dependence of the Auger and radiative transition probabilities of high Rydberg states on their principal and orbital quantum numbers was carried out by [Gau and Hahn \(1978\)](#), leading to a simple empirical  $l$  dependence. The scaling behavior of the transition probabilities associated with DR were studied by [Retter et al. \(1978\)](#), showing that  $\Gamma_s \propto Z^4$ ,  $\Gamma_a \sim \text{const}$ . These were tested against numerical computations using single configuration Hartree-Fock wave functions, for the Be and Ne isosequences. This simple scaling was found to break down at high  $Z$ , and a polynomial expression in  $Z$  was given which is a better approximation. Relativistic effects were shown to be important for Fe.

Calculations of DR using single configuration nonrelativistic Hartree-Fock wave functions in  $LS$  coupling include those of [Hahn \(1980\)](#), who studied the scaling of

$\alpha_{\text{DR}}$  with principal quantum number and with nuclear charge. A correction to Burgess (1965) general formula was suggested based on these results, which was carried out only for the Be and Ne isosequences. The importance of the contributions of high Rydberg states to DR of Ar<sup>7+</sup>, Fe<sup>15+</sup>, and Mo<sup>31+</sup> were studied by Lagattuta and Hahn (1981a), leading to derivation of approximate Auger rate coefficients and fluorescence yields for such states. Lagattuta and Hahn (1981b) calculated the DR rate for Na-like Mo<sup>31+</sup> and pointed out the importance of cascades to all excited levels, not just the ground level, which reduces the total rate, and of including doubly excited states which increases the total rate. Lagattuta and Hahn (1982b) demonstrated the importance of 2p-3d core excitations and Auger decays from excited states using a calculation of DR for Cl<sup>7+</sup> (Ne-like). These effects cause departures from  $n^{-3}$  scaling for the transition probabilities. Lagattuta and Hahn (1982a) calculated DR of Mg<sup>+</sup> and pointed out the importance of cascades to autoionizing levels, which leads to a reduction of the net rate. Lagattuta and Hahn (1983a) calculated DR for C<sup>+</sup>, for which the dominant excitation is 2s-2p. The capture states are at high  $n > 100$ , and so are densely packed in energy close to threshold. Lagattuta and Hahn (1983b) calculated DR for Ar<sup>14+</sup>, examining the influence of  $n^{-3}$  scaling and pointing out the effects of 1s excitation at high energy. McLaughlin and Hahn (1983a) calculated DR for C<sup>3+</sup>, and McLaughlin and Hahn (1983b) calculated DR for B<sup>2+</sup> with an improved treatment of high- $n$  states. McLaughlin and Hahn (1983c) calculated DR for O<sup>5+</sup> and discussed scaling of  $\Gamma_a$  and  $\Gamma_s$  vs  $Z$  for various ions in the isosequence. Lagattuta et al. (1986) discussed the effect on the DR cross section of electric-field-induced mixing of high Rydberg state levels, for both Mg<sup>+</sup> and Ca<sup>+</sup> target ions. Omar and Hahn (1987) calculated DR for Ca<sup>12+</sup>, Ca<sup>11+</sup>, and Ca<sup>10+</sup>. Moussa et al. (1988) calculated DR into Ne-like Mg<sup>2+</sup>, P<sup>3+</sup>, Cl<sup>7+</sup>, in which DR involves  $\Delta n \neq 0$  core excitation, and results were compared with the experiment of Dittner et al. (1983). Nasser and Hahn (1989) calculate DR for N<sup>2+</sup>, O<sup>3+</sup> in order to compare with the experiments of Dittner et al. (1988). Ramadan and Hahn (1989) calculated DR for the B-like ions of C, O, Ar, and Fe. They pointed out the importance of accurate energies for  $\Delta n = 0$ . Owing to shortcomings of the single configuration Hartree-Fock treatment for this purpose, these authors use the HFR code. They estimate field effect enhancement based on state counting arguments, and derive an expression for the reduction:  $r_F \sim n_f / (1 + l_{\max})$ , and  $n_f = 3.2 \times 10^8 / F^{1/4}$ , in which  $F$  is the field strength in V cm<sup>-1</sup> and  $l_{\max}$  is the maximum  $l$  which contributes to DR. Agreement is obtained with the experiment by Dittner et al. (1988) using  $r_F = 2$  for C<sup>+</sup>, but the experimental uncertainty is large. Metastables in the recombining ion can affect experimental results from beams, and these were calculated by Hahn (1989) and Hahn and Bellantone (1989), who calculated DR cross sections for metastable O<sup>6+</sup> and found them to be large,  $\sim 10^{-15}$  cm<sup>2</sup> for resonances, leading to rate coefficients

which are  $\sim 10^{-9}$  cm<sup>3</sup> s<sup>-1</sup>. With some field enhancement and assuming that the initial ion beam is a mixture of metastable 1s2s (<sup>1</sup>S and <sup>3</sup>S) states, the overall feature of the experimental data of Andersen, Pan, Schmidt, Pindzola, et al. (1992) was reproduced, including the broad peaks at the incident-electron kinetic energies of 4.7 and 12.5 eV, and partially also at 2.5 and 6.8 eV. With a different mixture, the C<sup>4+</sup> data were reproduced. Janjusevic and Hahn (1989) calculated DR rate coefficients and cross sections for the O<sup>3+</sup> ion where the 2s and 2p electrons of the initial state are excited to higher,  $n \geq 3$  states ( $\Delta n \neq 0$  transitions). The 2p electron excitation dominates the  $\Delta n \neq 0$  process, while the 2s excitation is suppressed by the cascade corrections that strongly affect the intermediate states 1s<sup>2</sup>2s2p3snl and 1s<sup>2</sup>2s2p3dn. The 2s contribution is approximately 15% of the  $\Delta n \neq 0$  mode, while the total  $\Delta n \neq 0$  contribution is roughly 10% of the  $\Delta n = 0$  cross section. Bellantone and Hahn (1989) calculated DR cross sections and rate coefficients for the H-like and He-like C and O ions. The DR cross sections for the initial metastable states of the He-like ions were also estimated for a few low-lying resonance states near the DR threshold. Comparison between various electron coupling schemes was discussed and it was pointed out that configuration interaction (CI) will reduce the contrast between various coupling choices. Hahn (1993) obtained rate formulas for DR by fitting all of the existing DR data for ions with core charges ( $Z_c$ ) less than 50 and the number of electrons in the target ions less than 13. A review of the physics of RR and DR was presented by Hahn (1997), in addition pointing out more exotic modes of recombination. These include off-shell dielectronic recombination (radiative DR, RDR), in which an electron capture is accompanied by simultaneous radiative emission and excitation of the target ion.

Similar techniques were used by Roszman (1979), who calculated the total rate of DR for Mo<sup>32+</sup> (Ne-like) using radial orbitals obtained from central field solution and a Hartree-Fock calculation for ground states. The structure was LS term resolved, not configuration averaged. Agreement with the GF for the total rate is good in the temperature range 1.0–6.0 keV, but poor below 1.0 keV, which is attributed to the GF use of hydrogenic Coulomb wave functions for continuum and hydrogenic wave functions for bound states. Roszman (1987a) calculated DR for members of the fluorine isoelectronic sequence, Ar<sup>9+</sup>, Fe<sup>17+</sup>, and others using the single-configuration, LS-coupled, frozen-core approximation. These calculations employed a different treatment for the ground-state orbitals, in which the Hartree-Fock exchange is replaced with Cowan HXR exchange potential, and continuum exchange is treated using a semiclassical exchange potential. A significant discrepancy is found with the only other available calculation, that of Jacobs et al. (1977a). This may be due to the overestimate of the decays to autoionizing levels by Jacobs et al. (1977a), as discussed below. The results also differ from the rate coefficients calculated using the GF. Similar re-

sults were found by Roszman (1987b) from calculations of DR for O-like  $\text{Ar}^{10+}$  and  $\text{Fe}^{18+}$  using similar techniques. Roszman (1987c) calculated DR for ions of the Li isoelectronic sequence:  $\text{Ne}^{7+}$ ,  $\text{Ar}^{15+}$ ,  $\text{Fe}^{23+}$ , and  $\text{Kr}^{33+}$ . When compared with the results of McLaughlin and Hahn (1983a) a large discrepancy is found, which is attributed to an incorrect assumption by McLaughlin and Hahn (1983a) that all transitions from states  $1s3pn'l'$  and  $1s4pn'l'$  to  $1s2pn''l''$  are treated as stabilizing, while in fact many are not since for  $n'' > n_0$  they are not below the first ionization limit. Roszman (1989a) used the same technique to calculate rate coefficients for  $\text{O}^{5+}$  and  $\text{O}^{2+}$ . Comparison with Badnell (1988) and the Burgess (1965) general formula shows differences of  $\approx 40\%$ . The effect of density-dependent correction formulas for DR are examined by Roszman (1989b), along with the effects of metastables. Another single-configuration Hartree-Fock calculation is that of Younger (1983), who calculated DR for He-like ions of C, Al, Ar, and Fe using DW and including CI for a limited set of states. The results compare well with those of Bely-Dubau *et al.* (1979a).

Jacobs *et al.* (1977a) pointed out that autoionization can occur to another level besides the ground level of the recombining ion, and that this may be more probable than the inverse of the initial capture. This would lead to a greater autoionization probability and a smaller net recombination cross section. Also, the autoionizing level can be collisionally ionized as well, if the density is high, leading to a net reduction in the recombination cross section. These processes were incorporated into DR rate coefficients for  $\text{Fe}^{8+}$ – $\text{Fe}^{24+}$  (Jacobs *et al.*, 1977a), and all ions of Si (Jacobs *et al.*, 1977b), S (Jacobs *et al.*, 1979), Ca, and Ni (Jacobs *et al.*, 1980). These calculations were widely adopted and were later shown to be inaccurate owing to inclusion of autoionization into excited states which are energetically inaccessible (Bandell, 1986a). For example, for  $\text{Fe}^{22+}$  Jacobs *et al.* (1977a) included dipole autoionization of  $1s^22s3p(^1P)nl \rightarrow 1s^22s3s(^1S)E_c l_c$ , but Bandell (1986a) showed that this is only energetically allowed for  $n > 19$ . At  $T = 10^7$  K this translates into a factor of 2.5 difference in the total rate. Bandell (1986a) also showed that nondipole autoionizing transitions are important for this case.

The effects of fine structure were included in single configuration intermediate coupling calculations of DR rate coefficients for excited configurations of iron ions by Dasgupta (1995). Comparison with Savin *et al.* (1999) shows adequate agreement, although their work leaves out important autoionizing channels by not explicitly calculating capture to states with  $n \geq 15$ . Scaled rate coefficients for O- and F-like ions were calculated by Dasgupta and Whitney (1990) and Dasgupta (1995).

MCDF orbitals were used for DR calculations by Chen and co-workers. M. H. Chen (1986b) carried out calculations for the He isoelectronic sequence. Relativistic effects drastically alter the satellite structure of  $\text{Fe}^{24+}$ , but only affect the total rate by 20%. Relativistic effects can alter the rate coefficients by as much as a

factor of 3 by altering the Auger energies for higher  $Z$  elements (e.g.,  $\text{Mo}^{40+}$ ). In nonrelativistic treatments and LS coupling the total rate is dominated by a few capture levels, while relativistic effects redistribute the rate to more levels. Calculations were carried out for Ne-like ions ( $Z=18, 26$  and greater) by M. H. Chen (1986a) and for F-like ions ( $Z=26$  and greater) by Chen (1988a). Coster-Kronig channels are those in which an ion with an inner-shell vacancy decays by autoionization of an electron with the same principal quantum number as the initial vacancy. The influence of these channels on DR rate coefficients was examined in the calculations of Chen (1988b). The total DR coefficients for  $\text{B}^{3+}$ ,  $\text{N}^{5+}$ , and  $\text{F}^{7+}$  ions are reduced by 60%, 13%, and 4%, respectively, due to the inclusion of Coster-Kronig channels. These effects are found to be negligible for  $Z > 10$ . Chen and Crasemann (1988) carried out DR calculations for Be-like ions with atomic numbers  $Z=30, 34, 36, 42, 47$ , and 54. Effects of relativity and configuration interaction on the DR satellite spectra and rate coefficients were studied by comparing the theoretical results from non-relativistic and relativistic single-configuration and multiconfiguration Hartree-Fock calculations with and without the Breit interaction by Chen (1988c). Explicit calculations for H-like Ne, Cr, Mo, and Xe show that relativistic and CI effects are important in calculating satellite spectra. For light ions, nonrelativistic calculations in intermediate coupling with configuration interaction may be sufficient. For medium heavy and heavy ions, however, *ab initio* relativistic calculations in intermediate coupling with CI including the Breit interaction are necessary. DW calculations using MCDF orbitals were carried out for Li-like ions by Chen (1991). It was shown that the total rate coefficients for the fine-structure states for ions with  $Z \geq 4$  can differ by as much as one order of magnitude at low temperatures due to the effects of relativity and intermediate coupling. Comparison with the results of Roszman (1987a) one finds  $\Delta n = 0$  rate coefficients 20% larger for  $\text{Ne}^{7+}$  at low temperature, which is likely due to Roszman's (1987a) neglect of  $1s2pnl$  for  $l > 8$  and the use of nonrelativistic  $2s$ - $2p$  energies. For  $\Delta n > 0$ , computed rate coefficients are lower at low  $T$  and higher at high  $T$  than those of Roszman (1987a). The discrepancy at low temperatures is likely due to discrepancy in Auger energies, and at high temperatures it is due to inclusion of  $K$  excitation channels in the work of Chen. DW calculations using MCDF orbitals have been carried out for B-like ions by Chen, Reed, Guo, and Savin (1998). Comparison with experiment (Savin *et al.*, 1999) shows that the MCDF rate coefficients agree with experiment to within  $\approx 30\%$ . The discrepancy may be due to the neglect of  $l \geq 8$  Rydberg states, and possibly also due to overestimate of resonance energies.

Badnell showed the importance of the intermediate coupling and CI effects on DR rate coefficients in a series of papers reporting calculations using his AUTO-STRUCTURE code in  $\text{Fe}^{22+}$  and  $\text{Fe}^{21+}$ . This enables the relatively rapid calculation of large numbers of radiative

and autoionization transition rates for arbitrary atomic configurations which are needed to calculate DR rate coefficients. [Badnell \(1986a\)](#) calculated configuration-mixing *LS* coupling or intermediate coupling autoionization rate coefficients for  $\text{Fe}^{24+}$ , and pointed out omissions in the state contribution in work on the same ion by [Bely-Dubau et al. \(1979a\)](#). Calculations using the same techniques for  $\text{Fe}^{21+}$  and  $\text{Fe}^{22+}$  were carried out by [Badnell \(1986b\)](#). This was also done for Be-like ions ([Badnell, 1987](#)), B-like ions ([Badnell et al. 1991](#))  $\text{S}^+ \text{-} \text{S}^{5+}$  ([Badnell, 1991](#)), and oxygen ions ([Badnell, 1989, 1992](#)). Intermediate coupling calculations were carried out by [Badnell and Pindzola \(1989a\)](#) for the boron iso-electronic sequence, by [Badnell and Pindzola \(1989b\)](#) for oxygen, and by [Badnell and Pindzola \(1989c\)](#) for Na-like P and Cl. The effects of coupling are expected to be less important for highly charged ions, i.e., charge greater than 20, since the change from *LS* coupling does not open significant additional radiative channels. DR for the ground and excited states of He-like C and O were calculated by [Badnell et al. \(1990\)](#), and for Li-like Al by [Badnell \(1990\)](#). These were compared with *R*-matrix calculations by [Terao and Burke \(1990\)](#), and the importance of high angular momentum states and stabilization were pointed out. The importance of fine structure and CI were examined in detail for He-like ions by [Pindzola et al. \(1990\)](#), and compared with storage ring experimental results. [Gorczyca and Badnell \(1996b\)](#) demonstrated the importance of CI in Na-like ions, including  $\text{Fe}^{15+}$ .

Calculations of DR cross sections are most often done perturbatively, using bound-state wave functions which are calculated separately from the continuum. [Gorczyca et al. \(1996\)](#) compared calculations using *R* matrix with an optical potential against perturbative methods for calculating DR in the  $\text{Ar}^{15+}$  ion, showing agreement between the methods. This provides validation for the use of *R*-matrix methods for cases where the isolated resonance approximation is likely to be inaccurate. Rate coefficients which use continuum wave functions calculated in the *R*-matrix method and which combine both RR and DR into a unified rate coefficient have been calculated by [Nahar and Pradhan \(1994\)](#) and [Nahar \(1995, 1996\)](#). Total recombination rate coefficients were calculated using *R* matrix for DR into Si,  $\text{Si}^+$ ,  $\text{S}^+$ ,  $\text{S}^{2+}$ ,  $\text{C}^+$ , C,  $\text{N}^+$ ,  $\text{O}^{2+}$ ,  $\text{F}^{3+}$ ,  $\text{Ne}^{4+}$ ,  $\text{Na}^{5+}$ ,  $\text{Mg}^{6+}$ ,  $\text{Al}^{7+}$ ,  $\text{Si}^{8+}$ , and  $\text{S}^{10+}$  ([Nahar, 1995](#)), and for iron ions ([Nahar, 1996](#)).

Important to any close-coupling treatment of DR is the effect of radiation damping. This corresponds physically to the effect of radiative decays on the resonant capture state, and which formally determines the width of the resonance and therefore its effect on the rate coefficient. The importance of this effect, and the limitations of *R*-matrix calculations of DR, were discussed by [Gorczyca et al. \(2002\)](#) by comparing computational techniques applied to recombination into  $\text{Fe}^{16+}$ . They showed the importance of accurate treatment of resonance damping, adequate numerical resolution of resonances and inclusion of radiative decays to autoionizing

states, and that these effects can be treated efficiently and accurately using perturbative calculations.

#### *d. Recent developments*

In a series of papers beginning with [Savin et al. \(1997\)](#), measurements were made of the resonance strengths and energies for several iron ions in the Li-Ne isoelectronic sequences using the heavy-ion Test Storage Ring in Heidelberg, Germany. This apparatus has the combined advantages of low background and negligible metastable content. [Savin et al. \(1999\)](#) measured the energy-dependent cross section for  $\text{Fe}^{17+} \rightarrow \text{Fe}^{16+}$  and  $\text{Fe}^{18+} \rightarrow \text{Fe}^{17+}$   $\Delta n=0$  DR and calculated DR rate coefficients. They found significant discrepancies between rate coefficients inferred from their measured cross sections and those of other published calculations. In a comparison with the calculations of [Jacobs et al. \(1977a\)](#) and [Roszman \(1987a\)](#), who only published Maxwellian-averaged rate coefficients, [Savin et al. \(1999\)](#) demonstrated that such comparison can be used to identify discrepant calculations, but cannot clearly identify the approximation responsible for the error, and that agreement between measured and calculated rate coefficients is not a reliable test of the validity of a calculation. The accuracy of DR calculations can best be evaluated by comparison of resonance strengths and energies in the cross section. [Savin et al. \(1999\)](#) showed that single configuration *LS* coupling calculations overestimate  $\text{Fe}^{18+} \rightarrow \text{Fe}^{17+}$  by a factor of 1.6. This may be due to the use of *LS* coupling which leaves out important autoionizing channels, or it could be due to inaccurate resonance energies.

[Savin et al. \(2002a\)](#) measured resonance strengths and energies for DR of  $\text{Fe}^{18+} \rightarrow \text{Fe}^{17+}$  via  $n=2 \rightarrow n'=2$  and  $n=2 \rightarrow n'=3$  core excitations. They have also calculated these resonance strengths and energies using two independent techniques: the perturbative multiconfiguration Breit-Pauli (MCBP) and multiconfiguration Dirac-Fock (MCDF) methods, finding reasonable agreement between experimental results and theoretical calculations. The left panel (a) of Fig. 9 shows the results of measurements made using tokamaks by [Isler, Crume, and Arnarius \(1982\)](#) and [Wang, Griem, et al. \(1988\)](#), theoretical calculations by [Jacobs et al. \(1977a\)](#), [Roszman \(1987a\)](#), and [Dasgupta and Whitney \(1994\)](#), those adopted in the compilation of [Mazzotta et al. \(1998\)](#), and the RR rate coefficients calculated by [Arnaud and Raymond \(1992\)](#). This shows the dispersion in rate coefficients obtained by various workers is a factor of  $\sim 10$  at low temperatures, and a factor of  $\sim 3$  at coronal temperatures, far greater than the estimated experimental uncertainties. The right panel (b) of Fig. 9 shows the storage ring measurements of [Savin et al. \(2002a\)](#), along with calculations using MCBP (AUTOSTRUCTURE) and MCDF. [Savin et al. \(2002b\)](#) measured the resonance strengths and energies for DR of  $\text{Fe}^{19+} \rightarrow \text{Fe}^{18+}$   $\Delta n=0$  core excitations. They have also calculated the DR resonance strengths and energies using four different theoretical techniques: AUTOSTRUCTURE, HULLAC, MCDF, and

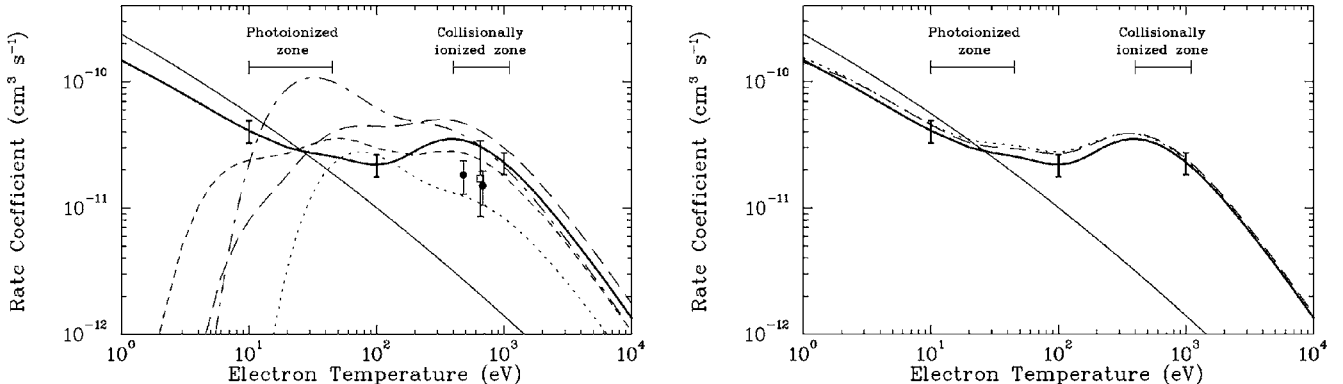


FIG. 9.  $\text{Fe}^{18+} - \text{Fe}^{17+}$  rate coefficient for recombination. Left panel (a): The thick solid curve represents the experimentally derived rate coefficient from Savin *et al.* (2002b). The thick error bars show the estimated experimental uncertainty of 20%. Symbols show tokamak results of Isler, Crume, and Arnurius (1982) (filled circles) and Wang, Griem, *et al.* (1988) (open squares). Curves are DR rate coefficients calculated by Jacobs *et al.* (1977a) as fitted by Shull and van Steenberg (1982a, 1982b) (dotted curve), Roszman (1987a) (short-dashed curve), and of Dasgupta and Whitney (1994) (long-dashed curve), and recommended DR rate coefficient of Mazzotta *et al.* (1998) (dot-long-dashed curve), and recommended RR rate coefficient of Arnaud and Raymond (1992) (thin solid curve). None of the experimental or theoretical DR rate coefficients include RR. The range of temperatures at which these processes are likely to occur in equilibrium are denoted for photoionized and collisionally ionized plasmas. Right panel (b): As in (a) the thick solid curve represents the rate coefficient derived from the storage ring experiment of Savin *et al.* (2002a), and the thin solid curve shows the recommended RR rate. Dotted curve shows the MCBP calculations and the dashed curve shows the MCDF calculations of the DR rate coefficients calculated by Savin *et al.* (2002a). Both calculations are for capture into states including capture states for all values of  $nl$  (i.e.,  $n_{\max} = \infty$ ) and both include DR via  $1 \rightarrow 2$ ,  $2 \rightarrow 2$ , and  $2 \rightarrow 3$  core excitations. None of the experimental or theoretical DR rate coefficients in (a) or (b) include RR. From Savin *et al.*, 2002a.

$R$ -matrix methods. On average the theoretical resonance strengths agree to within  $\leq 10\%$ . However, the  $1\sigma$  scatter in the comparison is 30%, so that calculations of individual emission lines due to DR will have a scatter of approximately this magnitude, although the ensemble will be more accurate.

Savin *et al.* (2003) measured DR resonance strengths and energies for  $\text{Fe}^{20+} \rightarrow \text{Fe}^{19+}$  for  $\text{Fe}^{21+} \rightarrow \text{Fe}^{20+}$  via  $\Delta n = 0$  core excitations. They have also calculated these resonance strengths and energies using three techniques: multiconfiguration Breit-Pauli (MCBP) method using AUTOSTRUCTURE, MCDF, and FAC. Although there is general agreement between experiment and theoretical calculations, discrepancies occur for collision energies  $\leq 3$  eV. Nonetheless, the storage ring experiments and careful comparison with various computational platforms provide crucial benchmarks. These make it clear which computational techniques and approximations are most reliable, and the level of accuracy which can be expected. These techniques can then be applied on a large scale to provide DR cross sections and rate coefficients for astrophysical applications.

Other storage ring measurements include those of De-Witt *et al.* (1995) for  $\text{He}^+$ , Zong *et al.* (1997) for  $\text{Ar}^{15+}$ , Mannervik *et al.* (1998) for  $\text{C}^{3+}$ , Glans *et al.* (1999) for  $\text{F}^{6+}$ , Glans *et al.* (2001) for  $\text{N}^{4+}$ , Bohm *et al.* (2002, 2003) for  $\text{O}^{5+}$ , Bohm *et al.* (2001) for  $\text{Ne}^{7+}$ , Fogle *et al.* (2003) for  $\text{Ni}^{17+}$ , and Nikolić *et al.* (2004) for  $\text{Na}^{8+}$ ; these are summarized by Glans *et al.* (2004). Many of these include comparison with calculations which utilize relativistic many-body perturbation theory, and take into account QED effects in the position and strengths of resonances. Kenntner *et al.* (1995) measured DR for Li-

like Cl and Si and Fogle *et al.* (2005) measured DR for Be-like C, N, and O using a similar apparatus. Measurements of DR have been done using a single-pass merged beam by Andersen, Pan, Schmidt, Badnell, *et al.* (1992) and Andersen, Pan, Schmidt, Pindzola, *et al.* (1992) for He-like and Li-like ions of nitrogen, fluorine, and silicon. These authors point out the importance of resonances associated with the  $1s2s(^3S)$  metastable state in the He-like case. They also point out the importance of intermediate coupling in determining the resonance structure and hence the DR rate coefficient in situations when the electron velocities sample resonances close to the ionization threshold for the metastable state. The use of merged beams for DR, electron collisional excitation, and charge transfer has been reviewed by Phaneuf *et al.* (1999), and the use of storage rings for measurements of recombination has been reviewed by Schippers (1999).

Building on the experimental results of Savin and co-workers, large-scale calculations of state-selected cross sections and rate coefficients for DR in intermediate coupling using the AUTOSTRUCTURE (Badnell *et al.*, 2003) code have been carried out by Badnell, Gorczyca, and co-workers. These include calculations for the various isoelectronic sequences H-Na (Colgan *et al.*, 2003, 2004, 2005; Zatsarinsky *et al.*, 2003, 2004a, 2004b, 2005a, 2005b, 2006; Altun *et al.*, 2004, 2005, 2006; Mitnik and Badnell, 2004; Badnell, 2006). In a complementary effort Gu (2003b) has used FAC to calculate total DR rate coefficients for the H-like through Ne-like isoelectronic sequences for the seven elements Mg, Si, S, Ar, Ca, Fe, and Ni. Together these remove the shortcomings of early calculations, namely, that of  $LS$  coupling and the

choice of energetically allowed channels for applications at coronal temperatures. For applications at temperatures characteristic of photoionized plasmas, large uncertainties remain owing to the use of *ab initio* energy-level structure intrinsic in this work. This has been shown by the storage ring measurements of [Schippers et al. \(2004\)](#), who demonstrated the existence of strong resonances in the recombination cross section for Mg<sup>8+</sup> at electron energies 20–70 meV. They point out that errors in the location of these resonances of only 100 meV can result in changes of up to a factor of  $\sim 3$  in the total recombination rate coefficient at low temperatures. However, with these calculations and their experimental validation, the rate coefficients for DR at coronal temperatures for many ions of astrophysical interest have reached a level accuracy previously unattained.

One remaining area of uncertainty is the role of external fields on DR. According to [Badnell et al. \(2003\)](#), this renders pointless efforts to compute field-free rate coefficients to an accuracy of better than 20%. It has long been known that the high Rydberg states that frequently dominate the DR process can be Stark mixed by weak electric fields ([Burgess and Summers, 1969](#)), such as the plasma microfield ([Jacobs et al., 1976](#)), and so increase the partial rate coefficients by factors of 2 or more over a wide range of  $n$ . Recently, the picture has been further complicated by the discovery that magnetic fields, when crossed with an electric field, strongly affect the electric-field enhancement by reducing it in most cases ([Robicheaux and Pindzola, 1997; Bartsch et al., 1999](#)). This suppression of the electric-field enhancement improves the applicability of field-free DR rates, but does not remove the uncertainty due to field effects in modeling of real plasmas. The importance of field effects, and the field strengths themselves, can be derived through collisional radiative modeling of the dynamic part of the plasma microfield ([Badnell et al. 2003](#)). Previously it appeared that a reasonable approach would be to use the values of the plasma microfield for the electric-field strength for use in the generation of field-dependent data as input to plasma modeling, but the added sensitivity to the magnetic field makes this impractical.

### 3. Collisional excitation

#### a. Background

Collisional excitation or deexcitation by electrons or protons is closely associated with discrete diagnostics, since it is the dominant mechanism affecting the level populations associated with many diagnostic features. However, it also is key to the calculation of synthetic spectra and for cooling. For spectrum synthesis, comprehensiveness is important in order to accurately calculate cooling rate coefficients and pseudocontinuum emission due to large arrays of blended weak lines.

In tabulating collisional excitation data it is customary to work with the collision strength ([Hebb and Menzel, 1940](#)) rather than the cross section. The collision strength between a given pair of levels  $\Omega_{ij}$  is defined

such that  $\Omega_{ij} = \Omega_{ji}$ , and the excitation cross section is given by

$$\sigma_{ij} = \frac{\pi a_0^2}{\omega_i k_i^2} \Omega_{ij}, \quad (29)$$

where  $\omega_i$  is the statistical weight of level  $i$ . The Maxwellian-averaged collision strength is denoted  $Y_{ij}$  and preserves this symmetry.

Although calculations are of greater practical importance to collisional excitation than experiments owing to the large number of transitions which may be of interest, measurement of plasma spectra can be used to infer collision rates. This makes use of assumptions about the excitation mechanism and with independent measurements of the gas density and temperature. Examples include the measurements of [Datla et al. \(1976\)](#), who deduced ionization rate coefficients for He-like B and C from the time histories of the lines emitted by these ions in a theta pinch plasma and compared theoretical estimates using the semiclassical formula of Burgess with experimental results, corrected for the effects of metastables. [Johnston and Kunze \(1971\)](#) determined electron collision-excitation rate coefficients experimentally for  $n=2, 3$ , and 4 levels of Be-like N<sup>3+</sup>, O<sup>4+</sup>, Ne<sup>6+</sup>, and Si<sup>8+</sup> using plasma produced in a theta pinch device. [Tondello and McWhirter \(1971\)](#) measured excitation rate coefficients for 18 transitions in Ne<sup>7+</sup>. A review of methods and some results were presented by [Kunze \(1972\)](#).

A general review of experimental techniques and results has been given by [Dunn et al. \(1995\)](#). The use of merged beams for electron collisional excitation and for charge transfer has been reviewed by [Phaneuf et al. \(1999\)](#). Recent measurements of 2s-2p excitation in Li-like ions C<sup>3+</sup> and O<sup>5+</sup> have been carried out using merged beams by [Greenwood et al. \(1999\)](#) and [Lozano et al. \(2001\)](#), and for S<sup>3+</sup> by [Smith, Chutjian, et al. \(2000\)](#). Measurements of selected transitions have provided crucial checks on calculations ([Beiersdorfer et al., 2002](#)) for spectra such as Fe<sup>16+</sup>, and the EBIT apparatus has been used to benchmark cross sections and density-dependent line ratios for N<sup>5+</sup>, Ar<sup>13+</sup>, and Fe<sup>21+</sup> ([Chen et al., 2004](#)).

An early review of computational techniques for collisional excitation is that of [Bely \(1966\)](#). These include the Born approximation, in addition to other computational methods which require the consideration of many partial waves and so are slow when carried out on older computers. For this reason the Bethe approximation was widely used in early work. This is based on the fact that at very high energy distant encounters are most important and the projectile remains outside the atom most of the time. Then the cross section can be expressed as a proportionality with the oscillator strength of the transition. The proportionality is expressed as a Gaunt factor, and values of effective  $\bar{g}$  were derived by [van Regemorter \(1962\)](#). This allowed the use of radiative transition probabilities directly in modeling of collisional plasmas. This formula was used, for example, in calculation of structure and collision strengths for Fe<sup>7+</sup> by [Czyzak and Krueger \(1966\)](#) and compared with results

from Hartree-Fock with exchange self-consistent wave functions. This approximation is no longer in widespread use, since more accurate methods can now be conveniently applied to large numbers of transitions.

Coulomb-Born-Oppenheimer (CBO) calculations of collisional excitation in H-like ions were performed by Burgess *et al.* (1970) and Golden and Sampson (1971). Screened hydrogenic calculations of collisional excitation for atoms with less than four electrons were performed by Sampson and Parks (1974). Golden *et al.* (1981) calculated scaled collision strengths for hydrogenic ions using the CBO method, and Clark *et al.* (1982) calculated scaled collision strengths for excitation of highly charged ions.

An early mention of the importance of CI for collisional excitation rate coefficients was by Layzer (1951). Jones (1970) extended the Eissner-Nussbaumer CI code to include relativity, and illustrated that drastic changes in  $A$  values can occur depending on the treatment of CI. Ermolaev and Jones (1972) explored the importance of CI in He-like ions and mixing between  $^1P$  and  $^3P$ , especially for  $Z > 2$  using both Breit-Pauli and  $Z$  expansion techniques. Nussbaumer (1972) discussed the importance of CI for the ion  $C^{2+}$ . Flower (1972) estimated collision strengths and showed that Li-like lines are useful temperature diagnostics in solar corona if 2-2 and 2-3 lines can both be measured. Bely-Dubau (1973) and Flower and Pineau des Forets (1973) performed CI calculations for  $Fe^{12+}$ . The pitfalls of CI calculations which have deficient sets of configurations and can lead to errors were examined by Nussbaumer (1973), with the ion  $Fe^{12+}$  (Flower and Pineau des Forets, 1973) used as an example. Loulergue and Nussbaumer (1973) demonstrated the effects of blending on the 17.06-Å line in a CI calculation of the structure and excitation rate coefficients for  $Fe^{16+}$ . Jones (1974) calculated collision strengths for He-like ions of Si, Ca, Fe comparing the results of LS coupling and intermediate coupling using a DW method. The effects of relativity were examined by Walker (1974), who calculated electron impact excitation of the  $n=1$  and  $n=2$  states of hydrogenic ions in the Coulomb-Born approximation using Dirac wave functions.

A comparison of distorted-wave and close-coupling calculations of collision strengths for transitions in  $C^{2+}$  excited by electron collisions (Flower and Launay, 1972) indicates that the distorted-wave method is sufficiently accurate for many astrophysical and laboratory applications. DW calculations for many ions have been carried out by Bhatia, Mason, and co-workers, cited in Sec. VI. Calculations using similar techniques have been made for  $S^{10+}$  (Landi and Bhatia, 2003a),  $Ca^{6+}$  (Landi and Bhatia, 2003b),  $Fe^{17+}$  (Cornille *et al.*, 1992),  $Fe^{20+}$  (Phillips *et al.*, 1996),  $Ne^{2+}$  (Landi and Bhatia, 2005c),  $Ca^{13+}$  (Landi and Bhatia, 2005b),  $Ca^{12+}$  (Landi and Bhatia, 2005a), and  $Ar^{11+}$  (Eissner *et al.*, 2005). Fawcett and Mason (1991) calculated collision strengths and oscillator strengths for  $Fe^{8+}$ . Collisional excitation rate coefficients for H-like and He-like ions calculated using a relativistic

DW method have been calculated by Sampson *et al.* (1983) and Zhang and Sampson (1987). This has also been applied to F (Sampson *et al.*, 1991), Na (Sampson *et al.*, 1990), B (Sampson *et al.*, 1986; Zhang and Sampson, 1994a, 1994b), Li (Zhang *et al.*, 1990), Be (Zhang and Sampson, 1992), and C (Zhang and Sampson, 1996) iso-electronic sequences. Collections of references to calculations of collisional excitation have been provided by Kato (1976), Raymond and Smith (1977), Mewe and Gronenschield (1981), and Mewe *et al.* (1985, 1986). Reviews of calculations of available electron excitation cross sections for many ions of interest were presented as part of a 1994 conference on collisions by Berrington (1994), Bhatia *et al.* (1994), Callaway (1994), Cornille, Dubau, and Jacquemot (1994), Dubau (1994), Dufton and Kingston (1994), Fossi and Landini (1994), Kato (1994), Lang and Summers (1994), Mason (1994), McWhirter (1994), Pradhan (1994), and Sampson *et al.* (1994).

### b. Recent developments

Close-coupling calculations are available for an increasing fraction of transitions needed to model coronal plasmas.  $R$ -matrix calculations of collisional excitation have been carried out for hydrogenic ions of C (Aggarwal and Kingston, 1991a), Ne (Aggarwal and Kingston, 1991b), Si (Aggarwal and Kingston, 1992a), Ca (Aggarwal and Kinston, 1992b), Fe (Aggarwal and Kingston, 1993).  $R$ -matrix intermediate coupling calculations have been made for He-like and Li-like Ar and Fe by Whiteford *et al.* (2001, 2002). Calculations for Be-like ions have been reviewed by Berrington (1994). The breakdown of the isolated resonance approximation and the importance of accurate treatment of radiation damping in calculations of collisional excitation, in contrast with the situation for DR, was pointed out by Badnell and Pindzola (1993). The point is that two or more Rydberg series of resonances will interfere only if they overlap because coupling through the background is weak, or absent. In contrast, for electron-impact excitation there is strong coupling through the background. There is no dipole selection rule and consequently the number of resonances increases greatly, so that close-coupling technique or a perturbative approach to overlapping resonances are needed. Such a situation is seldom met in photoionization and DR cross section because the number of accessible resonances is limited by dipole selection rules.

A comparison of relativistic DW and  $R$ -matrix calculations for  $Fe^{21+}$  was carried out by Gu (2004). In order to test for the importance of channel coupling and breakdown of the isolated resonance approximation, the two calculations were compared using the same energy level structure, and good agreement was found for most transitions, both for resonance structure and for the background cross section. This is in contrast to the results of Badnell and Pindzola (1993), who demonstrated factor of  $\sim 2$  errors in the dominant resonant contributions to the excitation of Mg-like ions. Thus uncertain-

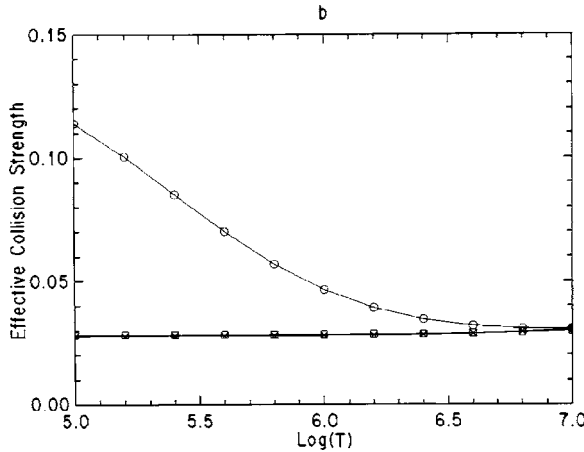


FIG. 10. The effective collision strength for the  $3s^2 \text{ } 1S_0 \rightarrow 3s3p \text{ } ^3P_1^o$  transition in  $\text{Fe}^{14+}$  as a function of temperature for close-coupling (circles) and DW calculations (squares). From Eissner *et al.*, 1999.

ties introduced by the DW and isolated resonance approximation can be significant. *R*-matrix calculation of excitation of many x-ray transitions have been carried out by the Iron Project (Hummer *et al.*, 1993). This work is continuing and the results are contained in the TIPTOPbase database (Cunto and Mendoza, 1992). A sample of publications include those for  $\text{Fe}^{20+}$  (Butler and Zeippen, 2000),  $\text{Fe}^{19+}$  (Butler and Zeippen, 2001a),  $\text{Fe}^{18+}$  (Butler and Zeippen, 2001b),  $\text{Fe}^{11+}$  (Binello *et al.*, 1998a, 1998b), the oxygen isosequence (Butler and Zeippen, 1994),  $\text{Ca}^{7+}$  (Landi *et al.*, 2004),  $\text{Fe}^{15+}$  (Eissner *et al.*, 1999), the Cl isosequence (Pelan and Berrington, 1995),  $\text{Fe}^{13+}$  fine structure (Storey *et al.*, 1996), the B isosequence (Zhang *et al.*, 1994) and for  $\text{Fe}^{2+}$  (Zhang, 1996). *R*-matrix calculations have been done for the fine-structure levels of  $\text{Fe}^{12+}$  and for  $\text{Fe}^{10+}$  (Gupta and Tayal, 1998, 1999). Most of these do not include levels in the  $n=4$  manifold, but do account for relativistic effects using the Breit-Pauli Hamiltonian and intermediate coupling. Exceptions include the *R*-matrix calculations for He-like O by Delahaye and Pradhan (2002) and He-like Ne by Bautista *et al.* (2003). The mission of the Iron Project has been extended into the x-ray region by the UK RmaX Network ([http://amdpp.phys.strath.ac.uk/UK\\_RmaX](http://amdpp.phys.strath.ac.uk/UK_RmaX)).

Close-coupling calculations which include  $n=4$  and intermediate coupling have been carried out for  $\text{Fe}^{20+}$  by Badnell and Griffin (2001) and for  $\text{Fe}^{21+}$  by Badnell *et al.* (2001), and show general consistency with the Iron Project results. The difference between collision strengths calculated using the close-coupling approximation from those calculated using DW is illustrated in Fig. 10, taken from Eissner *et al.* (1999). This shows the effective collision strength for the  $3s^2 \text{ } 1S_0 \rightarrow 3s3p \text{ } ^3P_1^o$  transition in  $\text{Fe}^{14+}$  as a function of temperature for close-coupling (circles) and DW calculations (squares). The difference at low temperatures is due to the cumulative effect of resonances, which are not accounted for by DW method. At the temperature corresponding to the

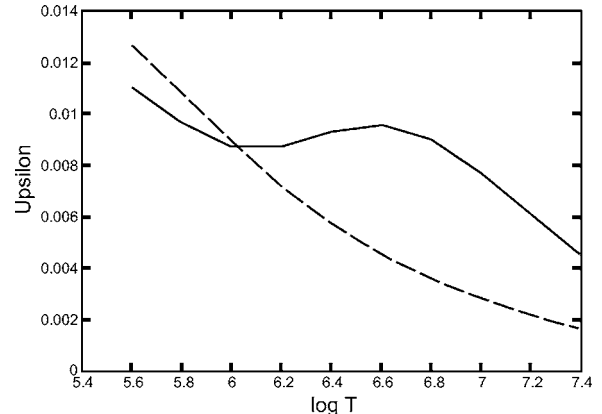


FIG. 11. Comparison of the collision strength for the  $2s^2 2p^2 ({}^3P_0^e) \rightarrow 2s^2 2p^2 ({}^1D_2^e)$  transition in  $\text{Fe}^{20+}$  calculated using BPRM (solid curve; Butler and Zeippen, 2000) with calculated using MCDF by Aggarwal (1991) (dashed curve) as a function of temperature. From Butler and Zeippen, 2000.

peak abundance of this ion in coronal equilibrium,  $\log(T) \approx 6.4$ , the two methods give very nearly the same result. The role of CI in collisional calculations is illustrated in Fig. 11. This shows comparison of the effective collision strength for the  $2s^2 2p^2 ({}^3P_0^e) \rightarrow 2s^2 2p^2 ({}^1D_2^e)$  transition in  $\text{Fe}^{20+}$  as a function of temperature calculated using BPRM (Butler and Zeippen, 2000) with those of Aggarwal (1991) which used MCDF. The latter, although it includes a more complete treatment of relativistic interactions, omits the  $n=3$  configurations and so under-predicts the resonance structure at high temperature, where these resonances can be excited.

Measured line ratios and absolute rate coefficient are important for validating calculations. Absolute cross sections have been measured for electron impact excitation of a few ions, for example,  $\text{C}^{3+} \text{ } 2s({}^2S_{1/2}) \rightarrow 2p({}^2P_{1/2,3/2})$  for energies near threshold by Savin *et al.* (1995) [see also Janzen *et al.* (1999) for further work and references to other measurements], for  $\text{Fe}^{16+}$  by Brown, Beiersdorfer, and Widman (2001), and Beiersdorfer *et al.* (2002, 2004), and for  $\text{Fe}^{20+}$ – $\text{Fe}^{23+}$  by Chen *et al.* (2005). These serve as important tests for close-coupling calculations such as those of Chen and Pradhan (2002). An example is shown in Fig. 12, which shows a comparison of the collision strength for the  $3s^2 ({}^1P_0) \rightarrow 3s3p ({}^3D)$  transition in  $\text{Ar}^{6+}$  calculated using an *R*-matrix calculation (Griffin *et al.*, 1993); an isolated-resonance DW calculations and experimental merged beam measurements (Smith *et al.*, 2003). These illustrate the importance of resonances, which are more prominent in the spin-forbidden transition shown here, and the difficulty in accurately calculating resonance strength. An added uncertainty in experimental measurements comes from the fact that experiments such as those shown in Fig. 12 must detect scattered electrons in order to discriminate between various excitation channels, and the angular scattering distribution must be understood in order to correct for electrons which miss the detectors. Similar comparisons have been performed by Djurić *et al.* (2002).

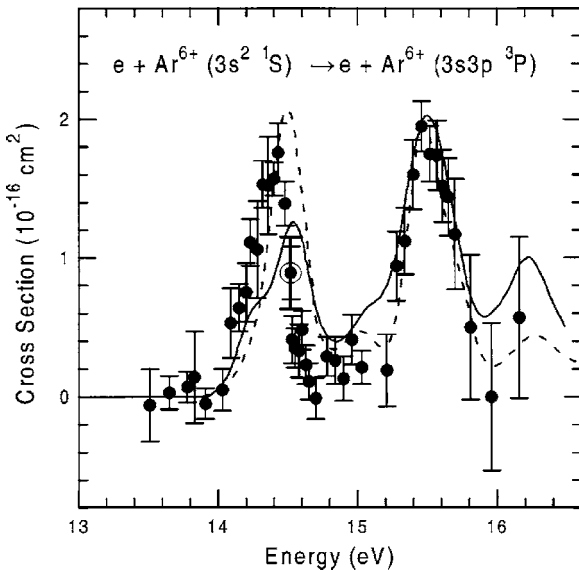


FIG. 12. Comparison of the collision strength for the  $3s^2 1P_0 \rightarrow 3s3p ^3D$  transition in  $\text{Ar}^{6+}$  calculated using an  $R$ -matrix calculation (solid curve) (Griffin *et al.*, 1993), an isolated-resonance DW calculation (dashed curve), and experimental merged beam measurements (Smith *et al.*, 2003). From Smith *et al.*, 2003.

Bibliographies of the available data for collisional excitation were published by Itikawa *et al.* (1984) and Itikawa (1991, 1996, 2002), all designed primarily for fusion applications, and by Pradhan and Gallagher (1992). Reviews organized by isosequence include the aforementioned conference proceedings from 1994 [see, e.g., Berrington (1994), etc.]. Much recent work relevant to x-ray astronomy is contained in the CHIANTI database. These include papers by Dere *et al.* (1997, 2001), Landi *et al.* (1999, 2004, 2005), Young *et al.* (2003), and Landi and Phillips (2005) and papers describing the Arcetri spectral code (Landi and Landini, 1998, 2002).

#### 4. Radiative transition probabilities

##### a. Background

Traditional modeling of coronal plasmas assumed that radiative decay to the ground level is more rapid than excitation or decay to excited levels. As a consequence, all dipole-allowed line emission and cooling could be calculated without explicit reference to the rate coefficients for radiative decay. Recent plasma models, such as APEC (Smith *et al.*, 2001), calculate all level populations explicitly, and therefore require transition probabilities for transitions in all decay paths of excited levels.

Radiative transition probabilities are conveniently parametrized in terms of the oscillator strength, which has a value of unity by definition for a classical point charge. Nonrelativistic quantum-mechanical oscillator strengths for hydrogen have been tabulated by Menzel and Pekeris (1935). It is also customary to define the oscillator strength for hydrogen in terms of the semiclassical Kramers expression:

$$f_K(n, n') = \frac{32}{3\pi\sqrt{3}} \left( \frac{1}{n'^2} - \frac{1}{n^2} \right)^{-3} \left( \frac{1}{n^3 n'^5} \right) g_I(n', n) \quad (30)$$

along with a Gaunt factor  $g_I(n', n)$ . These have been tabulated by Baker and Menzel (1938).

Classic tabulations of these include the H-like oscillator strengths of Wiese *et al.* (1966), along with the compilations of NIST (Fuhr *et al.*, 1999). For hydrogenlike ions without relativity an exact calculation is possible (Bethe and Salpeter, 1972). Treatment of non-dipole-allowed processes such as two-photon decay (Shapiro and Breit, 1959) and magnetic dipole rate coefficients (Parpia and Johnson, 1972) requires treatment of the effects of QED and nuclear size.

Examples of DW calculations include transition probabilities for lines from Al-like ions (Nussbaumer, 1977), transition probabilities within the  $2s^2-2s2p-2p^2$  manifold in the Be isosequence (Muehlethaler and Nussbaumer, 1976), radiative data for the Mg isosequence (Christensen *et al.*, 1986), transition probabilities for the ground configuration of  $S^{3+}$  (Johnson *et al.*, 1986), transition probabilities for transitions within the ground configuration of  $S^{2+}$  and other Si-like ions (Huang, 1985), and oscillator strengths for He-like allowed lines and collision strengths among fine-structure levels (Zhang and Sampson, 1987). It is worth noting that, although ground-state fine-structure transitions often fall outside of what is typically considered the x-ray band, the structure and transition probabilities are relevant to the x-ray spectrum from these ions seen in absorption, and they may also be useful for study of higher energy transitions which belong to the same isoelectronic sequence. Martin *et al.* (1993) calculated transition probabilities in the lithium sequence. DW calculations of oscillator strengths have been carried out for  $2s-2p$  transitions Be, B, C, N, and O (Fawcett *et al.*, 1978), and for  $\Delta n=0,1$  transitions in the O, S, P (Fawcett, 1986a, 1986b, 1986c), and C (Fawcett, 1987) isosequences.

Cowan *et al.* (1984) presented theoretical calculations of wavelengths and oscillator strengths for  $\text{Fe}^{9+}$ . They pointed out the importance of spin-orbit and configuration-mixing effects in the calculation of wavelengths and oscillator strengths for heavy-element moderately charged ions. This technique involves calculation of the energy-level structure and line spectrum for a variety of ions by collecting available experimental data from laboratory and solar measurements, adjusting in order to obtain smooth variation along isoelectronic sequence, and then using these levels to calculate the structure of model ions using a semiempirical code (Cowan, 1981). This was done for  $\text{Fe}^{11+}$  and  $\text{Fe}^{12+}$ ,  $3p-3d$  and  $3s-3p$  transitions (Bromage, Fawcett, and Cowan, 1978), Be-like and B-like iron (Bromage, Fawcett, Ridgeley, *et al.*, 1978), the  $2p^2-2p3d$  transition array of  $\text{Fe}^{20+}$  and isoelectronic spectra (Bromage and Fawcett, 1977a), the  $2s^22p^n-2s^22p^{n-1}4d$   $\text{Fe}^{17+}$  and  $\text{Fe}^{18+}$  lines (Bromage, Fawcett, and Cowan, 1977), much of which was updated by Cornille *et al.* (1992), the  $2p^3-2p^23d$  transition array in  $\text{Fe}^{19+}$  and isoelectronic ions (Bromage and

Fawcett, 1977b), and the  $3s^23p^n$ - $3s^23p^{n-1}3d$  transitions in  $\text{Fe}^{9+}$  and  $\text{Fe}^{10+}$  (Bromage, Cowan, and Fawcett, 1977). A compilation of collisional excitation and radiative decay rate coefficients for lines of  $2s^22p^k$ ,  $2s2p^{k+1}$ , and  $2p^{k+2}$  configurations and for the O, N, C, B, and Be isoelectronic sequences of Ti, Cr, Fe, Ni was produced by Feldman *et al.* (1982). A compilation of transition probabilities for Cr, Fe, Ni ions in the B, C, N, O, and F isosequences was produced by Feldman *et al.* (1980).

### b. Recent developments

Close-coupling transition probabilities for many dipole-allowed transitions of interest have been calculated by the Opacity Project (Seaton, 1987) and are contained in the TOPbase database (Cunto and Mendoza, 1992). These use LS coupling and are tabulated with theoretical wavelengths, and therefore are not directly applicable to synthesis of spectra and do not include forbidden transitions. Their application to observations has been aided by the work of Fuhr *et al.* (1999) who have matched these with experimental wavelengths where possible and redistributed the oscillator strength among fine-structure levels. Other CI calculations of transition probabilities include oscillator strengths of F-like ions for  $18 < Z < 33$  using CIV3 (Blackford and Hibbert, 1994). Iron Project calculations include intermediate coupling and relativistic effects in the Breit-Pauli approximation. These include extensive work on forbidden transitions within the ground configuration of complex ions, whose wavelengths generally place them outside the scope of this review (Galavis *et al.*, 1997). An annotated bibliography of transition probabilities for allowed and forbidden transitions with some overlap to the x-ray and EUV band is presented by Biemont and Zeippen (1996). Quinet (2000) calculated the wavelengths and oscillator strengths using HFR for the  $3p4s$ ,  $3p4d$ ,  $3p5s$ , and  $3p5d$  transitions in  $\text{Fe}^{8+}$ - $\text{Fe}^{13+}$  appearing in the soft x-ray region. Close-coupling calculations of transition probabilities for fine-structure transitions in  $\text{S}^{3+}$  have been calculated by Tayal (1999). Storey and Zeippen (2000) presented transition probabilities for transitions within the ground configuration of the carbon and oxygen isoelectronic sequences. Opacity Project line strengths have been incorporated into the line list for use in absorption line studies by Verner, Verner, and Ferland (1996). These used a compilation of experimental energy levels similar to that used by NIST and Opacity Project wavelengths derived using LS coupling rules for lines originating from ground-term multiplets in the spectral region 1–200 Å. Experimental measurements of radiative lifetimes for excited levels of many ions have been reviewed by Träbert (2002).

## B. Photoionized plasmas

In gases exposed to strong ionizing radiation, or in the absence of strong mechanical or nonradiative heating, the ionization balance can be determined by the effects of photoionization and recombination. In this case the

gas temperature is determined by a balance between heating and cooling due to photon interactions. Heating processes include slowing down of fast photoelectrons, and Compton scattering, while cooling is due to emission processes analogous to those in a coronal plasma. Early discussion of this was given by Tarter and Salpeter (1969) and Tarter *et al.* (1969). Traditional application for photoionization models was HII regions and planetary nebulae (Flower, 1968, 1983), but it is now apparent that photoionization is dominant in many x-ray sources as well, such as active galaxies (see, e.g., Figs. 1 and 4).

The condition for photoionization to dominate over collisions depends on the rate of mechanical heating, if any, and on the ratio of the ionizing flux to the gas density  $n$ , which is called the photoionization parameter. Various definitions are in use, those most widely quoted are  $U=N/nc$ , where  $N$  is the number flux of ionizing photons (i.e., photons with energies greater than 1 Ry), and  $\xi=4\pi F/n$ , where  $F$  is the energy flux of ionizing photons, typically in the 1–1000 Ry energy range.

The choice of convention for ionization parameter definition is arbitrary. Any accurate calculation of photoionization rate coefficients or heating must take into account the shape of the ionizing spectrum in detail; the ionization parameter serves as a constant of proportionality for use in describing model results. Certain choices of the ionization parameter are more directly related to the problem to be solved, which explains in part the origins of the differing conventions. Photoionization rate integrals can be written

$$\text{rate} = \int_{\varepsilon_{\text{th}}}^{\infty} F_{\varepsilon} \sigma(\varepsilon) \frac{d\varepsilon}{\varepsilon}, \quad (31)$$

where  $\varepsilon_{\text{th}}$  is the ionization threshold energy for the bound level in question,  $F_{\varepsilon}$  is the ionizing flux in units  $\text{erg cm}^{-2} \text{s}^{-1} \text{erg}^{-1}$ , and the photoionization cross section is  $\sigma(\varepsilon)$ . This quantity scales with energy above threshold as  $\sigma(\varepsilon) \propto \varepsilon^{-\gamma}$  where  $\gamma \sim 3$ . So the photoionization rate and heating integrals are always dominated by the behavior at threshold if  $d \log(F_{\varepsilon})/d \log(\varepsilon) \leq \gamma$ . In classical photoionized nebulae, such as HII regions or planetary nebulae, the behavior of the model depends most sensitively on the ionizing photon flux at 1 Ry. The total number of ionizing photons  $N$  is also weighted toward the flux at 1 Ry unless  $F_{\varepsilon}$  increases faster than  $\propto \varepsilon^1$ . However, photons at 1 Ry have less influence on the ionization of ions typically observed in the x-ray band than do photons at energies greater than  $\sim 0.25$  keV. Study of x-ray photoionized plasmas differs from classical photoionized nebulae in that it is often possible to directly observe the photons responsible for the ionization of gas responsible for line emission or absorption, which is motivation for an ionization parameter which is more closely coupled to the continuum in the x-ray band than is  $N$ . This has led to the suggestion by Netzer (1996) of the use of the parameter  $U_X=N_X/nc$ , where  $N_X$  is the number flux of ionizing photons above 0.1 keV. The choice of  $\xi$  is motivated by the fact that it is more heavily weighted toward the x-ray band by using ioniz-

ing energy flux rather than number flux. Also heating by Compton scattering is proportional to the photon energy flux.  $\xi$  has units implied (typically erg s cm<sup>-1</sup>), while  $U$  is dimensionless. The study of photoionized gases in which the pressure is prescribed rather than the density has led to the further definition of an ionization parameter  $\Xi = F/cP$ , where  $P$  is the gas pressure (Krolik *et al.*, 1981). This quantity is dimensionless. It is important to note that no matter what definition of ionization parameter is adopted, it serves only as a convenient scaling quantity. Real calculations take into account the full frequency dependence of the radiation spectrum, and so do not depend ultimately on the convention which is used.

Since the ionizing radiation spectrum may not, in general, be a pure thermal spectrum, photoionization is not conveniently parametrized by a rate coefficient depending on temperature. Rather, it is customary to consider the full energy-dependent cross section, and perform the calculation of the ionization rate by integrating this over the photon flux distribution. Photoionization cross sections are also important for calculations of the inverse process, RR, via the Milne relation (Osterbrock and Ferland, 2006). In the case of RR, cross sections to excited levels are important. In many cases of astrophysical interest the equilibrium populations of excited levels are negligible, so that for the purpose of calculating the ionization rates it is only necessary to consider photoionization from the ground level or term. For this reason many traditional calculations were applied only to the ground term. Recent calculations have addressed rate coefficients for excited levels, which are increasingly being self-consistently included in level population calculations for most ions. An added feature of photoionization is that, owing to the nonthermal nature of the radiation field, ionization from inner electronic shells can be important for ions with three or more electrons. In contrast, EII generally results in a smaller contribution from inner-shell ionization. A thermal electron energy distribution has too few electrons at the high energies needed for inner-shell ionization (at least five to ten times the valence threshold), although excitation autoionization is important for many isoelectronic sequences.

## 1. Photoionization

### a. Background

Analytic expressions for the photoionization cross section of hydrogen can be obtained in the same way as for bound-bound transition oscillator strengths if the upper level is allowed to have an imaginary principle quantum number  $ik$ . The oscillator strength can then be written

$$f_{nk} = \frac{32}{3\pi\sqrt{3}} \left( \frac{1}{n^2} + \frac{1}{k^2} \right)^{-3} \left( \frac{1}{k^3 n^5} \right) g_{II}(n, k), \quad (32)$$

where  $g_{II}(n, k)$  is the bound-free Gaunt factor (Menzel and Pekeris, 1935; Karzas and Latter, 1961). The cross section involves the density of states, and if this is calcu-

lated in the limit of large  $n$  then a reasonably accurate approximation is

$$\sigma(E) = (2.815 \times 10^{29}) \frac{g_{II}(n, k)}{n^5 \nu^3}. \quad (33)$$

This is a hydrogenic approximation and is independent of angular momentum. The Gaunt factor can take angular momentum into account; the asymptotic dependence of the cross section on energy is  $\propto \epsilon^{-l-7/2}$  (Fano and Cooper, 1968). The exact analytic nonrelativistic cross section for  $l=0,1$  has been given by Bethe and Salpeter (1972).

A widely used simple parametrization of photoionization cross sections is that of Seaton (1958). This has been fitted to monoconfigurational Hartree-Fock results for the moderately ionized ions important to planetary nebulae by Henry and Williams (1968), Henry (1970), and Chapman and Henry (1971, 1972). Photoionization cross sections for He-like ions were calculated by Brown (1971). Photoionization cross sections using Hartree-Slater wave functions were calculated by Barfield (1979), who derived a simple scaling behavior along isonuclear sequences which could be used to relate ionic cross sections to those for neutrals. Reilman and Manson (1978, 1979) performed the first large-scale calculations of photoionization cross sections using Hartree-Slater wave functions, resulting in tabulations of cross sections for all ions of the elements with  $Z$  up to 30, including inner shells. Cross sections for excited levels of many ions based on a hydrogenic approximation were calculated by Clark *et al.* (1986).

The behavior of photoionization cross sections near the thresholds in multielectron ions is affected by resonance structure due to quasibound states. Accurate models for these require calculations using the close-coupling approximation. Near inner-shell edges these take the form of photoexcited core (PEC) resonances below the threshold, and the net effect is to fill in the cross section below threshold and smooth the inner-shell edge.

### b. Recent developments

A large scale compilation of close coupling calculations is included in the Opacity Project (Seaton, 1987), with results contained in the TOPbase, which is in turn part of TIPTOPbase (Cunto and Mendoza, 1992), <http://cdsweb.u-strasbg.fr/topbase/home.html>. Also included as part of TIPTOPbase is the Iron Project database and the OP server, which can calculate Rosseland mean opacities (Mihalas, 1978) for various elemental mixtures using the Opacity Project cross sections. These are LS coupling calculations including channel couplings, carried out for ground and excited states for all ions of elements with  $Z$  up to 30. A widely used compilation was presented by Verner and Yakovlev (1995), who calculated central field cross sections including inner shells based on the Dirac-Slater potential, for most astrophysically important ions. These were scaled to fit the behavior of the  $R$ -matrix calculations near threshold, while

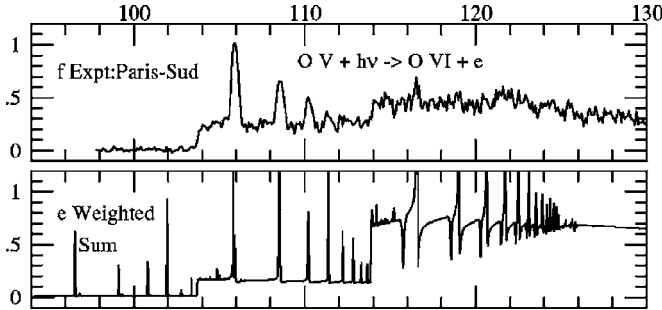


FIG. 13. Comparison of BPRM calculation of the photoionization of  $O^{4+}$  with experiment (Champeaux *et al.*, 2003) in the energy range 90–130 eV. Below 103 eV the cross section is due to ionization from the  $2s2p$  excited configuration, and  $2s^2$  above. From Nahar, 2004.

also having the correct behavior in the high-energy asymptotic limit. These are convenient to use, and provide an approximation to the resonance structure near threshold, and therefore can be used to calculate integral quantities such as photoionization rates. However, they do not contain the detailed resonance structure near threshold, and so should not be applied to calculations of monochromatic opacity or synthetic spectra. Opacity Project opacities have been recently revised to include inner-shell contributions, using the AUTOSTRUCTURE package, and these are available through the Opacity Project on line database TIPTOPbase (Badnell *et al.*, 2005). Figure 13 shows a comparison of BPRM calculations for  $O^{4+}$  with experiment (Champeaux *et al.*, 2003) in the vicinity of the threshold for ground-state ionization, showing the extensive resonance structure and general consistency between the measured and calculated cross sections.

Even when the total ionization rate is so low that the gas is neutral, or if photoionization is not the dominant ionization mechanism, the spectrum of the radiation field transmitted in the x-ray band is affected by the photoionization cross section. Thus knowledge of the cross section is needed to interpret observations of x-ray absorption. In this case, spectroscopic accuracy can be important, since features in the cross section can be used to diagnose the conditions in the absorbing gas (Paerels *et al.*, 2001). Examples of such features include the line features due to  $K$ -shell photoexcitation in oxygen and its ions, which is abundant in the interstellar medium. The importance of this process has been emphasized by Pradhan (2000) and Pradhan *et al.* (2003). An early detection of interstellar oxygen  $K$  absorption was done by Schattenburg and Canizares (1986).

The calculation of photoionization from inner shells is affected by the resonance structure associated with excitation of states with one  $np$  excited electron and a  $K$ -shell vacancy. They decay predominantly by spectator Auger transitions, in which the  $np$  electron does not participate, and have widths nearly independent of principle quantum number  $n$ . This leads to a series of resonances with constant width close to the threshold for photoionization, thereby smearing and lowering the lo-

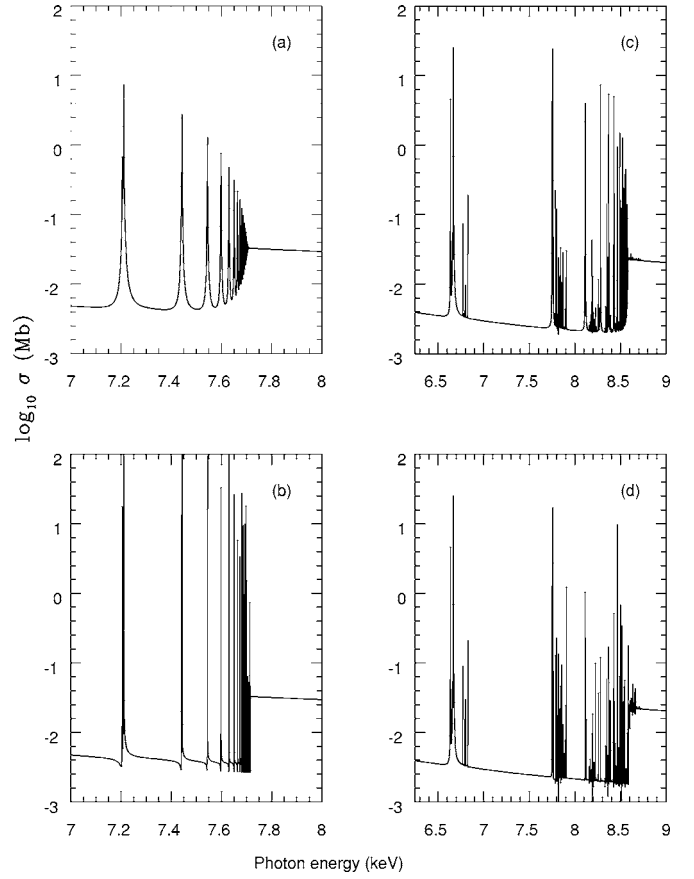


FIG. 14. High-energy total photoabsorption cross sections of the ground level of (a)  $Fe^{16+}$  including radiative and Auger damping effects; (b)  $Fe^{16+}$  excluding damping effects for resonances with  $n > 2$ ; (c)  $Fe^{22+}$  including damping; and (d)  $Fe^{22+}$  excluding damping for resonances with  $n > 2$ . This demonstrates that when damping is included the resonance widths are constant for high  $n$  leading to a smearing of the  $K$  edge. From Bautista *et al.*, 2004.

cation of the edge. This effect, called Auger damping, has also been observed in the laboratory (Farhat *et al.*, 1997). It was emphasized and pointed out earlier in calculations of inner-shell ionization by Gorczyca and McLaughlin (2000) for oxygen [cf. Gorczyca and Robicheaux (1999)] and Ne (Gorczyca, 2000). Computation of these effects using an  $R$ -matrix technique relies on the use of an optical potential to mimic the decays to spectator channels not explicitly included in the close-coupling expansion. BPRM photoionization cross sections including Auger damping have been carried out for inner shells of all ions of iron (Palmeri *et al.*, 2002; Bautista *et al.*, 2003, 2004; Palmeri, Mendoza, Kallman, and Bautista, 2003; Palmeri, Mendoza, Kallman, Bautista, *et al.*, 2003; Kallman *et al.*, 2004; Mendoza *et al.*, 2004) and for oxygen (Garcia *et al.*, 2005). An example of these effects is shown in Fig. 14, which shows the photoionization cross sections of  $Fe^{16+}$  and  $Fe^{22+}$  near the threshold for the  $K$  shell, taken from Bautista *et al.* (2004). The left panels show the resonance structure with the effects of damping by resonances with  $n > 2$  included, while the right panels show the resonance

structure with damping by resonances with  $n > 2$  excluded.

The vacancies created by inner shell photoionization are filled by fluorescence or Auger decays. The rates for these processes have been calculated by Jacobs and Rozsnyai (1986) using configuration-average energy levels and by Kaastra and Mewe (1993) based on isoelectronic scaling from the calculations of McGuire (1969, 1970, 1971a, 1971b, 1972). The validity of these approximations has been discussed by Gorczyca *et al.* (2003, 2006). Level-resolved intermediate coupling calculations of  $K$  Auger and fluorescence rates have been calculated for iron by Palmeri *et al.* (2002), Bautista *et al.* (2003, 2004), Palmeri, Mendoza, Kallman, and Bautista (2003), Palmeri, Mendoza, Kallman, Bautista, *et al.* (2003), and Mendoza *et al.* (2004).

## 2. Radiative recombination

Radiative recombination (RR) is more important as a line emission mechanism in photoionized plasmas than in coronal plasmas and therefore receives more discussion in this context. Rate coefficients can be calculated using detailed balance arguments via the Milne relation (Osterbrock and Ferland, 2006). The rate coefficient can be expressed in the form defined by Seaton (1959) for hydrogenic ions:

$$\alpha_n(Z, T) = \frac{1}{c^2} \left( \frac{2}{\pi} \right)^{1/2} (mkT)^{-3/2} 2n^2 e^{I_n/kT} \times \int_{I_n}^{\infty} (h\nu)^2 e^{-h\nu/kT} \sigma_n(Z, h\nu) d(h\nu), \quad (34)$$

where  $I_n$  is the ionization potential and the photoionization cross section can be written

$$\sigma_n(Z, h\nu) = \frac{2^6 \alpha \pi a_0^2}{3\sqrt{3}} \frac{n}{Z^2} (1 + n^2 \epsilon)^{-3} g_{II}(n, \epsilon), \quad (35)$$

where  $\alpha$  is the fine-structure constant,  $a_0$  is the Bohr radius, and energy conservation requires that  $h\nu = hRcZ^2(1/n^2 + \epsilon)$ . The Kramers-Gaunt factor can be expanded as a polynomial in  $u = n^2 \epsilon$ , and the rate coefficient can be expressed as

$$\alpha_n(Z, T) = DZ \frac{\lambda^{1/2}}{n} x_n S_n(\lambda), \quad (36)$$

where  $D = (2^6/3)(\pi/3)^{1/2} \alpha^4 c a_0^2 = 5.197 \times 10^{14} \text{ cm}^3 \text{ s}^{-1}$ ,  $\lambda = hRcZ^2/kT = 157890 Z^2/T$ ,  $x_n = \lambda/n^2$ ,

$$S_n(\lambda) = \int_0^{\infty} \frac{g_{II}(n, \epsilon) e^{-x_n u}}{1 + u} du, \quad (37)$$

and  $u = n^2 \epsilon$ . Seaton (1959) used the asymptotic expansion for  $g_{II}(n, \epsilon)$  to evaluate  $S_n(\lambda)$ . Numerical tables for  $S_n(\lambda)$ , for the total recombination rate coefficients for  $\alpha_S(Z, T) = \sum_{n=1}^{\infty} \alpha_n(Z, T)$ , and for the spectrum of recombining electrons have been published by Seaton (1959). When  $RZ^2/n^2 \gg kT$  then  $\alpha_n(1, T) \propto n^{-1} T^{-1/2}$  and when  $RZ^2/n^2 \ll kT$  then, for  $Z=1$ ,

$$\alpha_n(1, T) \propto n^{-3} T^{-3/2} \left[ \log \left( \frac{n^2 T}{157890} \right) - 0.5772 + 8.56 \times 10^{-3} T^{1/3} - 2.3 \times 10^{-5} T^{2/3} \right]. \quad (38)$$

The first term in the brackets becomes less important at high temperatures, corresponding to the fact that excited levels contribute more at low temperatures than at high temperatures.

Such calculations are typically tabulated as total recombination rates, in which all the possible radiative transitions from the lowest continuum state (i.e., the ground state of the next highest ion stage) to the bound states of a given ion are summed. This requires a sum over all rate coefficients into excited levels of an ion, and implicitly assumes that all recombinations to excited levels decay to the ground level. Such sums traditionally use ground-state photoionization cross sections appropriate to the ion, together with hydrogenic photoionization cross sections for the excited levels. Tarter (1971) calculated RR rate coefficients for many ions of astrophysical interest, as did Gould (1978). A widely used compilation has been given by Aldrovandi and Pequignot (1973, 1976) who calculated RR and DR rate coefficients for many ions of astrophysical interest, calculated using the Burgess (1965) general formula for DR and the Milne relation. Pequignot *et al.* (1991) calculated total and effective RR coefficients for all ions with  $Z \leq 10$  for important optical and UV transitions of these ions. Woods *et al.* (1981) calculated RR rate coefficients for iron, using the cross sections of Reilman and Manson (1979). Pradhan (1983) calculated the RR for the ground states of Li-like ions. Verner and Ferland (1996) calculated rate coefficients for RR based on Opacity Project photoionization cross sections. Gu (2003c) has provided total RR rate coefficients for the H-like through Ne-like isoelectronic sequences for the seven elements Mg, Si, S, Ar, Ca, Fe, and Ni, and Gu (2003d) has provided x-ray line emission rate coefficients for  $\text{Fe}^{17+}$ – $\text{Fe}^{23+}$  due to both RR cascades and DR. The need for tabulations of total rate coefficients or of effective rate coefficients is reduced by advances in computer speed, which allow plasma modeling codes to calculate or make use of state-specific recombination rates.

## 3. Dielectronic recombination

Dielectronic recombination (DR) in photoionized plasmas is generally less important than in coronal plasmas, but it is not negligible. As shown in Fig. 9, contributions of radiative and DR are comparable for  $\text{Fe}^{18+}$  DR at temperatures characteristic of photoionized plasmas. For  $\text{Fe}^{19+}$ – $\text{Fe}^{22+}$  DR dominates RR by a factor of 2 or more (Savin *et al.*, 2002a, 2002b, 2003). Theoretical rate coefficients are less certain at low temperatures, owing to the fact that the electron velocity distribution samples low-energy states. Theory cannot calculate the resonance energies for the relevant DR resonances at low energy with sufficient precision. Kraemer *et al.* (2004) and Netzer (2004) provided examples of the sen-

sitivity of astrophysical results to DR rates in photoionized plasmas, and also pointed out the consequences of errors in the rate coefficients which are in widespread use for astrophysical modeling.

The importance of low-temperature DR was pointed out by [Storey \(1981\)](#), who showed that the  $C^{2+}2p^2\ ^3D \rightarrow 2s2p\ ^1P_0\lambda 2296$  line observed from planetary nebulae is likely excited by DR. This was extended to ions of C, N, and O by [Nussbaumer and Storey \(1983\)](#), who calculated rates for these ions using LS coupling. The associated satellite spectra were calculated by [Nussbaumer and Storey \(1984\)](#). These were extended to Mg, Al, Si by [Nussbaumer and Storey \(1986\)](#) and to Ne by [Nussbaumer and Storey \(1987\)](#). Calculations of low-temperature DR are most affected by uncertainties in the low-energy resonance structure, and this in turn is affected by the assumption of LS coupling in many calculations. LS coupling can be applied when the fine-structure splitting is small compared to the term separation which is caused by the Coulomb interaction.

Recent experimental measurements using storage rings ([Savin, 2000](#); [Savin et al., 2002b](#)) and calculations using AUTOSTRUCTURE ([Colgan et al., 2003, 2004, 2005](#); [Zatsarinny et al., 2003, 2004a, 2004b, 2005a, 2005b, 2006](#); [Altun et al., 2004, 2005, 2006](#); [Mitnik and Badnell, 2004](#); [Badnell, 2006](#)) of DR include intermediate coupling structure calculations, and so are likely to be more accurate for low-temperature DR than previous calculations. Nonetheless, as pointed out by [Gu \(2003b\)](#) and by [Schipper et al. \(2004\)](#), DR at low temperatures continues to be a major source of uncertainty in calculations of ionization balance under photoionization conditions.

#### 4. Charge transfer

##### a. Background

Charge transfer is of potential importance in photoionized plasmas owing to the fact that the charge-transfer rate coefficient for an ion with neutral H or He can exceed that for electron recombination by a factor  $\geq 10^4$  ([Kingdon and Ferland, 1996](#)). Photoionized plasmas can have a hydrogen neutral fraction as great as  $\sim 0.1$  coexisting with several times ionized metals, depending on the shape of the ionizing spectrum. Another application for charge-transfer rate coefficients was pointed out by [Savin et al. \(2004\)](#), who calculated the rate coefficients for  $H^++H_2 \rightarrow H+H_2^+$  using recently published theoretical cross sections, and showed that uncertainties in these rate coefficients can affect the cooling and formation of primordial structures such as stars and galaxies.

The importance of charge transfer in the interstellar medium was pointed out by [Field and Steigman \(1971\)](#) and [Steigman et al. \(1971\)](#) who also calculated rate coefficients for  $C^{2+}+He \rightarrow C^++He^+$  ([Steigman, 1975](#)) and discussed the influence of charge transfer on the O<sup>+</sup> and N<sup>+</sup> ionization balance. The potential importance of charge transfer and, for the first time, charge transfer involving ions more than singly ionized on the structure of planetary nebulae was pointed out by [Pequignot, Stasinska,](#)

and [Aldrovandi \(1978\)](#) and [Pequignot \(1980\)](#). This led to efforts to calculate cross sections and rates, including calculations of the charge transfer of N<sup>+</sup> with H, and of C<sup>+</sup> and S<sup>+</sup> with H and He using a distorted-wave calculation by [Butler and Dalgarno \(1979, 1980a\)](#). [Butler and Dalgarno \(1980b\)](#) calculated the charge transfer of a variety of multiply charged ions with H and He using a Landau-Zener calculation. [Watson and Christensen \(1979\)](#) calculated the charge transfer of C<sup>3+</sup>+H and N<sup>3+</sup>+H using a close-coupling approximation. A review and compilation by [Kingdon and Ferland \(1996\)](#) provides a collection of rate coefficients in a form useful for modeling.

##### b. Recent developments

The most accurate calculations at the low energies of interest to astrophysics ( $\leq 1$  eV/amu) are techniques similar to molecular calculations, using the molecular-orbital close-coupling (MOCC) technique ([Heil et al., 1985](#)). Recent MOCC calculations include O<sup>3+</sup>+H ([Wang et al., 2003](#)), Si<sup>4+</sup>+He ([Stancil et al., 1997](#)), N<sup>4+</sup>+H ([Zygelman et al., 1997](#)), S<sup>4+</sup>+H ([Stancil et al., 2001](#)), and S<sup>4+</sup>+He ([Wang et al., 2003](#)). These show large ( $\geq 10^2$ ) differences with Landau-Zener calculations in some cases. Recent measurements include Si<sup>3+</sup>, Si<sup>4+</sup>, Si<sup>5+</sup>+He ([Tawara et al., 2001](#)), Ne<sup>3+</sup>+H ([Rejoub et al., 2004](#)), Ne<sup>2+</sup>+H ([Mroczkowski et al., 2003](#)), C<sup>4+</sup>+H ([Bliet et al., 1997](#)), N<sup>2+</sup>+H ([Pieksma et al., 1997](#)), and C<sup>+</sup>+H ([Stancil et al., 1998a, 1998b](#)).

A review of the charge-transfer process has been given by [Janev and Winter \(1985\)](#). Recent reviews of charge-transfer data for photoionized plasmas are given by [Stancil \(2001\)](#) for theory and by [Havener \(2001\)](#) for experiment. Although quantum-mechanical MOCC calculations provide the most reliable results when no experimental data are available ([Stancil, 2001](#)), still large discrepancies between theory and experiment at collision energies of less than a few hundreds eV/amu point to the difficulty of theory at this energy range and the need for benchmark measurements ([Havener, 2001](#)).

#### C. Charge transfer in cometary and planetary atmospheres

The discovery of x-ray emission from comets by the ROSAT x-ray astronomy satellite ([Lisse et al., 1996](#)) led to the appreciation of the importance of charge transfer of solar wind nuclei with neutrals in comets and gaseous planets. This process has a distinct spectral signature associated with the cascade of the captured electron from the excited state where capture initially occurs. The most probable states are determined by the energetics of the collision and the level structure of the reactants.

[Haberli et al. \(1997\)](#) extended this idea to look at individual spectral lines produced from C, O, and Ne ions. The excited state of the ion following capture was assumed to have a principal quantum number  $n$  which is the nearest integer to the quantity  $q^{0.75}$ , where  $q$  is the charge on the ion, followed by a cascading decay of  $\Delta n$

$\lambda=1$ . This assumption leads to x-ray spectra which fits to the observed x-ray spectra in a subset of the cases. A recent review of the physics of cometary x-ray emission was presented by Cravens (2002). EBIT simulations of cometary charge exchange were performed by Beiersdorfer *et al.* (2003). Additional models for the cascade, level populations, and x-ray line emission associated with cometary charge transfer have been calculated by Kharchenko and Dalgarno (2000).

Measurements for various species have been carried out using beam techniques. Total cross sections for C, N, and O have been tabulated by Phaneuf *et al.* (1987), Haavener *et al.* (1989), and Huq *et al.* (1989). For interpreting x-ray spectra, and for testing theoretical calculations, state-selective measurements are needed. This need along with the relatively low collision energy make the x-ray astronomy data need distinct from those for fusion plasmas. Techniques for measuring state-selected charge transfer include energy-loss spectroscopy and photon emission spectroscopy. Energy-loss spectroscopy provides greater counting rates, while photon emission spectroscopy allows higher energy resolution. Measurements have been made using energy-loss spectroscopy of  $O^{2+}$  in H,  $H_2$ , and He (McLaughlin *et al.*, 1990),  $C^{4+}$  ions in collisions with  $H_2$  and  $O_2$  (McLaughlin *et al.*, 1992),  $Fe^{3+}$  and  $Fe^{4+}$  ions with H and He atoms (McLaughlin *et al.*, 1993),  $S^{2+}$  with H and  $H_2$  (Wilson *et al.*, 1990b), and  $S^{3+}$  with H,  $H_2$ , and He (Wilson *et al.*, 1990a). Using similar techniques, Kimura *et al.* (1987) have studied highly stripped Ne, O, N, and C in collisions with H and  $H_2$ , and Kamber *et al.* (1996) have studied  $N^{3+}$  colliding with  $H_2$ , He, Ne, and Ar. Beam measurements have been made using photon emission spectroscopy to obtain state-selective cross sections of single-electron charge transfer of  $C^{4+}$  on H and  $H_2$  (Hoekstra *et al.*, 1990),  $O^{3+}$  on H and  $H_2$  (Beijers *et al.*, 1996),  $C^{4+}$ ,  $N^{5+}$ ,  $O^{6+}$  with H,  $H_2$ , and He (Dijkkamp *et al.*, 1985a),  $C^{6+}$ ,  $N^{6+}$ ,  $O^{6+}$ , and  $Ne^{6+}$  onto  $H_2$ , He, Ar (Dijkkamp *et al.*, 1985b). Similar techniques have been used to study  $C^{5+}$  and  $N^{6+}$  with He and  $H_2$  (Suraud *et al.*, 1991), and  $C^{5+}$  and  $N^{6+}$  with He and  $H_2$  (Ciric *et al.*, 1985). Double charge exchange can be an important loss process for highly charged ions incident on neutrals, but in many cases it leads to the production of autoionizing states, and therefore does not contribute to x-ray emission. Cross sections with molecular targets other than  $H_2$  have been measured for ions of C, N, O, and Ne colliding with He,  $H_2$ ,  $CO_2$ , and  $H_2O$  by Greenwood *et al.* (2001). Some of these experimental data have been collected at the ORNL/UGA charge-transfer database website, <http://cfadc.phy.ornl.gov/astro/ps/data/home.html>, including both total and state-specific cross sections and rates, along with fits to many of these.

Computational techniques for charge-exchange collisions include the classical trajectory Monte Carlo technique (Cornelius *et al.*, 2000), in which the motion of the projectile, target, and electron are calculated by integrating Hamilton's equations including only the Coulomb interactions. This technique is of limited use at

energies below 1 keV/amu, where the structure of the projectile ion is important. Another method is the semi-classical impact parameter close-coupling method, in which the wave function of electrons is calculated from a set of orbitals appropriate to the projectile ion. This technique is most suitable to systems with a small number of electrons (Saha, 1995; Kumar and Saha, 1998), and so has not been applied to the study of many ions. The Landau-Zener model has also been widely applied, and involves the use of avoided level crossings in order to determine the cross sections for various processes. It turns out that especially for energies below 200 eV/amu there are considerable differences between experiment and theory in both relative and state-selective cross sections.

## VIII. DISCUSSION

Basic needs and physical processes important to atomic data for x-ray astronomy have been known since the advent of solar x-ray astronomy. This has led to steady production of rate coefficients and cross sections for use in modeling and interpreting observed astrophysical x-ray spectra, and with considerable overlap with the needs for fusion plasmas. Prior to the launch of Chandra and XMM-Newton a great deal of work had been done toward the goal of developing an atomic database for coronal plasmas. Much of this was devoted to the study of discrete diagnostics, since the spatial and temporal structures of the x-ray emission limits the accuracy of global modeling for the Sun.

The launch of instruments capable of observing spectra from extrasolar objects with comparable resolution and good counting statistics has added motivation for data production and it has changed the emphasis somewhat from that of studies of solar x rays. Extrasolar objects often cannot be spatially resolved and the sensitivity to temporal variability is limited. Arguments based on other knowledge of their properties motivates attempts to construct global models based on a single set of physical conditions, such as the assumption of a single temperature or a cooling flow for the coronal emission from a cluster of galaxies. For some objects a simple distribution of conditions is assumed, such as a differential emission measure analysis performed for a cool star. In addition, the spectra of distant objects often do not have sufficient statistical accuracy to allow the application of detailed discrete diagnostics. This creates a greater need for global modeling, in which the ionization balance and spectrum can be calculated based on simple assumptions about the conditions, such as temperature and density. In addition, extrasolar data have broadened the range of physical processes of interest to include charge exchange, photoionized plasmas, inner-shell processes, and opacities associated with interstellar gas.

Significant advances in the calculation and measurement of atomic cross sections and rate coefficients needed for x-ray astronomy have occurred in parallel with the launch of the new observatories. Notable among these are the energetic application of experimen-

tal apparatus such as the EBIT and storage rings, and improvements in computer technology and campaigns to calculate large quantities of data such as the Iron Project and Opacity Project. At the same time, long-term efforts to compile reliable data from more traditional laboratory sources have continued to yield results, and the advent of free on-line databases, such as the NIST database, has aided in their use. Other important databases are those developed primarily for the fusion energy program at ORNL (<http://www-cfadc.phy.ornl.gov/>) and ALADDIN and AMBDIS at the IAEA (<http://www-amdis.iaea.org/>). As a result, there now exist accurate experimental datasets for line wavelengths and cross sections or rate coefficients for some key processes, along with computations using the most accurate known algorithms for many quantities. Laboratory measurements have been made for DR of many ions, and comparison with calculations allows benchmarking of computational techniques. Comprehensive calculations of state-specific DR, which have been benchmarked against the measurements, are available for many ions of interest. Measurements of EII exist for most ions of astrophysical interest, although verification is needed for many of these. Calculations, including close-coupling calculations with adequate treatment of intermediate coupling, relativistic effects, CI and radiation damping, have been made for radiative transition probabilities and electron impact collision strengths of many ions of interest. Measurements of absolute electron impact excitation cross sections have proven to be crucial in benchmarking these calculations. Beam measurements have yielded state-selective cross sections for charge exchange for many ions of interest to solar system x-ray studies.

In addition to the databases discussed above, a great deal of useful data have been collected and made publicly available as part of the databases associated with analysis packages such as CHIANTI (Landi and Bhatia, 2005a), APEC (Smith *et al.*, 2001), and MEKAL/SPEX (Kaastra, Mewe, and Nieuwenhuijzen, 1996). It is important to point out that the ultimate source of all databases and compilations is extensive computational and experimental work, and that the credit for this work is often neglected when the compilation or database is used. Astrophysicists and modelers should, whenever possible, attempt to cite original sources even when using the compilation or database as a guide or repository for atomic data.

As a result of accuracy demanded by the new instruments for x-ray astronomy some of the atomic calculations which were in widespread use for modeling astrophysical plasmas are no longer adequate for application to many observations. The approximations necessitated by early computers or analytic work provide valuable insight and constraints on the more recent work, and therefore have been crucial in the development of modern tools. However, there are few remaining processes or ions for which rate coefficients calculated using simple approximations are all that is available. These include the use of the Born approximation, or CBO, in

collisional ionization cross sections, the Bethe approximation for collisional excitation, *ab initio* wavelengths for strong lines in the x-ray band, the Burgess general formula for DR, hydrogenic or central field cross sections for photoionization or radiative recombination, and Landau-Zener rate coefficients for charge exchange. An added consequence of the capabilities of new computers is that it is no longer necessary to use total recombination rates when calculating ionization balance. Rather, collisional-radiative models [e.g., Summers *et al.* (2006)] can be quickly calculated which take into account state-specific recombination and ionization rates, and so are applicable to a wide range of gas densities and radiation environments.

Areas where there are still critical needs include the accumulation of energy-level structures and transition wavelengths which are of sufficient accuracy. These are needed for applications including line identification, where the observations have an accuracy of  $10^{-3}$  in many cases, and for calculations of DR at low temperature. Experiments have the most promise for useful work in this area, but new theoretical techniques are needed for this challenge as well. There are few experimental measurements of inner-shell photoabsorption for ions of interest to astronomy. Similarly, many lines in observed spectra such as that of NGC 3783 remain unidentified, and these may be associated with inner shell transitions not typically observed from coronal plasmas. X-ray processes involving molecules, including detailed spectra associated with charge transfer and inner-shell opacities, have not been studied for many species. Experimental work is needed to continue the campaign to measure all the DR and CI rate coefficients needed to benchmark the calculation of coronal ionization balance both in electron ionization and photoionization driven plasmas and in cometary and planetary atmospheres.

The most probable choices for future x-ray instrumentation will likely be only a partial continuation of the trends of the recent past. Both technological challenges and astronomical priorities suggest that x-ray astronomy satellites following Chandra and XMM-Newton will have significantly greater sensitivity, so that the number of objects which can be observed spectroscopically, the statistical quality of the spectra, and the ability to study time variability will all be greatly enhanced. However, it is less likely that either the spectral resolution or the spectral bandpass will be improved in such instruments. Thus spectral resolution comparable to that available from the best optical or UV instruments will not be attained. In view of this it seems likely that the interpretation of data from such future missions will continue to rely on tools similar to those currently in use, tools which attempt to calculate ionization, excitation, and synthesize the spectrum over a wide range of wavelengths. New targets for these observations will likely include galaxies, clusters of galaxies, and intergalactic gas in order to study the formation of structure, nucleosynthesis, and cosmological parameters. More sensitive instruments will also study spectra of fainter nearby objects such as stars and supernova remnants, and allow

improved statistics and more detailed study of time variability of the brightest objects. This is in contrast to what might be expected if the trend toward both greater spectral resolution and greater sensitivity were to occur, which might lead to more extensive application of discrete diagnostics and a reduced reliance on global modeling. If so, the atomic data needed for the foreseeable future will not be greatly altered, in the sense that the precision required will be comparable to the best currently available, and physical processes of interest will span those covered in this review. Spectra with improved statistical accuracy, or time resolution, are likely to reveal physical effects which have not been incorporated into the available atomic database. These may include departures from ionization equilibrium, nonstationary processes, optical depth effects, magnetic field effects, and interactions with energetic particles and non-Maxwellian electron energy distributions. This implies the need for cross sections at energies significantly both above and below the traditional range of energies prescribed by coronal equilibrium. In addition, it is likely that x-ray astronomers will further explore molecular, or solid matter in astrophysics using charge transfer and also absorption features near edges or inner-shell lines.

#### ACKNOWLEDGMENTS

We thank Manuel Bautista, Nigel Badnell, Greg Madejski, Alfred Müller, and Daniel Savin for careful reading, many valuable comments, and suggestions. We also thank Professor Claude Canizares and the Center for Space Research for access to the MIT libraries. This work was supported in part by a grant from NASA through the Astrophysics Theory program.

#### GLOSSARY

Acronym	Meaning
AMA	Angular momentum average
APEC	Atomic physics emission code
BP	Breit-Pauli
BPRM	Breit-Pauli <i>R</i> -matrix code package
CB	Coulomb Born approximation
CBE	Coulomb Born with exchange
CBO	Coulomb Born Oppenheimer
CCD	Charge-coupled device
CI	Configuration interaction
DI	Direct ionization
DR	Dielectronic recombination
DW	Distorted-wave approximation
EA	Excitation autoionization
EBIS	Electron-beam ion source
EBIT	Electron-beam ion trap
ECIP	Exchange classical impact parameter
EII	Electron impact ionization
FAC	Flexible atomic code
GF	Burgess general formula
HETG	High-energy transmission grating
HFR	Hartree-Fock relativistic code
HRS	High Rydberg states
HULLAC	Hebrew University LLNL Code

HXR	Hartree-Fock exchange potential
LLNL	Lawrence Livermore National Laboratory
LTE	Local thermodynamic equilibrium
MBPT	Many-body perturbation theory
MC	Multiconfiguration
MCBP	Multiconfiguration Breit Pauli
MCDF	Multiconfiguration Dirac Fock
MCHF	Multiconfiguration Hartree Fock
ORNL	Oak Ridge National Laboratory
QED	Quantum electrodynamic
READI	Resonant excitation auto-double ionization
REDA	Resonant excitation double autoionization
RGS	Reflection grating spectrograph
RTE	Resonant transfer of excitation
SCF	Self-consistent field

#### REFERENCES

- Abrahamsson, K., *et al.*, 1993, Nucl. Instrum. Methods Phys. Res. B **79**, 26.  
 Aggarwal, K. M., 1991, Astrophys. J., Suppl. Ser. **77**, 677.  
 Aggarwal, K. M., and A. E. Kingston, 1991a, J. Phys. B **24**, 4583.  
 Aggarwal, K. M., and A. E. Kingston, 1991b, J. Phys. B **44**, 517.  
 Aggarwal, K. M., and A. E. Kingston, 1992a, Phys. Scr. **46**, 193.  
 Aggarwal, K. M., and A. E. Kingston, 1992b, J. Phys. B **25**, 751.  
 Aggarwal, K. M., and A. E. Kingston, 1993, Astrophys. J., Suppl. Ser. **85**, 187.  
 Aichele, K., W. Shi, F. Scheuermann, H. Teng, E. Salzborn, and A. Müller, 2001, Phys. Rev. A **63**, 014701.  
 Aichele, K., M. Steidl, U. Hartenfeller, D. Hathiramani, F. Scheuermann, M. Westermann, E. Salzborn, and M. S. Pindzola, 2001, J. Phys. B **34**, 4113.  
 Aichele, K., *et al.*, 1998, J. Phys. B **31**, 2369.  
 Aitken, K. L., and M. F. A. Harrison, 1971, J. Phys. B **4**, 1176.  
 Aitken, K. L., F. A. Harrison, and R. D. Rundel, 1971, J. Phys. B **4**, 1189.  
 Ait-Tahar, S., I. P. Grant, and P. H. Norrington, 1996, Phys. Rev. A **54**, 3984.  
 Aldrovandi, S. M. V., and D. Pequignot, 1973, Astron. Astrophys. **25**, 137.  
 Aldrovandi, S. M. V., and D. Pequignot, 1976, Astron. Astrophys. **47**, 321.  
 Ali, R., C. P. Bhalla, C. L. Cocke, and M. Stockli, 1990, Phys. Rev. Lett. **64**, 633.  
 Allen, J. W., and A. K. Dupree, 1969, Astrophys. J. **155**, 27.  
 Altun, Z., A. Yumak, N. R. Badnell, J. Colgan, and M. S. Pindzola, 2004, Astron. Astrophys. **420**, 775.  
 Altun, Z., A. Yumak, N. R. Badnell, J. Colgan, and M. S. Pindzola, 2005, Astron. Astrophys. **433**, 395.  
 Altun, Z., A. Yumak, N. R. Badnell, S. D. Loch, and M. S. Pindzola, 2006, Astron. Astrophys. **447**, 1165.  
 Andersen, L. H., G.-Y. Pan, H. T. Schmidt, N. R. Badnell, and M. S. Pindzola, 1992, Phys. Rev. A **45**, 7868.  
 Andersen, L. H., G.-Y. Pan, H. T. Schmidt, M. S. Pindzola, and N. R. Badnell, 1992, Phys. Rev. A **45**, 6332.  
 Ansari, B., and C. Alam, 1975, Sol. Phys. **41**, 97.  
 Antonucci, R. R. J., and J. S. Miller, 1985, Astrophys. J. **297**, 621.

- Arnaud, M., and J. Raymond, 1992, *Astrophys. J.* **398**, 394.
- Arnaud, M., and R. Rothenflug, 1985, *Astron. Astrophys., Suppl. Ser.* **60**, 425.
- Avgoustoglou, E., W. R. Johnson, D. R. Plante, J. Sapirstein, S. Sheinerman, and S. A. Blundell, 1992, *Phys. Rev. A* **46**, 5478.
- Badnell, N. R., 1986a, *J. Phys. B* **19**, 1541.
- Badnell, N. R., 1986b, *J. Phys. B* **19**, 3827.
- Badnell, N. R., 1987, *J. Phys. B* **20**, 2081.
- Badnell, N. R., 1988, *J. Phys. B* **21**, 749.
- Badnell, N. R., 1989, *Phys. Scr.* **T28**, 33.
- Badnell, N. R., 1990, *J. Phys. B* **23**, L565.
- Badnell, N. R., 1991, *Astrophys. J.* **379**, 356.
- Badnell, N. R., 1992, *Phys. Rev. A* **46**, 660.
- Badnell, N. R., 1997, *J. Phys. B* **30**, 1.
- Badnell, N. R., 2006, *Astron. Astrophys.* **447**, 389.
- Badnell, N. R., M. A. Bautista, K. Butler, F. Delahaye, C. Mendoza, P. Palmeri, C. J. Zeippen, and M. J. Seaton, 2005, *Mon. Not. R. Astron. Soc.* **360**, 458.
- Badnell, N. R., and D. C. Griffin, 2001, *J. Phys. B* **34**, 681.
- Badnell, N. R., D. C. Griffin, and D. Mitnik, 2001, *J. Phys. B* **34**, 5071.
- Badnell, N. R., and D. L. Moores, 1994, *At. Data Nucl. Data Tables* **57**, 329.
- Badnell, N. R., and M. S. Pindzola, 1989a, *Phys. Rev. A* **39**, 1685.
- Badnell, N. R., and M. S. Pindzola, 1989b, *Phys. Rev. A* **39**, 1690.
- Badnell, N. R., and M. S. Pindzola, 1989c, *Phys. Rev. A* **39**, 6165.
- Badnell, N., and M. Pindzola, 1993, *Phys. Rev. A* **47**, 2937.
- Badnell, N. R., M. S. Pindzola, L. H. Andersen, J. Bolko, and H. T. Schmidt, 1991, *J. Phys. B* **24**, 4441.
- Badnell, N. R., M. S. Pindzola, I. Bray, and D. C. Griffin, 1998, *J. Phys. B* **31**, 911.
- Badnell, N. R., M. S. Pindzola, W. J. Dickson, H. P. Summers, D. C. Griffin, and J. Lang, 1993, *Astrophys. J. Lett.* **407**, L91.
- Badnell, N. R., M. S. Pindzola, and D. C. Griffin, 1990, *Phys. Rev. A* **41**, 2422.
- Badnell, N. R., *et al.*, 2003, *Astron. Astrophys.* **406**, 1151.
- Baker, J., and D. Menzel, 1938, *Astrophys. J.* **88**, 52.
- Ballance, C. P., D. C. Griffin, J. A. Ludlow, and M. S. Pindzola, 2004, *J. Phys. B* **37**, 4779.
- Bannister, M. E., 1996, *Phys. Rev. A* **54**, 1435.
- Barfield, W. D., 1979, *Astrophys. J.* **229**, 856.
- Bar-Shalom, A., M. Klapisch, and J. Oreg, 2001, *J. Quant. Spectrosc. Radiat. Transf.* **71**, 169.
- Bartiromo, R., F. Bombarda, and R. Giannella, 1985, *Phys. Rev. A* **32**, 531.
- Bartsch, T., *et al.*, 1999, *Phys. Rev. Lett.* **82**, 3779.
- Bartschat, K., and I. Bray, 1996, *J. Phys. B* **30**, L577.
- Bartschat, K., and I. Bray, 1997, *J. Phys. B* **30**, L109.
- Bates, D. R., and A. Dalgarno, 1962, in *Atomic and Molecular Processes*, edited by D. R. Bates (Academic, New York), p. 245.
- Bautista, M. A., 2000, *J. Phys. B* **33**, 71.
- Bautista, M. A., and T. R. Kallman, 2000, *Astrophys. J.* **544**, 581.
- Bautista, M. A., and T. R. Kallman, 2001, *Astrophys. J., Suppl. Ser.* **134**, 139.
- Bautista, M. A., T. R. Kallman, and A. K. Pradhan, 2000, Conference Proceedings, NASA/CP-2000-209968; Rept-2000-04370-0; NAS 1.55:209968, <http://heasarc.gsfc.nasa.gov/docs/heasarc/atomic/>
- Bautista, M. A., C. Mendoza, T. R. Kallman, and P. Palmeri, 2003, *Astron. Astrophys.* **403**, 339.
- Bautista, M. A., C. Mendoza, T. R. Kallman, and P. Palmeri, 2004, *Astron. Astrophys.* **418**, 1171.
- Becker, C., H. Knopp, J. Jacobi, H. Teng, S. Schippers, A. Müller, 2004, *J. Phys. B* **37**, 1503.
- Behar, E., J. Cottam, and S. M. Kahn, 2001, *Astrophys. J.* **548**, 966.
- Behar, E., and H. Netzer, 2002, *Astrophys. J.* **570**, 165.
- Behar, E., M. Sako, and S. M. Kahn, 2001, *Astrophys. J.* **563**, 497.
- Behring, W. E., L. Cohen, and U. Feldman, 1972, *Astrophys. J.* **175**, 493.
- Beiersdorfer, P., 2003, *Annu. Rev. Astron. Astrophys.* **41**, 343.
- Beiersdorfer, P., T. Phillips, V. L. Jacobs, K. W. Hill, M. Bitter, S. von Goeler, and S. M. Kahn, 1993, *Astrophys. J.* **409**, 846.
- Beiersdorfer, P., *et al.*, 1990, *Rev. Sci. Instrum.* **61**, 2338.
- Beiersdorfer, P., *et al.*, 1992, *Phys. Rev. A* **46**, 3812.
- Beiersdorfer, P., *et al.*, 2002, *Astrophys. J. Lett.* **576**, L169.
- Beiersdorfer, P., *et al.*, 2003, *Science* **300**, 1558.
- Beiersdorfer, P., *et al.*, 2004, *Astrophys. J.* **610**, 616.
- Beijers, J. P. M., R. Hoekstra, and R. Morgenstern, 1996, *J. Phys. B* **29**, 1397.
- Belic, D. S., G. H. Dunn, T. J. Morgan, D. W. Mueller, and C. Timmer, 1983, *Phys. Rev. Lett.* **50**, 339.
- Bell, K. L., H. B. Gilbody, J. G. Hughes, A. E. Kingston, and F. J. Smith, 1983, *J. Phys. Chem. Ref. Data* **12**, 891.
- Bellantone, R., and Y. Hahn, 1989, *Phys. Rev. A* **40**, 6913.
- Bely, O., 1966, *Ann. Astrophys.* **29**, 683.
- Bely, O., 1968, *J. Phys. B* **1**, 23.
- Bely, O., and H. van Regemorter, 1970, *Annu. Rev. Astron. Astrophys.* **8**, 329.
- Bely-Dubau, F., 1973, *Astron. Astrophys.* **25**, 431.
- Bely-Dubau, F., P. Faucher, J. Dubau, and A. H. Gabriel, 1982, *Mon. Not. R. Astron. Soc.* **198**, 239.
- Bely-Dubau, F., A. H. Gabriel, and S. Volonte, 1979a, *Mon. Not. R. Astron. Soc.* **186**, 405.
- Bely-Dubau, F., A. H. Gabriel, and S. Volonte, 1979b, *Mon. Not. R. Astron. Soc.* **189**, 801.
- Bely-Dubau, F., *et al.*, 1982, *Mon. Not. R. Astron. Soc.* **201**, 1155.
- Bely-Dubau, F., *et al.*, 1983, *Phys. Lett.* **93A**, 189.
- Berrington, K. A., 1994, *At. Data Nucl. Data Tables* **57**, 71.
- Bethe, H. A., and E. E. Salpeter, 1972, *Quantum Mechanics of One- and Two-Electron Atoms* (Springer, Berlin).
- Bevington, P. R., 1969, *Data Reduction and Error Analysis for Physicists* (McGraw-Hill, New York).
- Bhalla, C. P., A. H. Gabriel, and L. P. Presnyakov, 1975, *Mon. Not. R. Astron. Soc.* **172**, 359.
- Bhalla, C. P., and K. R. Karim, 1986, *Rev. Sci. Instrum.* **57**, 2055.
- Bhalla, C. P., and K. R. Karim, 1988, *Rev. Sci. Instrum.* **59**, 1527.
- Bhatia, A. K., and G. A. Doschek, 1992, *At. Data Nucl. Data Tables* **52**, 1.
- Bhatia, A. K., and G. A. Doschek, 1993, *At. Data Nucl. Data Tables* **53**, 195.
- Bhatia, A. K., and G. A. Doschek, 1995, *At. Data Nucl. Data Tables* **60**, 97.
- Bhatia, A. K., and G. A. Doschek, 1996, *At. Data Nucl. Data Tables* **64**, 183.
- Bhatia, A. K., and G. A. Doschek, 1998, *At. Data Nucl. Data Tables* **68**, 49.

- Bhatia, A. K., and G. A. Doschek, 1999, At. Data Nucl. Data Tables **71**, 69.
- Bhatia, A. K., and G. A. Doschek, 2003, At. Data Nucl. Data Tables **85**, 1.
- Bhatia, A. K., G. A. Doschek, and W. Eissner, 2002, At. Data Nucl. Data Tables **82**, 211.
- Bhatia, A. K., B. C. Fawcett, K. J. H. Phillips, J. R. Lemen, and H. E. Mason, 1989, Mon. Not. R. Astron. Soc. **240**, 421.
- Bhatia, A. K., and S. O. Kastner, 1980, Sol. Phys. **65**, 181.
- Bhatia, A. K., and S. O. Kastner, 1985, Sol. Phys. **96**, 11.
- Bhatia, A. K., and S. O. Kastner, 1999, Astrophys. J. **516**, 482.
- Bhatia, A. K., S. O. Kastner, F. P. Keenan, E. S. Conlon, and K. G. Widing, 1994, Astrophys. J. **427**, 497.
- Bhatia, A. K., and E. Landi, 2003a, Astrophys. J. **585**, 587.
- Bhatia, A. K., and E. Landi, 2003b, Astrophys. J., Suppl. Ser. **147**, 409.
- Bhatia, A. K., and E. Landi, 2003c, At. Data Nucl. Data Tables **85**, 169.
- Bhatia, A. K., and E. Landi, 2003d, At. Data Nucl. Data Tables **85**, 317.
- Bhatia, A. K., E. Landi, and H. E. Mason, 2003, At. Data Nucl. Data Tables **83**, 71.
- Bhatia, A. K., and H. E. Mason, 1980, Astron. Astrophys. **83**, 380.
- Bhatia, A. K., and H. E. Mason, 1981, Astron. Astrophys. **103**, 324.
- Bhatia, A. K., and H. E. Mason, 1983, Astron. Astrophys., Suppl. Ser. **52**, 115.
- Bhatia, A. K., and H. E. Mason, 1986a, Astron. Astrophys. **155**, 413.
- Bhatia, A. K., and H. E. Mason, 1986b, Astron. Astrophys. **155**, 417.
- Bhatia, A. K., and H. E. Mason, 1997, At. Data Nucl. Data Tables **66**, 119.
- Bhatia, A. K., J. F. Seely, and U. Feldman, 1987, At. Data Nucl. Data Tables **36**, 453.
- Biemont, E., P. Quinet, A. Ya Faenov, I. Skobolev, J. Nilsen, V. M. Romanova, M. Scholz, L. Karpinski, and A. Szydlowski, 2000, Phys. Scr. **61**, 555.
- Biemont, E., and C. J. Zeippen, 1996, Phys. Scr. **T65**, 192.
- Binello, A. M., H. E. Mason, and P. J. Storey, 1998a, Astron. Astrophys., Suppl. Ser. **131**, 153.
- Binello, A. M., H. E. Mason, and P. J. Storey, 1998b, Astron. Astrophys., Suppl. Ser. **127**, 545.
- Bitter, M., K. W. Hill, N. R. Sauthoff, P. C. Efthimion, E. Meserve, W. Roney, S. von Goeler, R. Horton, M. Goldman, and W. Stodieck, 1979, Phys. Rev. Lett. **43**, 129.
- Bitter, M., et al., 1984, Phys. Rev. A **29**, 661.
- Blackford, H. M. S., and A. Hibbert, 1994, At. Data Nucl. Data Tables **58**, 101.
- Blanchet, L., M. Cornille, J. Dubau, P. Faucher, and J. Lion, 1985, Astron. Astrophys. **152**, 417.
- Bliek, F. W., Hoekstra R., Bannister M. E., and C. C. Havener, 1997, Phys. Rev. A **56**, 426.
- Blumenthal, G. R., G. W. F. Drake, and W. H. Tucker, 1972, Astrophys. J. **172**, 205.
- Bohm, S., A. Müller, S. Schippers, W. Shi, N. Eklov, R. Schuch, H. Danared, and N. R. Badnell, 2003, Astron. Astrophys. **405**, 1157.
- Bohm, S., et al., 2001, Phys. Scr. **T92**, 395.
- Bohm, S., et al., 2002, Phys. Rev. A **65**, 052728.
- Boiko, V. A., Faenov, A. I., and S. A. Pikuz, 1978, J. Quant. Spectrosc. Radiat. Transf. **19**, 11.
- Boiko, V. A., A. Y. Faenov, S. A. Pikuz, and U. L. Safranova, 1977, Mon. Not. R. Astron. Soc. **181**, 107.
- Breton, C., C. DeMichelis, M. Finkenthal, and M. Mattioli, 1978, Phys. Rev. Lett. **41**, 110.
- Briand, J. P., P. Charles, J. Arianer, H. Laurent, C. Goldstein, J. Dubau, M. Loulergue, and F. Bely-Dubau, 1984, Phys. Rev. Lett. **52**, 617.
- Brickhouse, N. S., J. C. Raymond, and B. W. Smith, 1995, Astrophys. J., Suppl. Ser. **97**, 551.
- Brinkman A. C., J. S. Kaastra, R. L. J. van der Meer, A. Kinkhabwala, E. Behar, S. M. Kahn, F. B. S. Paerels, and M. Sako, 2002, Astron. Astrophys. **396**, 761.
- Brinkman, B. C., et al., 2000, Proc. SPIE **4012**, 81.
- Bromage, G. E., R. D. Cowan, and B. C. Fawcett, 1977, Phys. Scr. **15**, 177.
- Bromage, G. E., and B. C. Fawcett, 1977a, Mon. Not. R. Astron. Soc. **178**, 605.
- Bromage, G. E., and B. C. Fawcett, 1977b, Mon. Not. R. Astron. Soc. **178**, 591.
- Bromage, G. E., B. C. Fawcett, and R. D. Cowan, 1977, Mon. Not. R. Astron. Soc. **178**, 599.
- Bromage, G. E., B. C. Fawcett, and R. D. Cowan, 1978, Mon. Not. R. Astron. Soc. **183**, 19.
- Bromage, G. E., B. C. Fawcett, A. Ridgeley, and R. D. Cowan, 1978, J. Opt. Soc. Am. **68**, 48.
- Brook, E., A. C. H. Smith, and M. F. A. Harrison, 1978, J. Phys. B **11**, 3115.
- Brown, G. J. N., M. P. Scott, and K. A. Berrington, 1999, J. Phys. B **32**, 737.
- Brown, G. V., P. Beiersdorfer, D. A. Liedahl, K. Widmann, and S. M. Kahn, 1998, Astrophys. J. **502**, 1015.
- Brown, G. V., P. Beiersdorfer, and K. Widmann, 2001, Phys. Rev. A **63**, 032719.
- Brown, G. V., et al., 2001, Phys. Scr. **T92**, 130.
- Brown, R. T., 1971, Astrophys. J. **170**, 387.
- Bruch, R., D. Schneider, M. H. Chen, K. T. Chung, and B. F. Davis, 1992, Phys. Rev. A **45**, 4476.
- Bruch, R., et al., 1979, Phys. Rev. A **19**, 587.
- Bruch, R., et al., 1987, Phys. Rev. A **35**, 4114.
- Brueckner, K. A., 1955, Phys. Rev. **97**, 1353.
- P. Bryans, N. R. Badnell, T. W. Gorczyca, J. M. Laming, W. Mitthumsiri, and D. W. Savin, 2006, Astrophys. J. Suppl. (to be published).
- Burgess, A., 1964, Mem. R. Astron. Soc. **69**, 1.
- Burgess, A., 1965, Astrophys. J. **141**, 1588.
- Burgess, A., and M. C. Chidichimo, 1983, Mon. Not. R. Astron. Soc. **203**, 1269.
- Burgess, A., D. G. Hummer, and J. A. Tully, 1970, Philos. Trans. R. Soc. London, Ser. A **266**, 225.
- Burgess, A., and V. B. Sheorey, 1974, J. Phys. B **7**, 2403.
- Burgess, A., and H. P. Summers, 1969, Astrophys. J. **157**, 1007.
- Burgess, A., and H. P. Summers, 1976, Mon. Not. R. Astron. Soc. **174**, 345.
- Burgess, A., H. P. Summers, R. W. P. McWhirter, and D. M. Cochrane, 1977, Mon. Not. R. Astron. Soc. **179**, 275.
- Burgess, A., and A. S. Tworkowski, 1976, Astrophys. J., Lett. Ed. **205**, L105.
- Burke, P. G., and K. A. Berrington, 1993, *Atomic and Molecular Processes: an R-matrix Approach* (IOP, Bristol and Philadelphia).
- Butler, K., and D. L. Moores, 1985, J. Phys. B **18**, 1247.
- Butler, K., and C. J. Zeippen, 1994, Astron. Astrophys., Suppl. Ser. **108**, 1.

- Butler, K., and C. J. Zeippen, 2000, Astron. Astrophys., Suppl. Ser. **143**, 483.
- Butler, K., and C. J. Zeippen, 2001a, Astron. Astrophys. **372**, 1078.
- Butler, K., and C. J. Zeippen, 2001b, Astron. Astrophys. **372**, 1083.
- Butler, S. E., and A. Dalgarno, 1979, Astrophys. J. **234**, 765.
- Butler, S. E., and A. Dalgarno, 1980a, Astron. Astrophys. **85**, 144.
- Butler, S. E., and A. Dalgarno, 1980b, Astrophys. J. **241**, 838.
- Callaway, J., 1994, At. Data Nucl. Data Tables **57**, 9.
- Canizares, C. R., *et al.*, 2000, Astrophys. J. Lett. **539**, L41.
- Canizares, C. R., *et al.*, 2005, Publ. Astron. Soc. Pac. **117**, 1144.
- Champeaux, J.-P., J.-M. Bizau, D. Cubaynes, C. Blancard, S. Nahar, D. Hitz, J. Bruneau, and F. J. Wuilleumier, 2003, Astron. Astrophys., Suppl. Ser. **148**, 583.
- Chapman, R. D., and R. J. W. Henry, 1971, Astrophys. J. **168**, 169.
- Chapman, R. D., and R. J. W. Henry, 1972, Astrophys. J. **173**, 243.
- Chen, G. X., and A. K. Pradhan, 2002, Phys. Rev. Lett. **89**, 013202.
- Chen, G. X., A. K. Pradhan, and W. Eissner, 2003, J. Phys. B **36**, 453.
- Chen, H., P. Beiersdorfer, L. A. Heeter, D. A. Liedahl, K. L. Naranjo-Rivera, E. Trabert, M. F. Gu, and J. K. Lepson, 2004, Astrophys. J. **611**, 598.
- Chen, H., *et al.*, 2005, Astrophys. J. **618**, 1086.
- Chen, M. H., 1986a, Phys. Rev. A **34**, 1073.
- Chen, M. H., 1986b, Phys. Rev. A **33**, 994.
- Chen, M. H., 1988a, Phys. Rev. A **38**, 2332.
- Chen, M. H., 1988b, Phys. Rev. A **38**, 6430.
- Chen, M. H., 1988c, Phys. Rev. A **38**, 3280.
- Chen, M. H., 1991, Phys. Rev. A **44**, 4215.
- Chen, M. H., and B. Crasemann, 1988, Phys. Rev. A **38**, 5595.
- Chen, M. H., K. J. Reed, D. S. Guo, and D. W. Savin, 1998, Phys. Rev. A **58**, 4539.
- Chen, M. H., *et al.*, 1990, Phys. Rev. Lett. **64**, 1350.
- Chen, M. S., 1986, At. Data Nucl. Data Tables **34**, 301.
- Christensen, R. B., D. W. Norcross, and A. K. Pradhan, 1986, Phys. Rev. A **34**, 4704.
- Ciric, D., A. Brazuk, D. Dijkkamp, F. J. de Heers, and H. Winter, 1985, J. Phys. B **18**, 3629.
- Clark, M., D. Brandt, J. K. Swenson, and S. M. Shafrroth, 1985, Phys. Rev. Lett. **54**, 544.
- Clark, R. E. H., R. D. Cowan, and F. W. Bobrowicz, 1986, At. Data Nucl. Data Tables **34**, 415.
- Clark, R. E. H., D. H. Sampson, and S. J. Goett, 1982, Astron. Astrophys., Suppl. Ser. **49**, 545.
- Cohen, M., K. Fournier, and W. Goldstein, 1998, Phys. Rev. A **57**, 2651.
- Colgan, J., M. S. Pindzola, and N. R. Badnell, 2004, Astron. Astrophys. **417**, 1183.
- Colgan, J., M. S. Pindzola, and N. R. Badnell, 2005, Astron. Astrophys. **429**, 369.
- Colgan, J., M. S. Pindzola, A. D. Whiteford, and N. R. Badnell, 2003, Astron. Astrophys. **412**, 597.
- Connerade, J. P., N. J. Peacock, and R. J. Speer, 1970, Sol. Phys. **14**, 159.
- Corliss, C., and J. Sugar, 1982, J. Phys. Chem. Ref. Data **11**, 135.
- Cornelius, K. R., K. Wojtkowski, and R. E. Olson, 2000, J. Phys. B **33**, 2017.
- Cornille, M., J. Dubau, and S. Jacquemot, 1994, At. Data Nucl. Data Tables **58**, 1.
- Cornille, M., J. Dubau, M. Loulergue, F. Bely-Dubau, and P. Faucher, 1992, Astron. Astrophys. **259**, 669.
- Cornille, M., *et al.*, 1994, Astron. Astrophys., Suppl. Ser. **105**, 77.
- Cowan, R. D., 1981, *The Theory of Atomic Structure and Spectra* (University of California Press, Berkeley).
- Cowan, R. D., G. E. Bromage, and B. C. Fawcett, 1984, Mon. Not. R. Astron. Soc. **210**, 439.
- Cowan, R. D., and J. B. Mann, 1979, Astrophys. J. **232**, 940.
- Cox, D. P., and E. Daltabuit, 1971, Astrophys. J. **167**, 113.
- Cox, D. P., and W. H. Tucker, 1969, Astrophys. J. **157**, 1157.
- Crandall, D. H., R. A. Phaneuf, R. A. Falk, D. S. Belic, and G. H. Dunn, 1982, Phys. Rev. A **25**, 143.
- Crandall, D. H., R. A. Phaneuf, and D. C. Gregory, 1979, "Electron Impact Ionization of Multicharged Ions," ORNL/TM-7020, Oak Ridge National Laboratory.
- Crandall, D. H., R. A. Phaneuf, D. C. Gregory, A. M. Howald, D. W. Mueller, T. J. Morgan, G. H. Dunn, D. C. Griffin, and R. J. W. Henry, 1986, Phys. Rev. A **34**, 1757.
- Crandall, D. H., R. A. Phaneuf, B. E. Hasselquist, and D. C. Gregory, 1979, J. Phys. B **12**, L249.
- Cravens, T. E., 2002, Science **296**, 1042.
- Culhane, J. L., and L. W. Acton, 1974, Annu. Rev. Astron. Astrophys. **12**, 359.
- Cunto, W., and C. Mendoza, 1992, Rev. Mex. Astron. Astrofis. **23**, 107.
- Curdt, W., E. Landi, K. Wilhelm, and U. Feldman, 2000, Phys. Rev. A **62**, 022502.
- Czyzak, S. J., and T. K. Krueger, 1966, Astrophys. J. **144**, 381.
- Dance, D. F., M. F. A. Harrison, and R. D. Rundel, 1967, Proc. R. Soc. London, Ser. A **299**, 525.
- Danjo, A., *et al.*, 1984, J. Phys. Soc. Jpn. **43**, 4091.
- Dasgupta, A., 1995, Astron. Astrophys., Suppl. Ser. **101**, 401.
- Dasgupta, A., and K. G. Whitney, 1990, Phys. Rev. A **42**, 2640.
- Dasgupta, A., and K. G. Whitney, 1994, At. Data Nucl. Data Tables **58**, 77.
- Datla, R. U., L. J. Nugent, and H. R. Griem, 1976, Phys. Rev. A **14**, 979.
- Decaux, V., P. Beiersdorfer, S. M. Kahn, and V. L. Jacobs, 1997, Astrophys. J. **482**, 1076.
- Decaux, V., M. Bitter, H. Hsuan, K. W. Hill, S. von Goeler, H. Park, and C. P. Bhalla, 1991, Phys. Rev. A **44**, R6987.
- Decaux, V., V. L. Jacobs, P. Beiersdorfer, D. A. Lie Dahl, and S. M. Kahn, 2003, Phys. Rev. A **68**, 012509.
- Decaux, V., *et al.*, 1991, Phys. Rev. A **43**, 228.
- Defrance, P., *et al.*, 1990, J. Phys. B **23**, 2333.
- Delahaye, F., and A. K. Pradhan, 2002, J. Phys. B **35**, 3377.
- Dere, K. P., E. Landi, H. E. Mason, B. C. Monsignori Fossi, and P. R. Young, 1997, Astron. Astrophys., Suppl. Ser. **125**, 149.
- Dere, K. P., E. Landi, P. R. Young, and G. DelZanna, 2001, Astrophys. J., Suppl. Ser. **134**, 331.
- Derevianko, A., and W. R. Johnson, 1997, Phys. Rev. A **56**, 1288.
- Deutschman, W. A., and L. L. House, 1966, Astrophys. J. **144**, 435.
- Deutschman, W. A., and L. L. House, 1967, Astrophys. J. **149**, 451.
- Dewitt, D. R., E. Lindroth, R. Schuch, H. Gao, T. Quinteros, and W. Zong, 1995, J. Phys. B **28**, L147.

- Dijkkamp, D., D. Ceric, E. Vlieg, A. de Boer, and F. J. de Heer, 1985a, *J. Phys. B* **18**, 4763.
- Dijkkamp, D., Yu. S. Gordeev, A. Brazuk, A. G. Drentje, and F. J. de Heer, 1985b, *J. Phys. B* **18**, 737.
- Diserens, M. J., M. F. A. Harrison, and A. C. H. Smith, 1984, *J. Phys. B* **17**, L621.
- Diserens, M. J., M. F. A. Harrison, and A. C. H. Smith, 1988, *J. Phys. B* **21**, 2129.
- Dittner, P. F., S. Datz, R. Hippler, H. F. Krause, and P. D. Miller, 1988, *Phys. Rev. A* **38**, 2762.
- Dittner, P. F., *et al.*, 1983, *Phys. Rev. Lett.* **51**, 31.
- Djuric, N., E. W. Bell, X. Q. Guo, R. A. Phaneuf, M. E. Bannister, M. S. Pindzola, and D. C. Griffin, 1993, *Phys. Rev. A* **47**, 4786.
- Djuric, N., *et al.*, 2002, *Phys. Rev. A* **65**, 052711.
- Dolder, K. T., M. F. A. Harrison, and P. C. Thonemann, 1961, *Proc. R. Soc. London, Ser. A* **264**, 367.
- Dolder, K. T., M. F. A. Harrison, and P. C. Thonemann, 1963, *Proc. R. Soc. London, Ser. A* **274**, 546.
- Doschek, G. A., 1972, *Space Sci. Rev.* **13**, 765.
- Doschek, G. A., and R. D. Cowan, 1984, *Astrophys. J., Suppl. Ser.* **56**, 67.
- Doschek, G. A., and U. Feldman, 1987, *Astrophys. J.* **313**, 883.
- Drake, G. W., 1988, *Can. J. Phys.* **66**, 586.
- Dubau, J., 1994, *At. Data Nucl. Data Tables* **57**, 21.
- Dubau, J., M. Loulergue, A. H. Gabriel, L. Steenman-Clark, and S. Volonte, 1981, *Mon. Not. R. Astron. Soc.* **195**, 705.
- Dubau, J., M. Loulergue, and L. Steenman-Clark, 1980, *Mon. Not. R. Astron. Soc.* **190**, 125.
- Dubau, J., D. Porquet, and O. Z. Zabaydullin, 2003, *J. Quant. Spectrosc. Radiat. Transf.* **81**, 117.
- Dubau, J., and S. Volonte, 1980, *Rep. Prog. Phys.* **43**, 199.
- Dufton, P. L., and A. E. Kingston, 1994, *At. Data Nucl. Data Tables* **57**, 273.
- Dunn, G. H., N. Djuric, Y.-S. Chung, M. Bannister, and A. C. H. Smith, 1995, *Nucl. Instrum. Methods Phys. Res. B* **98**, 107.
- Duponchelle, M., M. Khouilid, E. M. Oualim, H. Zhang, and P. Defrance, 1997, *J. Phys. B* **30**, 729.
- Dyall, K. G., I. P. Grant, C. T. Johnson, F. A. Parpia, and E. P. Plummer, 1989, *Comput. Phys. Commun.* **55**, 425.
- Dzifcakova, E., 1992, *Sol. Phys.* **140**, 247.
- Dzifcakova, E., 1998, *Sol. Phys.* **178**, 317.
- Dzifcakova, E., and A. Kulinova, 2002, *ESASP-477: Solspa2001, Proceedings of the Second Solar Cycle and Space Weather Euroconference*, p. 9.
- Edlen, B., 1983, *Phys. Scr.* **28**, 51.
- Edlen, B., 1984, *Phys. Scr.* **30**, 135.
- Edlen, B., 1985, *Phys. Scr.* **31**, 345.
- Edmonds, A. R., 1960, *Angular Momentum in ‘Quantum Mechanics’* (Princeton University Press, Princeton).
- Eissner, W., M. E. Galavís, C. Mendoza, and C. J. Zeippen, 1999, *Astron. Astrophys., Suppl. Ser.* **136**, 385.
- Eissner, W., M. Jones, and H. Nussbaumer, 1974, *Comput. Phys. Commun.* **8**, 270.
- Eissner, W., E. Landi, and A. K. Bhatia, 2005, *At. Data Nucl. Data Tables* **89**, 139.
- Erickson, G. W., 1977, *J. Phys. Chem. Ref. Data* **6**, 3.
- Ermolaev, A. M., and M. Jones, 1972, *J. Phys. B* **5**, L225.
- Faenov, A. Ya., S. A. Pikuz, and A. S. Shlyaptseva, 1994, *Phys. Scr.* **49**, 41.
- Falk, R. A., G. H. Dunn, C. Bottcher, D. C. Gregory, D. H. Crandall, M. S. Pindzola, and D. C. Griffin, 1981, *Phys. Rev. Lett.* **47**, 494.
- Falk, R. A., G. Stefani, R. Camilloni, G. H. Dunn, R. A. Phaneuf, D. C. Gregory, and D. H. Crandall, 1983, *Phys. Rev. A* **28**, 91.
- Fano, U., and J. W. Cooper, 1968, *Rev. Mod. Phys.* **40**, 441.
- Fano, U., and G. Racah, 1959, *Irreducible Tensorial Sets* (Academic, New York).
- Farhat, A., *et al.*, 1997, *Phys. Rev. A* **56**, 501.
- Fawcett, B. C., 1970, *J. Phys. B* **3**, 1152.
- Fawcett, B. C., 1971, *J. Phys. B* **4**, 1577.
- Fawcett, B. C., 1986a, *At. Data Nucl. Data Tables* **35**, 203.
- Fawcett, B. C., 1986b, *At. Data Nucl. Data Tables* **35**, 185.
- Fawcett, B. C., 1986c, *At. Data Nucl. Data Tables* **34**, 215.
- Fawcett, B. C., 1987, *At. Data Nucl. Data Tables* **37**, 367.
- Fawcett, B. C., G. E. Bromage, and R. W. Hayes, 1979, *Mon. Not. R. Astron. Soc.* **186**, 113.
- Fawcett, B. C., R. D. Cowan, and R. W. Hayes, 1974, *Astrophys. J.* **187**, 377.
- Fawcett, B. C., and R. W. Hayes, 1972, *J. Phys. B* **5**, 366.
- Fawcett, B. C., and R. W. Hayes, 1973, *Phys. Scr.* **8**, 244.
- Fawcett, B. C., E. Y. Kononov, R. W. Hayes, and R. D. Cowan, 1972, *J. Phys. B* **5**, 1255.
- Fawcett, B. C., and H. E. Mason, 1991, *At. Data Nucl. Data Tables* **47**, 17.
- Fawcett, B. C., A. Ridgeley, and G. E. Bromage, 1978, *Phys. Scr.* **18**, 315.
- Feldman, U., and L. Cohen, 1968, *Astrophys. J., Lett.* **151**, L55.
- Feldman, U., G. A. Doschek, and A. K. Bhatia, 1982, *J. Appl. Phys.* **53**, 8554.
- Feldman, U., G. A. Doschek, C.-C. Cheng, and A. K. Bhatia, 1980, *J. Appl. Phys.* **51**, 190.
- Feldman, U., G. A. Doschek, D. J. Nagel, W. E. Behring, and L. Cohen, 1973, *Astrophys. J., Lett. Ed.* **183**, L43.
- Ferland, G., and D. W. Savin, 2001, *Publ. Astron. Soc. Pac.* **113**, 1024.
- Fernley, J. A., K. T. Taylor, and M. J. Seaton, 1987, *J. Phys. B* **20**, 6457.
- Field, G. B., and G. Steigman, 1971, *Astrophys. J.* **166**, 59.
- Fischer, C. F., 1996, in *Atomic, Molecular and Optical Physics Handbook*, edited by G. Drake (AIP, New York), pp. 242–257.
- Fischer, C. F., T. Brage, and P. Jonsson, 1997, *Computational Atomic Structure—An MCHF Approach* (IOP, Bristol).
- Fite, W. L., and R. T. Brackmann, 1959, *Phys. Rev.* **113**, 815.
- Fite, W. L., W. E. Kauppila, and W. R. Ott, 1968, *Phys. Rev. Lett.* **20**, 409.
- Flower, D. R., 1968, in *Planetary Nebulae*, edited by Donald E. Osterbrock and Charles Robert O’Dell, *Proceedings of the IAU Symposium No. 34* (Reidel, Dordrecht), p. 205.
- Flower, D. R., 1972, *Astron. Astrophys.* **17**, 201.
- Flower, D. R., 1983, in *Planetary Nebulae*, *Proceedings of the IAU Symposium No. 103* (Reidel, Dordrecht), p. 576.
- Flower, D. R., and J. M. Launay, 1972, *J. Phys. B* **5**, L207.
- Flower, D. R., and G. Pineau des Forets, 1973, *Astron. Astrophys.* **24**, 181.
- Fogle, M., N. R. Badnell, P. Glans, S. D. Loch, S. Madzunkov, S. A. Abdel-Naby, M. S. Pindzola, and R. Schuch, 2005, *Astron. Astrophys.* **442**, 757.
- Fogle, M., N. Eklöw, E. Lindroth, T. Mohamed, R. Schuch, and M. Tokman, 2003, *J. Phys. B* **36**, 2563.
- Fossi, B. C. M., and M. Landini, 1994, *At. Data Nucl. Data Tables* **57**, 125.

- Freeman, F. F., and B. B. Jones, 1970, Sol. Phys. **15**, 288.
- Fuhr, J. R., *et al.*, 1999, NIST Atomic Spectra Database, version 2.0.
- Gabriel, A., and T. Paget, 1972, J. Phys. B **5**, 673.
- Gabriel, A. H., 1972, Mon. Not. R. Astron. Soc. **160**, 99.
- Gabriel, A. H., and C. Jordan, 1969, Mon. Not. R. Astron. Soc. **145**, 241.
- Gabriel, A. H., and K. J. H. Phillips, 1979, Mon. Not. R. Astron. Soc. **189**, 319.
- Galavis, M., C. Mendoza, and C. J. Zeippen, 1997, Astron. Astrophys., Suppl. Ser. **123**, 159.
- Garcia, J., C. Mendoza, M. A. Bautista, T. W. Gorczyca, T. R. Kallman, and P. Palmeri, 2005, Astrophys. J., Suppl. Ser. **158**, 68.
- Gau, J. N., and Y. Hahn, 1978, Phys. Lett. **68A**, 197.
- Gau, N., Y. Hahn, and J. A. Retter, 1980, J. Quant. Spectrosc. Radiat. Transf. **23**, 147.
- Gianetti, D., E. Landi, and M. Landini, 2000, Astron. Astrophys. **360**, 1148.
- Glans, P., E. Lindroth, N. R. Badnell, N. Eklow, W. Zong, E. Justiniano, and R. Schuch, 2001, Phys. Rev. A **64**, 043609.
- Glans, P., *et al.*, 1999, Nucl. Instrum. Methods Phys. Res. B **154**, 97.
- Glans, P., *et al.*, 2004, Phys. Scr. **T110**, 212.
- Goldberg, L., A. K. Dupree, and J. W. Allen, 1965, Ann. Astrophys. **28**, 589.
- Golden, L. B., R. E. H. Clark, S. J. Goett, and D. H. Sampson, 1981, Astrophys. J., Suppl. Ser. **45**, 603.
- Golden, L. B., and D. H. Sampson, 1971, Astrophys. J. **170**, 181.
- Golden, L. B., and D. H. Sampson, 1977, J. Phys. B **10**, 2229.
- Golden, L. B., and D. H. Sampson, 1980, J. Phys. B **13**, 2645.
- Golden, L. B., D. H. Sampson, and K. Omidvar, 1978, J. Phys. B **11**, 3235.
- Goldsmith, S., U. Feldman, L. Oren, and L. Cohen, 1972, Astrophys. J. **174**, 209.
- Goldsmith, S., L. O. Katz, A. M. Crooker, and L. Cohen, 1973, Astrophys. J. **184**, 1021.
- Goldstein, W. H., A. Osterheld, J. Oreg, and A. Bar-Shalom, 1989, Astrophys. J. Lett. **344**, L37.
- Goldstone, J., 1957, Proc. R. Soc. London, Ser. A **239**, 267.
- Gorczyca, T. W., 2000, Phys. Rev. A **61**, 024702.
- Gorczyca, T. W., and N. R. Badnell, 1996a, J. Phys. B **29**, L283.
- Gorczyca, T. W., and N. R. Badnell, 1996b, Phys. Rev. A **54**, 4113.
- Gorczyca, T. W., and N. R. Badnell, 2000, J. Phys. B **33**, 2511.
- Gorczyca, T. W., N. R. Badnell, and D. W. Savin, 2002, Phys. Rev. A **65**, 062707.
- Gorczyca, T. W., I. Dumitriu, M. F. Hasoglu, K. T. Korista, N. R. Badnell, D. W. Savin, and S. T. Manson, 2006, Astrophys. J. Lett. **638**, L121.
- Gorczyca, T. W., C. N. Kodituwakku, K. T. Korista, O. Zatsarinny, N. R. Badnell, E. Behar, M. H. Chen, and D. W. Savin, 2003, Astrophys. J. **592**, 636.
- Gorczyca, T. W., and B. M. McLaughlin, 2000, J. Phys. B **33**, L859.
- Gorczyca, T. W., and F. Robicheaux, 1999, Phys. Rev. A **60**, 1216.
- Gorczyca, T. W., F. Robicheaux, M. S. Pindzola, and N. R. Badnell, 1996, Phys. Rev. A **54**, 2107.
- Gould, R. J., 1978, Astrophys. J. **219**, 250.
- Grant, I. P., B. J. McKenzie, P. H. Norrington, D. F. Mayers, and N. C. Pyper, 1980, Comput. Phys. Commun. **21**, 207.
- Greenwood, J. B., S. J. Smith, A. Chutjian, and E. Pollack, 1999, Phys. Rev. A **59**, 1348.
- Greenwood, J. B., I. D. Williams, S. J. Smith, and A. Chutjian, 2001, Phys. Rev. A **63**, 062707.
- Gregory, D. C., D. H. Crandall, R. A. Phaneuf, A. M. Howald, G. H. Dunn, R. A. Falk, D. W. Mueller, and T. J. Morgan, 1985, *Electron Impact Ionization of Multicharged Ions at ORNL: 1980–1984*, ORNL/TM-9501.
- Gregory, D. C., P. F. Dittner, and D. H. Crandall, 1983, Phys. Rev. A **27**, 724.
- Gregory, D. C., and A. M. Howald, 1986, Phys. Rev. A **34**, 97.
- Gregory, D. C., F. W. Meyer, A. Müller, and P. Defrance, 1986, Phys. Rev. A **34**, 3657.
- Gregory, D. C., L. J. Wang, F. W. Meyer, and K. Rinn, 1987, Phys. Rev. A **35**, 3256.
- Grevesse, N., A. Noels, and A. Sauval, 1996, in *ASP Conference Series 99, Cosmic Abundances*, edited by S. Holt and G. Sonneborn (ASP, San Francisco), p. 117.
- Griffin, D. C., C. Bottcher, and M. S. Pindzola, 1982, Phys. Rev. A **25**, 1374.
- Griffin, D. C., and M. S. Pindzola, 1988, J. Phys. B **21**, 3253.
- Griffin, D. C., M. S. Pindzola, and N. R. Badnell, 1993, Phys. Rev. A **47**, 2871.
- Griffin, D. C., M. S. Pindzola, and C. Bottcher, 1987, Phys. Rev. A **36**, 3642.
- Gronenschild, E. H. B. M., and R. Mewe, 1978, Astron. Astrophys., Suppl. Ser. **32**, 283.
- Gronenschild, E. H. B. M., and R. Mewe, 1982, Astron. Astrophys., Suppl. Ser. **48**, 305.
- Gu, M. F., 2003a, Astrophys. J. **582**, 1241.
- Gu, M. F., 2003b, Astrophys. J. **590**, 1131.
- Gu, M. F., 2003c, Astrophys. J. **589**, 1085.
- Gu, M. F., 2003d, Astrophys. J. **593**, 1249.
- Gu, M. F., 2004, Phys. Rev. A **70**, 062704.
- Gu, M. F., 2005, Astrophys. J., Suppl. Ser. **156**, 105.
- Gu, M. F., S. M. Kahn, D. W. Savin, E. Behar, P. Beiersdorfer, G. V. Brown, D. A. Liedahl, and K. J. Reed, 2001, Astrophys. J. **563**, 462.
- Gu, M. F., M. Schmidt, P. Beiersdorfer, H. Chen, D. B. Thorn, E. Träbert, E. Behar, and S. M. Kahn, 2005, Astrophys. J. **627**, 1066.
- Gu, M. F., *et al.*, 2004, Astrophys. J. Lett. **607**, L143.
- Gupta, G. P., N. C. Deb, and A. Z. Msezane, 2000, At. Data Nucl. Data Tables **74**, 257.
- Gupta, G. P., and S. S. Tayal, 1998, Astrophys. J. **506**, 464.
- Gupta, G. P., and S. S. Tayal, 1999, Astrophys. J. **510**, 1078.
- Gwinner, G., D. W. Savin, D. Schwalm, A. Wolf, S. Schippers, A. Müller, N. R. Badnell, and M. H. Chen, 2001, Phys. Scr. **T92**, 319.
- Haberli, R. M., T. I. Gombosi, D. L. DeZeeuw, M. R. Combi, and K. G. Powell, 1997, Science **276**, 939.
- Hagelstein, P. L., and R. K. Jung, 1987, At. Data Nucl. Data Tables **37**, 121.
- Hahn, Y., 1977, Phys. Rev. Lett. **39**, 82.
- Hahn, Y., 1978, Phys. Rev. A **18**, 1028.
- Hahn, Y., 1980, Phys. Rev. A **22**, 2896.
- Hahn, Y., 1989, Phys. Scr. **T28**, 25.
- Hahn, Y., 1993, J. Quant. Spectrosc. Radiat. Transf. **49**, 81.
- Hahn, Y., 1997, Rep. Prog. Phys. **60**, 691.
- Hahn, Y., and R. Bellantone, 1989, Phys. Rev. A **40**, 6117.
- Hamdan, M., K. Burkinshaw, and J. B. Hasted, 1978, J. Phys. B **11**, 331.

- Hamilton, A. J. S., R. A. Chevalier, and C. L. Sarazin, 1983, *Astrophys. J., Suppl. Ser.* **51**, 115.
- Harra-Murnion, L. K., *et al.*, 1996, *Astron. Astrophys.* **308**, 670.
- Hartree, D. R., 1957, *The Calculation of Atomic Structures* (Wiley, New York).
- Havener, C. C., 2001, *ASP Conference Series 247: Spectroscopic Challenges of Photoionized Plasmas*, Vol. 247, p. 17.
- Havener, C. C., M. S. Huq, H. F. Krause, P. A. Schulz, and R. A. Phaneuf, 1989, *Phys. Rev. A* **39**, 1725.
- Hayton, S. J. T., and B. Peart, 1994, *J. Phys. B* **27**, 5331.
- Hebb, M. H., and D. H. Menzel, 1940, *Astrophys. J.* **92**, 408.
- Heil, T. G., G. J. Bottrell, and C. Bottcher, 1985, *Nucl. Instrum. Methods Phys. Res. B* **9**, 448.
- Henry, H. J. W., 1970, *Astrophys. J.* **161**, 1153.
- Henry, H. J. W., 1979, *J. Phys. B* **12**, L309.
- Henry, H. J. W., and R. Williams, 1968, *Publ. Astron. Soc. Pac.* **80**, 669.
- Henry, R. J. W., and A. Z. Msezane, 1982, *Phys. Rev. A* **26**, 2545.
- Hibbert, A., 1975, *Comput. Phys. Commun.* **9**, 141.
- Hoekstra, R., J. P. M. Beijers, A. R. Schlatmann, R. Morgenstern, and F. J. de Heer, 1990, *Phys. Rev. A* **41**, 4800.
- House, L. L., 1969, *Astrophys. J., Suppl.* **18**, 21.
- Howald, A. M., D. C. Gregory, F. W. Meyer, R. A. Phaneuf, A. Müller, N. Djuric, and G. H. Dunn, 1986, *Phys. Rev. A* **33**, 3779.
- Huang, K.-N., 1985, *At. Data Nucl. Data Tables* **32**, 503.
- Hudson, E. T., K. Bartschat, M. P. Scott, P. G. Burke, and V. M. Burke, 1996, *J. Phys. B* **29**, 5513.
- Hummer, D. G., K. A. Berrington, W. Eissner, A. K. Pradhan, H. E. Saraph, and J. A. Tully, 1993, *Astron. Astrophys.* **279**, 298.
- Huq, M. S., C. C. Havener, and R. A. Phaneuf, 1989, *Phys. Rev. A* **40**, 1811.
- Inokuti, M., and Y. Kim, 1968, *Phys. Rev.* **173**, 154.
- Isler, R. C., E. C. Crume, and D. E. Arnurius, 1982, *Phys. Rev. A* **26**, 2105.
- Itikawa, Y., 1991, *At. Data Nucl. Data Tables* **49**, 209.
- Itikawa, Y., 1996, *At. Data Nucl. Data Tables* **63**, 315.
- Itikawa, Y., 2002, *At. Data Nucl. Data Tables* **80**, 117.
- Itikawa, Y., K. Takayanagi, and T. Iwai, 1984, *At. Data Nucl. Data Tables* **31**, 215.
- Itoh, H., 1979, *Publ. Astron. Soc. Jpn.* **31**, 541.
- Jacobs, V. L., J. Davis, and P. C. Kepple, 1976, *Phys. Rev. Lett.* **37**, 1390.
- Jacobs, V. L., J. Davis, P. C. Kepple, and M. Blaha, 1977a, *Astrophys. J.* **211**, 605.
- Jacobs, V. L., J. Davis, P. C. Kepple, and M. Blaha, 1977b, *Astrophys. J.* **215**, 690.
- Jacobs, V. L., J. Davis, J. E. Rogerson, and M. Blaha, 1979, *Astrophys. J.* **230**, 627.
- Jacobs, V. L., and B. F. Rozsnyai, 1986, *Phys. Rev. A* **34**, 216.
- Jacobs, V. L., B. F. Rozsnyai, and J. W. Cooper, 1980, *Phys. Rev. A* **21**, 1917.
- Jain, N. K., and U. Narain, 1978, *Astron. Astrophys., Suppl. Ser.* **31**, 1.
- Janev, R. K., and H. Winter, 1985, *Phys. Rep.* **117**, 265.
- Janjusevic, M., and Y. Hahn, 1989, *Phys. Rev. A* **40**, 5641.
- Janzen, P. H., L. D. Gardner, D. B. Reisenfeld, D. W. Savin, J. L. Kohl, and K. Bartschat, 1999, *Phys. Rev. A* **59**, 4821.
- Johnson, C. T., A. E. Kingston, and P. L. Dufton, 1986, *Mon. Not. R. Astron. Soc.* **220**, 155.
- Johnston, W. D., and H.-J. Kunze, 1971, *Phys. Rev. A* **4**, 962.
- Jones, M., 1970, *J. Phys. B* **3**, 1571.
- Jones, M., 1974, *Mon. Not. R. Astron. Soc.* **169**, 211.
- Jordan, C., 1969, *Mon. Not. R. Astron. Soc.* **142**, 501.
- Jordan, C., 1970, *Mon. Not. R. Astron. Soc.* **148**, 17.
- Juett, A. M., N. S. Schulz, and D. Chakrabarty, 2004, *Astrophys. J.* **612**, 308.
- Jupen, C., R. C. Isler, and E. Träbert, 1993, *Mon. Not. R. Astron. Soc.* **264**, 627.
- Kaastra, J. S., 1992, *An X-Ray Spectral Code for Optically Thin Plasmas* (Internal SRON-Leiden Rep., updated version 2.0).
- Kaastra, J. S., and R. Mewe, 1993, *Astron. Astrophys., Suppl. Ser.* **97**, 443.
- Kaastra, J. S., R. Mewe, and H. Nieuwenhuijzen, 1996, in *UV and X-Ray Spectroscopy of Astrophysical and Laboratory Plasmas*, Proceedings of the 11th Colloquium 1995, edited by K. Yamashita and T. Watanabe, Frontiers Science Series No. 15 (Universal Academy, Tokyo), p. 411.
- Kaastra, J. S., *et al.*, 2004, *Astron. Astrophys.* **428**, 57.
- Kahn, S. M., E. Behar, A. Kinkhabwala, and D. W. Savin, 2004, *Frontiers of X-ray Astronomy*, edited by A. C. Fabian, K. A. Pounds, and R. D. Blandford (Cambridge University Press, Cambridge, UK).
- Kallman, T. R., P. Palmeri, M. A. Bautista, C. Mendoza, and J. H. Krolik, 2004, *Astrophys. J., Suppl. Ser.* **55**, 675.
- Kamber, E. Y., C. Akgungor, C. Leather, and A. G. Brenton, 1996, *Phys. Rev. A* **54**, 1452.
- Karim, K. R., and C. P. Bhalla, 1986, *Phys. Lett. A* **116**, 172.
- Karim, K. R., and C. P. Bhalla, 1988a, *Phys. Rev. A* **37**, 840.
- Karim, K. R., and C. P. Bhalla, 1988b, *Phys. Rev. A* **37**, 2599.
- Karim, K. R., and C. P. Bhalla, 1988c, *Phys. Rev. A* **37**, 1507.
- Karim, K. R., and C. P. Bhalla, 1989a, *Nucl. Instrum. Methods Phys. Res. B* **40**, 366.
- Karim, K. R., and C. P. Bhalla, 1989b, *Phys. Rev. A* **39**, 3548.
- Karim, K. R., and C. P. Bhalla, 1990, *Phys. Rev. A* **42**, 3555.
- Karim, K. R., and C. P. Bhalla, 1991, *Phys. Rev. A* **43**, 615.
- Karim, K. R., and C. P. Bhalla, 1995, *J. Phys. B* **28**, 5229.
- Karim, K. R., C. P. Bhalla, M. Ruesink, S. Biel, and M. Wilson, 1991, *J. Phys. B* **24**, L375.
- Karim, K. R., M. Ruesink, and C. P. Bhalla, 1992, *Phys. Rev. A* **46**, 3904.
- Karstensen, F., and M. Schneider, 1978, *J. Phys. B* **11**, 167.
- Karzas, W., and R. Latter, 1961, *Astrophys. J., Suppl.* **6**, 167.
- Kastner, S. O., 1983, *Astrophys. J.* **275**, 922.
- Kato, T., 1976, *Astrophys. J., Suppl.* **30**, 397.
- Kato, T., 1994, *At. Data Nucl. Data Tables* **57**, 181.
- Kato, T., K. Masai, and M. Arnaud, 1991, National Institute for Fusion Science, Nagoya, Japan, Research Report, NIFS-DATA-14.
- Kato, T., and S. Nakazaki, 1989, *At. Data Nucl. Data Tables* **42**, 313.
- Kato, T., U. Safronova, A. Shlyptseva, M. Cornille, J. Dubau, and J. Nilsen, 1997, *At. Data Nucl. Data Tables* **67**, 225.
- Kaufman, V., and W. C. Martin, 1991a, *J. Phys. Chem. Ref. Data* **20**, 775.
- Kaufman, V., and W. C. Martin, 1991b, *J. Phys. Chem. Ref. Data* **20**, 83.
- Kaufman, V., and W. C. Martin, 1993, *J. Phys. Chem. Ref. Data* **22**, 279.
- Keenan, F. P., A. E. Kingston, and D. L. McKenzie, 1986, *Astrophys. J.* **303**, 486.
- Kelly, R. L., 1987, *J. Phys. Chem. Ref. Data Suppl.* **16**, 1.

- Kenntner, J., *et al.*, 1995, Nucl. Instrum. Methods Phys. Res. B **98**, 142.
- Kharchenko, V., and A. Dalgarno, 2000, J. Geophys. Res. **105**, 18351.
- Kieffer, L. J., and G. H. Dunn, 1966, Rev. Mod. Phys. **38**, 1.
- Kimura, M., N. Kobayashi, S. Ohtani, and H. Tawara, 1987, J. Phys. B **20**, 3873.
- Kingdon, J. B., and G. J. Ferland, 1996, Astrophys. J., Suppl. Ser. **106**, 205.
- Kinkhabwala, A., *et al.*, 2002, Astrophys. J. **575**, 732.
- Kisielius, R., A. Hibbert, G. J. Ferland, M. E. Foord, S. J. Rose, P. A. M. vanHoof, and F. P. Keenan, 2003, Mon. Not. R. Astron. Soc. **344**, 696.
- Knapp, D., *et al.*, 1989, Phys. Rev. Lett. **62**, 2104.
- Knopp, H., H. Teng, S. Ricz, S. Schippers, A. Müller, 2001, Phys. Scr. **T92**, 379.
- Kotchigova, S., K. Kirby, P. Mohr, and S. Tupitsyn, 2005, in *X-ray Diagnostics for Astrophysical Plasmas*, edited by R. Smith (AIP, Melville, NY).
- Kraemer, S., *et al.*, 2004, Astrophys. J. **604**, 556.
- Krolik, J. H., C. F. McKee, and C. B. Tarter, 1981, Astrophys. J. **249**, 422.
- Krongold, Y., F. Nicastro, N. S. Brickhouse, M. Elvis, D. A. Liedahl, and S. Mathur, 2003, Astrophys. J. **597**, 832.
- Kumar, S., and K. Saha, 1998, J. Phys. B **31**, L937.
- Kunze, H.-J., 1972, Space Sci. Rev. **13**, 565.
- Kunze, H.-J., A. H. Gabriel, and H. R. Griem, 1968, Phys. Rev. **165**, 267.
- Lagattuta, K., and Y. Hahn, 1982a, J. Phys. B **15**, 2101.
- Lagattuta, K., and Y. Hahn, 1982b, Phys. Rev. A **26**, 1125.
- Lagattuta, K., and Y. Hahn, 1983a, Phys. Rev. Lett. **50**, 668.
- Lagattuta, K., and Y. Hahn, 1983b, Phys. Rev. A **27**, 1675.
- Lagattuta, K., I. Nasser, and Y. Hahn, 1986, Phys. Rev. A **33**, 2782.
- Lagattuta, K. J., and Y. Hahn, 1981a, Phys. Lett. **84A**, 468.
- Lagattuta, K. J., and Y. Hahn, 1981b, Phys. Rev. A **24**, 785.
- Landi, E., and A. K. Bhatia, 2003a, Astrophys. J., Suppl. Ser. **149**, 251.
- Landi, E., and A. K. Bhatia, 2003b, Astrophys. J. **589**, 1075.
- Landi, E., and A. K. Bhatia, 2005a, Astron. Astrophys. **444**, 305.
- Landi, E., and A. K. Bhatia, 2005b, At. Data Nucl. Data Tables **90**, 177.
- Landi, E., and A. K. Bhatia, 2005c, At. Data Nucl. Data Tables **89**, 195.
- Landi, E., K. P. Dere, P. R. Young, G. del Zanna, H. E. Mason, and M. Landini, 2005, in *X-ray Diagnostics of Astrophysical Plasmas: Theory, Experiment, and Observation*, edited by R. K. Smith, AIP Conf. Proc. No. 774 (AIP, Melville, NY), p. 409.
- Landi, E., and M. Landini, 1998, Astron. Astrophys., Suppl. Ser. **133**, 411.
- Landi, E., and M. Landini, 2002, Astron. Astrophys. **384**, 1124.
- Landi, E., M. Landini, K. P. Dere, P. R. Young, and H. E. Mason, 1999, Astron. Astrophys., Suppl. Ser. **135**, 339.
- Landi, E., and K. Phillips, 2005, Astrophys. J., Suppl. Ser. **160**, 286.
- Landi, E., P. J. Storey, and C. J. Zeippen, 2004, Astrophys. J. **607**, 640.
- Landini, M., and B. C. Monsignori Fossi, 1972, Astron. Astrophys., Suppl. Ser. **7**, 291.
- Lang, J., and H. P. Summers, 1994, At. Data Nucl. Data Tables **57**, 215.
- Layzer, D., 1951, Astron. J. **56**, 43.
- Lee, J. C., P. M. Ogle, C. R. Canizares, H. L. Marshall, N. S. Schulz, R. Morales, A. C. Fabian, and K. Iwasawa, 2001, Astrophys. J. Lett. **554**, L13.
- Lemen, J. R., K. J. H. Phillips, R. D. Cowan, J. Hata, and I. P. Grant, 1984, Astron. Astrophys. **135**, 313.
- Lennon, M. A., K. L. Bell, H. B. Gilbody, J. G. Hughes, A. E. Kingston, M. J. Murray, and F. J. Smith, 1988, J. Phys. Chem. Ref. Data **17**, 1285.
- Lepson, J. K., P. Beiersdorfer, E. Behar, and S. M. Kahn, 2003, Astrophys. J. **590**, 604.
- Lepson, J. K., P. Beiersdorfer, E. Behar, and S. M. Kahn, 2005a, Nucl. Instrum. Methods Phys. Res. B **235**, 131.
- Lepson, J. K., P. Beiersdorfer, E. Behar, and S. M. Kahn, 2005b, Astrophys. J. **625**, 1045.
- Liedahl, D., 2003, *Atomic Data for X-Ray Astronomy, 25th Meeting of the IAU, Joint Discussion 17, Sydney, Australia* (Kluwer, Dordrecht), p. 17.
- Liedahl, D. A., A. L. Osterheld, and W. H. Goldstein, 1995, Astrophys. J. Lett. **438**, L115.
- Lin, C. D., W. R. Johnson, and A. Dalgarno, 1977, Phys. Rev. A **15**, 154.
- Lin, S.-H., C.-S. Hsue, and K. T. Chung, 2001a, Phys. Rev. A **64**, 012709.
- Lin, S.-H., C.-S. Hsue, and K. T. Chung, 2001b, Phys. Rev. A **65**, 032706.
- Linkemann, J., A. Muller, J. Kenntner, D. Habs, D. Schwalm, A. Wolf, N. R. Badnell, and M. S. Pindzola, 1995, Phys. Rev. Lett. **74**, 4173.
- Lisse, C. M., *et al.*, 1996, Science **274**, 205.
- Loch, S. D., J. Colgan, M. S. Pindzola, M. Westermann, F. Scheuermann, K. Aichele, D. Hathiramani, and E. Salzborn, 2003, Phys. Rev. A **67**, 042714.
- Loch, S. D., M. S. Pindzola, C. P. Ballance, and D. C. Griffin, 2006, J. Phys. B **39**, 85.
- Loch, S. D., *et al.*, 2005, Phys. Rev. A **71**, 012716.
- Lotz, W., 1967, Astrophys. J., Suppl. **14**, 207.
- Lotz, W., 1968, Z. Phys. **216**, 241.
- Louergue, M., 1971, Astron. Astrophys. **15**, 216.
- Louergue, M., and H. Nussbaumer, 1973, Astron. Astrophys. **24**, 209.
- Louergue, M., and H. Nussbaumer, 1975, Astron. Astrophys. **45**, 125.
- Lozano, J. A., M. Niimura, S. J. Smith, A. Chutjian, and S. S. Tayal, 2001, Phys. Rev. A **63**, 042713.
- Man, K., A. C. H. Smith, and M. F. A. Harrison, 1987, J. Phys. B **20**, 2571.
- Man, K., A. C. H. Smith, and M. F. A. Harrison, 1993, J. Phys. B **26**, 1365.
- Mann, J. B., 1983, At. Data Nucl. Data Tables **29**, 407.
- Mannervik, S., D. Dewitt, L. Engström, J. Lidberg, E. Lindroth, R. Schuch, and W. Zong, 1998, Phys. Rev. Lett. **81**, 313.
- Marchalant, P. J., and K. Bartschat, 1997, J. Phys. B **30**, 4373.
- Marchalant, P. J., K. Bartschat, and I. Bray, 1997, J. Phys. B **30**, L435.
- Mariska, J. T., 1993, in *The Solar Transition Region*, edited by John T. Mariska (Cambridge University Press, Cambridge, UK).
- Martin, I., J. Karwowski, G. H. F. Diercksen, and C. Barrientos, 1993, Astron. Astrophys., Suppl. Ser. **100**, 595.
- Martin, S. O., B. Peart, and K. T. Dolder, 1968, J. Phys. B **1**, 537.

- Martin, W. C., and R. Zalubas, 1979, J. Phys. Chem. Ref. Data **8**, 817.
- Martin, W. C., and R. Zalubas, 1983, J. Phys. Chem. Ref. Data **12**, 323.
- Martin, W. C., R. Zalubas, and A. Musgrove, 1990, J. Phys. Chem. Ref. Data **19**, 821.
- Masai, K., 1997, Astron. Astrophys. **324**, 410.
- Masai, K., and M. Ishida, 2004, Astrophys. J. **607**, 76.
- Mason, H. E., 1994, At. Data Nucl. Data Tables **57**, 305.
- Mason, H. E., and A. K. Bhatia, 1983, Astron. Astrophys., Suppl. Ser. **52**, 181.
- Mason, H. E., G. A. Doschek, U. Feldman, and A. K. Bhatia, 1979, Astron. Astrophys. **73**, 74.
- Mason, H. E., and P. J. Storey, 1980, Mon. Not. R. Astron. Soc. **191**, 631.
- Massey, H. S. W., and D. R. Bates, 1942, Rep. Prog. Phys. **9**, 62.
- Matsumoto, A., et al., 1990, J. Phys. Soc. Jpn. **59**, 902.
- Mauche, C., 2005, in *X-ray Diagnostics of Astrophysical Plasmas: Theory, Experiment, and Observation*, edited by R. K. Smith, AIP Conf. Proc. No. 774 (AIP, Melville, NY), p. 133.
- Mazzotta, P., G. Mazzitelli, S. Colafrancesco, and N. Vittorio, 1998, Astron. Astrophys., Suppl. Ser. **133**, 403.
- McDowell, M. R. C., and J. H. Williamson, 1963, Phys. Lett. **4**, 159.
- McGowan, J. W., and E. M. Clarke, 1968, Phys. Rev. **167**, 43.
- McGuire, E. J., 1969, Phys. Rev. **185**, 1.
- McGuire, E. J., 1970, Phys. Rev. A **2**, 273.
- McGuire, E. J., 1971a, Phys. Rev. A **3**, 1801.
- McGuire, E. J., 1971b, Phys. Rev. A **3**, 587.
- McGuire, E. J., 1972, Phys. Rev. A **5**, 1052.
- McGuire, E. J., 1977, Phys. Rev. A **16**, 62.
- McGuire, E. J., 1982, Phys. Rev. A **26**, 125.
- McLaughlin, D. J., and Y. Hahn, 1982, Phys. Lett. **88**, 394.
- McLaughlin, D. J., and Y. Hahn, 1983a, Phys. Rev. A **27**, 1389.
- McLaughlin, D. J., and Y. Hahn, 1983b, Phys. Rev. A **28**, 493.
- McLaughlin, D. J., and Y. Hahn, 1983c, J. Phys. B **16**, L739.
- McLaughlin, T. K., J. M. Hodgkinson, H. Tawara, R. W. McCullough, and H. B. Gilbody, 1993, J. Phys. B **26**, 3587.
- McLaughlin, T. K., R. W. McCullough, and H. B. Gilbody, 1992, J. Phys. B **25**, 1257.
- McLaughlin, T. K., S. M. McCullough, and R. W. McCullough, H. B. Gilbody, 1990, J. Phys. B **23**, 737.
- McWhirter, R. W. P., 1994, At. Data Nucl. Data Tables **57**, 39.
- Meekins, J. F., R. W. Kreplin, T. A. Chubb, and H. Friedman, 1968, Science **162**, 891.
- Mendoza, C., T. R. Kallman, M. A. Bautista, and P. Palmeri, 2004, Astron. Astrophys. **414**, 377.
- Menzel, D., and C. Pekeris, 1935, Mon. Not. R. Astron. Soc. **96**, 77.
- Mewe, R., 1972a, Astron. Astrophys. **20**, 215.
- Mewe, R., 1972b, Sol. Phys. **22**, 459.
- Mewe, R., 1975, Sol. Phys. **44**, 383.
- Mewe, R., and E. H. B. M. Gronenschild, 1981, Astron. Astrophys., Suppl. Ser. **45**, 11.
- Mewe, R., E. H. B. M. Gronenschild, and G. H. J. van der Oord, 1985, Astron. Astrophys., Suppl. Ser. **62**, 197.
- Mewe, R., J. S. Kaastra, and D. A. Liedahl, 1995, Legacy **6**, 16.
- Mewe, R., J. S. Kaastra, C. J. Schrijver, G. H. J. van den Oord, and F. J. M. Alkemade, 1995, Astron. Astrophys. **296**, 477.
- Mewe, R., J. R. Lemen, and G. H. J. van den Oord, 1986, Astron. Astrophys., Suppl. Ser. **65**, 511.
- Mewe, R., and J. Schrijver, 1975, Astrophys. Space Sci. **38**, 345.
- Mewe, R., and J. Schrijver, 1978a, Astron. Astrophys., Suppl. Ser. **33**, 311.
- Mewe, R., and J. Schrijver, 1978b, Astron. Astrophys. **65**, 99.
- Mihalas, D., 1978, *Stellar Atmospheres* (Freeman, San Francisco).
- Mitchell, J. B. A., C. T. Ng, J. L. Forand, D. P. Levac, R. E. Mitchell, A. Sen, D. B. Miko, and J. W. McGowan, 1983, Phys. Rev. Lett. **50**, 335.
- Mitnik, D. M., and N. R. Badnell, 2004, Astron. Astrophys. **425**, 1153.
- Mitnik, D. M., M. S. Pindzola, D. C. Griffin, N. R. Badnell, 1999, J. Phys. B **32**, L479.
- Mitnik, D. M., J. A. Shaw, M. S. Pindzola, D. C. Griffin, and N. R. Badnell, 1998, Comput. Phys. Commun. **114**, 368.
- Montague, R. G., M. J. Diserens, and M. F. A. Harrison, 1984, J. Phys. B **17**, 2085.
- Moores, D. L., L. B. Golden, and D. H. Sampson, 1980, J. Phys. B **13**, 385.
- Moores, D. L., and M. S. Pindzola, 1990, Phys. Rev. A **42**, 5384.
- Moussa, A. H., H. H. Ramadan, and Y. Hahn, 1988, Phys. Rev. A **38**, 5076.
- Mroczkowski, T., D. W. Savin, R. Rejoub, P. S. Krstić, and C. C. Havener, 2003, Phys. Rev. A **68**, 032721.
- Muehlethaler, H. P., and H. Nussbaumer, 1976, Astron. Astrophys. **48**, 109.
- Mueller, D. W., T. J. Morgan, G. H. Dunn, D. C. Gregory, and D. H. Crandall, 1985, Phys. Rev. A **31**, 2905.
- Müller, A., 1991, in *Physics of Ion Impact Phenomena*, edited by D. Mathur, Springer Series in Chemical Physics Vol. 54 (Springer-Verlag, Berlin), pp. 13–90.
- Müller, A., K. Huber, K. Tinschert, R. Becker, and E. Salzborn, 1985, J. Phys. B **18**, 2993.
- Müller, A., H. Teng, G. Hofmann, R. A. Phaneuf, and E. Salzborn, 2000, Phys. Rev. A **62**, 062720.
- Müller, A., K. Tinschert, C. Achenbach, R. Becker, and E. Salzborn, 1985, J. Phys. B **18**, 3011.
- Nagy, P., et al., 1980, J. Phys. B **13**, 1249.
- Nahar, S. N., 1995, Astrophys. J., Suppl. Ser. **101**, 423.
- Nahar, S. N., 1996, Astrophys. J., Suppl. Ser. **106**, 213.
- Nahar, S. N., 2004, Phys. Rev. A **69**, 042714.
- Nahar, S. N., and A. K. Pradhan, 1994, Phys. Rev. A **49**, 1816.
- Nasser, I., and Y. Hahn, 1989, Phys. Rev. A **39**, 401.
- Netzer, H., 1996, Astrophys. J. **473**, 781.
- Netzer, H., 2004, Astrophys. J. **604**, 551.
- Nikolic, D., et al., 2004, Phys. Rev. A **70**, 062723.
- Nilsen, J., 1986, J. Phys. B **19**, 2401.
- Nilsen, J., 1987, At. Data Nucl. Data Tables **37**, 191.
- Nilsen, J., 1988, At. Data Nucl. Data Tables **38**, 339.
- Nussbaumer, H., 1972, Astron. Astrophys. **16**, 77.
- Nussbaumer, H., 1973, Astron. Astrophys. **27**, 303.
- Nussbaumer, H., 1977, Astron. Astrophys. **58**, 291.
- Nussbaumer, H., and P. J. Storey, 1983, Astron. Astrophys. **126**, 75.
- Nussbaumer, H., and P. J. Storey, 1984, Astron. Astrophys. **56**, 293.
- Nussbaumer, H., and P. J. Storey, 1986, Astron. Astrophys., Suppl. Ser. **64**, 545.
- Nussbaumer, H., and P. J. Storey, 1987, Astron. Astrophys., Suppl. Ser. **69**, 123.
- Oelgoetz, J., and A. K. Pradhan, 2001, Mon. Not. R. Astron. Soc. **327**, L42.
- Oelgoetz, J., and A. K. Pradhan, 2004, Mon. Not. R. Astron. Soc. **354**, 1093.
- Omar, G., and Y. Hahn, 1987, Phys. Rev. A **35**, 918.

- Osterbrock, D. E., and G. J. Ferland, 2006, in *Astrophysics of Gaseous Nebulae and Active Galactic Nuclei*, 2nd ed., edited by D. E. Osterbrock and G. J. Ferland (University Science Books, Sausalito, CA).
- Owocki, S. P., and J. D. Scudder, 1983, *Astrophys. J.* **270**, 758.
- Paerels, F., et al., 2001, *Astrophys. J.* **546**, 338.
- Paerels, F. B. S., and S. M. Kahn, 2003, *Annu. Rev. Astron. Astrophys.* **41**, 291.
- Palmeri, P., C. Mendoza, T. R. Kallman, and M. A. Bautista, 2002, *Astrophys. J. Lett.* **577**, L119.
- Palmeri, P., C. Mendoza, T. R. Kallman, and M. A. Bautista, 2003, *Astron. Astrophys.* **403**, 1175.
- Palmeri, P., C. Mendoza, T. R. Kallman, M. A. Bautista, and M. Meléndez, 2003, *Astron. Astrophys.* **410**, 359.
- Parkinson, J. H., 1973, *Astron. Astrophys.* **24**, 215.
- Parkinson, J. H., 1975, *Sol. Phys.* **42**, 183.
- Parpia, F. A., C. Froese Fischer, and I. P. Grant, 1996, *Comput. Phys. Commun.* **94**, 249.
- Parpia, F. A., and W. R. Johnson, 1972, *Phys. Rev. A* **26**, 1142.
- Peart, B., et al., 1991, *J. Phys. B* **24**, 4453.
- Pelan, J., and K. A. Berrington, 1995, *Astron. Astrophys., Suppl. Ser.* **110**, 209.
- Pequignot, D., 1980, *Astron. Astrophys.* **81**, 356.
- Pequignot, D., P. Petitjean, and C. Boisson, 1991, *Astron. Astrophys.* **251**, 680.
- Pequignot, D., G. Stasinska, and S. M. V. Aldrovandi, 1978, *Astron. Astrophys.* **63**, 313.
- Peterson, J. R., S. M. Kahn, F. B. S. Paerels, J. S. Kaastra, T. Tamura, J. A. M. Bleeker, C. Ferrigno, and J. G. Jernigan, 2003, *Astrophys. J.* **590**, 207.
- Phaneuf, R. A., C. C. Havener, G. H. Dunn, and A. Müller, 1999, *Rep. Prog. Phys.* **62**, 1143.
- Phaneuf, R. A., et al., 1987, Report No. ORNL-6090/V5 U.S. Dept. of Energy, Washington DC.
- Phillips, K. J. H., A. K. Bhatia, H. E. Mason, and D. M. Zarro, 1996, *Astrophys. J.* **466**, 549.
- Phillips, K. J. H., C. J. Greer, A. K. Bhatia, I. H. Coffey, R. Barnsley, and F. P. Keenan, 1997, *Astron. Astrophys.* **324**, 381.
- Phillips, K. J. H., J. R. Lemen, R. D. Cowan, G. A. Doschek, and J. W. Leibacher, 1983, *Astrophys. J.* **265**, 1120.
- Phillips, K. J. H., et al., 1982, *Astrophys. J.* **256**, 774.
- Pieksma, M., M. E. Bannister, W. Wu, and C. C. Havener, 1997, *Phys. Rev. A* **55**, 3526.
- Pindzola, M. S., N. R. Badnell, and D. C. Griffin, 1990, *Phys. Rev. A* **42**, 282.
- Pindzola, M. S., J. Colgan, F. Robicheaux, and D. C. Griffin, 2000, *Phys. Rev. A* **62**, 042705.
- Pindzola, M. S., D. C. Griffin, and C. Bottcher, 1986a, *Phys. Rev. A* **33**, 3787.
- Pindzola, M. S., D. C. Griffin, and C. Bottcher, 1986b, *Phys. Rev. A* **34**, 3668.
- Pindzola, M. S., D. C. Griffin, C. Bottcher, M. Buie, and D. Gregory, 1991, *Phys. Scr.* **T37**, 35.
- Pindzola, M. S., D. C. Griffin, C. Bottcher, D. H. Crandall, R. A. Phaneuf, and D. C. Gregory, 1984, *Phys. Rev. A* **29**, 1749.
- Pindzola, M. S., D. C. Griffin, and J. H. Macek, 1995, *Phys. Rev. A* **51**, 2186.
- Pindzola, M. S., D. M. Mitnik, J. A. Shaw, D. C. Griffin, N. R. Badnell, H. P. Summers, and D. R. Schultz, 1998, *Phys. Scr.* **57**, 514.
- Pindzola, M. S., D. L. Moores, and D. C. Griffin, 1989, *Phys. Rev. A* **40**, 4941.
- Pindzola, M. S., and F. J. Robicheaux, 2000, *Phys. Rev. A* **61**, 052707.
- Pindzola M. S., F. Robicheaux, N. R. Badnell, and T. W. Gorczyca, 1997, *Phys. Rev. A* **56** 1994.
- Podobedova, L. I., A. Musgrave, D. E. Kelleher, J. Reader, W. L. Wiese, J. S. Coursey, and K. Olsen, 2003, <http://physics.nist.gov/PhysRefData/Chandra/index.html>
- Porquet, D., and J. Dubau, 2000, *Astron. Astrophys., Suppl. Ser.* **143**, 495.
- Pradhan, A. K., 1983, *Astrophys. J.* **270**, 339.
- Pradhan, A. K., 1985, *Astrophys. J.* **288**, 824.
- Pradhan, A. K., 1994, *At. Data Nucl. Data Tables* **57**, 297.
- Pradhan, A. K., 2000, *Astrophys. J. Lett.* **545**, L165.
- Pradhan, A. K., G. X. Chen, F. Delahaye, S. N. Nahar, and J. Oelgoetz, 2003, *Mon. Not. R. Astron. Soc.* **341**, 1268.
- Pradhan, A. K., and J. W. Gallagher, 1992, *At. Data Nucl. Data Tables* **52**, 227.
- Pradhan, A. K., and J. M. Shull, 1981, *Astrophys. J.* **249**, 821.
- Quinet, P., 2000, *Phys. Scr.* **61**, 45.
- Racah, G., 1942, *Phys. Rev.* **62**, 438.
- Racah, G., 1943, *Phys. Rev.* **63**, 367.
- Rachafi, S., et al., 1991, *J. Phys. B* **24**, 1037.
- Ramadan, H. H., and Y. Hahn, 1989, *Phys. Rev. A* **39**, 3350.
- Rasmussen, A. P., E. Behar, S. M. Kahn, J. W. den Herder, and K. van der Heyden, 2001, *Astron. Astrophys.* **365**, L231.
- Raymond, J. C., and B. Smith, 1977, *Astrophys. J., Suppl.* **35**, 419.
- Raymond, J. C., and B. W. Smith, 1986, *Astrophys. J.* **306**, 762.
- Reilman, R. F., and S. T. Manson, 1978, *Phys. Rev. A* **18**, 2124.
- Reilman, R. F., and S. T. Manson, 1979, *Astrophys. J., Suppl.* **40**, 815.
- Rejoub, R., M. E. Bannister, C. C. Havener, D. W. Savin, C. J. Verzani, J. G. Wang, and P. C. Stancil, 2004, *Phys. Rev. A* **69**, 052704.
- Retter, J. A., J. N. Gau, and Y. Hahn, 1978, *Phys. Rev. A* **17**, 998.
- Rinn, K., D. C. Gregory, L. J. Wang, R. A. Phaneuf, and A. Müller, 1987, *Phys. Rev. A* **36**, 595.
- Robicheaux, F., and M. S. Pindzola, 1997, *Phys. Rev. Lett.* **79**, 2237.
- Roszman, L. J., 1979, *Phys. Rev. A* **20**, 673.
- Roszman, L. J., 1987a, *Phys. Rev. A* **35**, 2138.
- Roszman, L. J., 1987b, *Phys. Rev. A* **35**, 3368.
- Roszman, L. J., 1987c, *Phys. Rev. A* **35**, 2122.
- Roszman, L. J., 1989a, *Phys. Scr.* **T28**, 36.
- Roszman, L. J., 1989b, *Phys. Rev. A* **39**, 2073.
- Roszman, L. J., 1989c, *Phys. Rev. A* **39**, 913.
- Rothe, E. W., L. L. Marino, R. H. Neynaber, and S. M. Trujillo, 1962, *Phys. Rev.* **125**, 582.
- Ruszkowski, M., M. Brüggen, and M. C. Begelman, 2004, *Astrophys. J.* **611**, 158.
- Safranova, U., A. Vasiliev, and R. Smith, 2000, *Can. J. Phys.* **78**, 12.
- Safranova, U. I., and A. M. Urnov, 1980, *J. Phys. B* **13**, 869.
- Safranova, U. I., A. A. Vasilyev, and R. K. Smith, 2001, *Can. J. Phys.* **78**, 1055.
- Saha, B. C., 1995, *Phys. Rev. A* **51**, 5021.
- Sako, M., S. M. Kahn, F. Paerels, and D. A. Liedahl, 2000, *Astrophys. J. Lett.* **543**, L115.
- Sampson, D. H., 1982, *J. Phys. B* **15**, 2087.
- Sampson, D. H., S. J. Goett, and R. E. H. Clark, 1983, *At. Data Nucl. Data Tables* **29**, 467.

- Sampson, D. H., and L. B. Golden, 1979, *J. Phys. B* **12**, L785.
- Sampson, D. H., and L. B. Golden, 1981, *J. Phys. B* **14**, 903.
- Sampson, D. H., and A. D. Parks, 1974, *Astrophys. J., Suppl.* **28**, 323.
- Sampson, D. H., G. M. Weaver, S. J. Goett, H. Zhang, and R. E. H. Clark, 1986, *At. Data Nucl. Data Tables* **35**, 223.
- Sampson, D. H., H. L. Zhang, and C. J. Fontes, 1990, *At. Data Nucl. Data Tables* **44**, 209.
- Sampson, D. H., H. L. Zhang, and C. J. Fontes, 1991, *At. Data Nucl. Data Tables* **48**, 25.
- Sampson, D. H., H. L. Zhang, and C. J. Fontes, 1994, *At. Data Nucl. Data Tables* **57**, 97.
- Savin, D. W., 1999, *Astrophys. J.* **523**, 855.
- Savin, D. W., 2000, *Astrophys. J.* **533**, 106.
- Savin, D. W., 2005, in *X-Ray Diagnostics of Astrophysical Plasmas (XDAP 2000)*, edited by R. Smith (AIP, Melville, NY).
- Savin, D. W., L. D. Gardner, D. B. Reisenfeld, A. R. Young, and J. L. Kohl, 1995, *Phys. Rev. A* **51**, 2162.
- Savin, D. W., and J. M. Laming, 2002, *Astrophys. J.* **566**, 1166.
- Savin, D. W., *et al.*, 1997, *Astrophys. J. Lett.* **489**, L115.
- Savin, D. W., *et al.*, 1999, *Astrophys. J., Suppl. Ser.* **123**, 687.
- Savin, D. W., *et al.*, 2002a, *Astrophys. J.* **576**, 1098.
- Savin, D. W., *et al.*, 2002b, *Astrophys. J., Suppl. Ser.* **138**, 337.
- Savin, D. W., *et al.*, 2003, *Astrophys. J., Suppl. Ser.* **147**, 421.
- Savin, D. W., P. S. Krstic, Z. Haiman, and P. C. Stancil, 2004, *Astrophys. J. Lett.* **606**, L167.
- Schattenburg, M., and C. Canizares, 1986, *Astrophys. J.* **301**, 579.
- Schippers, S., 1999, *Phys. Scr.* **T80**, 158.
- Schippers, S., T. Bartsch, C. Brandau, G. Gwinner, J. Linkemann, A. Müller, A. A. Saghir, and A. Wolf, 1998, *J. Phys. B* **31**, 4873.
- Schippers, S., M. Schnell, C. Brandau, S. Kieslich, A. Müller, and A. Wolf, 2004, *Astron. Astrophys.* **421**, 1185.
- Schmidt, M., P. Beiersdorfer, H. Chen, D. B. Thorn, E. Träbert, and E. Behar, 2004, *Astrophys. J.* **604**, 562.
- Schultz, M., E. Justiniano, R. Schuch, P. H. Mokler, and S. Reusch, 1987, *Phys. Rev. Lett.* **58**, 1734.
- Seaton, M., 1987, *J. Phys. B* **20**, 6363.
- Seaton, M. J., 1958, *Rev. Mod. Phys.* **30**, 979.
- Seaton, M. J., 1959, *Mon. Not. R. Astron. Soc.* **119**, 81.
- Seaton, M. J., 1962, in *Atomic and Molecular Processes*, edited by D. R. Bates (Academic, New York), p. 375.
- Seaton, M. J., and P. J. Storey, 1976, in *Atomic Process and Applications*, edited by P. Burke and B. Moisewitch (North-Holland, New York).
- Seely, J. F., U. Feldman, and G. A. Doschek, 1987, *Astrophys. J.* **319**, 541.
- Seely, J. F., U. Feldman, and U. I. Safranova, 1986, *Astrophys. J.* **304**, 838.
- Shapiro, J., and G. Breit, 1959, *Phys. Rev.* **113**, 179.
- Shapiro, P. R., and R. T. Moore, 1976, *Astrophys. J.* **207**, 460.
- Shevelko, V. P., H. Tawara, F. Scheuermann, B. Fabian, A. Müller, and E. Salzborn, 2005, *J. Phys. B* **38**, 525.
- Shevelko, V. P., H. Tawara, I. Yu. Tolstikhina, F. Scheuermann, B. Fabian, A. Müller, and E. Salzborn, 2006, *J. Phys. B* **39**, 1499.
- Shevelko, V. P., A. M. Urnov, L. A. Vainshtein, and A. Müller, 1983, *Mon. Not. R. Astron. Soc.* **203**, 45P.
- Shirai, T., Y. Funatake, K. Mori, J. Sugar, W. L. Wiese, and Y. Nakai, 1990, *J. Phys. Chem. Ref. Data* **19**, 127.
- Shirai, T., *et al.*, 2000, *J. Phys. Chem. Ref. Data Monogr.* **8**, 1.
- Shklovsky, J. S., 1968, *Interscience Monographs and Texts in Physics and Astronomy* (Wiley, London).
- Shore, B. W., 1969, *Astrophys. J.* **158**, 1205.
- Shull, J. M., and M. van Steenberg, 1982a, *Astrophys. J., Suppl. Ser.* **48**, 95.
- Shull, J. M., and M. van Steenberg, 1982b, *Astrophys. J., Suppl. Ser.* **49**, 351.
- Silver, E. H., and S. M. Kahn, 1993, in *UV and X-ray Spectroscopy of Laboratory and Astrophysical Plasmas*, edited by Eric H. Silver and Steven M. Kahn, Proceedings from the 10th International Colloquium held at Berkeley, California (Cambridge University Press, Cambridge, UK).
- Smith, A. C. H., *et al.*, 2003, *Nucl. Instrum. Methods Phys. Res. B* **205**, 421.
- Smith, A. J., P. Beiersdorfer, V. Decaux, K. Widmann, K. J. Reed, and M. H. Chen, 1996, *Phys. Rev. A* **54**, 462.
- Smith, A. J., P. Beiersdorfer, K. J. Reed, A. L. Osterheld, V. Decaux, K. Widmann, and M. H. Chen, 2000, *Phys. Rev. A* **62**, 012704.
- Smith, A. J., M. Bitter, H. Hsuan, K. W. Hill, S. von Goeler, J. Timberlake, P. Beiersdorfer, and A. Osterheld, 1993, *Phys. Rev. A* **47**, 3073.
- Smith, B. W., J. B. Mann, R. D. Cowan, and J. C. Raymond, 1985, *Astrophys. J.* **298**, 898.
- Smith, R., 2005, in *X-ray Diagnostics of Astrophysical Plasmas: Theory, Experiment, and Observation*, edited by R. K. Smith, AIP Conf. Proc. No. 774 (AIP, Melville, NY).
- Smith, R. K., N. S. Brickhouse, D. A. Liedahl, and J. C. Raymond, 2001, *Astrophys. J. Lett.* **556**, L91.
- Smith, S. J., A. Chutjian, J. B. Greenwood, and S. S. Tayal, 2000, *Astrophys. J.* **541**, 501.
- Stancil, P. C., 2001, *ASP Conference Series No. 247: Spectroscopic Challenges of Photoionized Plasmas*, p. 3.
- Stancil, P. C., A. R. Turner, D. L. Cooper, D. R. Schultz, M. J. Rakovic, W. Fritsch, and B. Zygelman, 2001, *J. Phys. B* **34**, 2481.
- Stancil, P. C., B. Zygelman, N. J. Clarke, and D. L. Cooper, 1997, *Phys. Rev. A* **55**, 1064.
- Stancil, P. C., *et al.*, 1998a, *J. Phys. B* **31**, 3647.
- Stancil, P. C., *et al.*, 1998b, *Astrophys. J.* **502**, 1006.
- Steigman, G., 1975, *Astrophys. J.* **199**, 336.
- Steigman, G., M. W. Werner, and F. M. Geldon, 1971, *Astrophys. J.* **168**, 373.
- Stenke, M., K. Aichele, D. Hathiramani, G. Hofmann, M. Steidl, E. Salzborn, and R. Volpel, 1995, *Nucl. Instrum. Methods Phys. Res. B* **98**, 573.
- Stenke, M., D. Hathiramani, G. Hofmann, M. Steidl, E. Salzborn, R. Volpel, and V. P. Shevelko, 1995, *Nucl. Instrum. Methods Phys. Res. B* **98**, 138.
- Stenke, M., *et al.*, 1999, *J. Phys. B* **32**, 3627.
- Stephan, K., *et al.*, 1980, *J. Chem. Phys.* **73**, 3763.
- Stolterfoht, N., 1987, *Phys. Rep.* **146**, 315.
- Storey, P. J., 1981, *Mon. Not. R. Astron. Soc.* **195**, 27P.
- Storey, P. J., H. E. Mason, and H. E. Saraph, 1996, *Astron. Astrophys.* **309**, 677.
- Storey, P. J., and C. J. Zeippen, 2000, *Mon. Not. R. Astron. Soc.* **312**, 813.
- Stratton, B. C., H. W. Moos, and M. Finkenthal, 1984, *Astrophys. J., Lett. Ed.* **279**, L31.
- Sugar, J., and C. Corliss, 1979, *J. Phys. Chem. Ref. Data* **8**, 865.
- Sugar, J., and C. Corliss, 1985, *Atomic Energy Levels of the Iron-period Elements: Potassium through Nickel* (American Chemical Society, Washington).

- Summers, H. P., 1972, Mon. Not. R. Astron. Soc. **158**, 255.
- Summers, H. P., 1974, Mon. Not. R. Astron. Soc. **169**, 663.
- Summers, H. P., *et al.*, 2006, Plasma Phys. Controlled Fusion **48**, 263.
- Suraud, *et al.*, 1991, J. Phys. B **24**, 2543.
- Sutherland, R. S., and M. A. Dopita, 1993, Astrophys. J., Suppl. Ser. **88**, 253.
- Sylwester, J., J. R. Lemen, R. D. Bentley, A. Fludra, and M.-C. Zolcinski, 1998, Astrophys. J., Suppl. Ser. **501**, 397.
- Tanaka, K., 1986, Publ. Astron. Soc. Jpn. **38**, 225.
- Tanis, J. A., *et al.*, 1981, Phys. Rev. Lett. **47**, 828.
- Tarter, C. B., 1971, Astrophys. J. **168**, 313.
- Tarter, C. B., and E. E. Salpeter, 1969, Astrophys. J. **156**, 953.
- Tarter, C. B., W. H. Tucker, and E. E. Salpeter, 1969, Astrophys. J. **156**, 943.
- Tawara, H., K. Okuno, C. W. Fehrenbach, C. Verzani, M. P. Stockli, B. D. Depaola, P. Richard, and P. C. Stancil, 2001, Phys. Rev. A **63**, 062701.
- Tayal, S. S., 1999, J. Phys. B **32**, 5311.
- Teng, H., 2000, J. Phys. B **33**, L553.
- Teng, H., H. Knopp, S. Ricz, S. Schippers, K. A. Berrington, and A. Müller, 2000, Phys. Rev. A **61**, 060704.
- Terao, M., and P. G. Burke, 1990, J. Phys. B **23**, 1815.
- Thompson, J. S., and D. C. Gregory, 1994, Phys. Rev. A **50**, 1377.
- Tisone, G. C., and L. M. Branscomb, 1968, Phys. Rev. **170**, 169.
- Tondello, G., and R. W. P. McWhirter, 1971, J. Phys. B **4**, 715.
- Träbert, E., 2002, Can. J. Phys. **80**, 1481.
- Trefftz, E., 1963, Proc. R. Soc. London, Ser. A **271**, 379.
- Tucker, W. H., and M. Koren, 1971, Astrophys. J. **168**, 283.
- Vainshtein, L., and U. Safranova, 1978, At. Data Nucl. Data Tables **21**, 49.
- van Regemorter, H., 1962, Astrophys. J. **136**, 906.
- Verner, D. A., P. D. Barthel, and D. Tytler, 1994, Astron. Astrophys., Suppl. Ser. **108**, 287.
- Verner, D. A., and G. J. Ferland, 1996, Astrophys. J., Suppl. Ser. **103**, 467.
- Verner, D. A., E. M. Verner, and G. J. Ferland, 1996, At. Data Nucl. Data Tables **64**, 1.
- Verner, D. A., and D. G. Yakovlev, 1995, Astron. Astrophys., Suppl. Ser. **109**, 125.
- Volonte, S., J. Lion, P. Faucher, and J. Dubau, 1987, Astron. Astrophys. **182**, 167.
- Voronov, G. S., 1997, At. Data Nucl. Data Tables **65**, 1.
- Walker, A. B. C., and H. R. Rugge, 1970, Astron. Astrophys. **5**, 4.
- Walker, D. W., 1974, J. Phys. B **7**, 97.
- Wang, J. G., P. C. Stancil, A. R. Turner, and D. L. Cooper, 2003, Phys. Rev. A **67**, 012710.
- Wang, J.-S., H. R. Griem, R. Hess, and W. L. Rowan, 1988, Phys. Rev. A **38**, 4761.
- Wang, L. J., K. Rinn, and D. C. Gregory, 1988, J. Phys. B **21**, 2117.
- Wargelin, B. J., S. M. Kahn, and P. Beiersdorfer, 2001, Phys. Rev. A **63**, 022710.
- Watson, W. D., and R. B. Christensen, 1979, Astrophys. J. **231**, 627.
- Wetzel, R. C., *et al.*, 1987, Phys. Rev. A **35**, 559.
- Whiteford, A. D., N. R. Badnell, C. P. Ballance, S. D. Loch, M. G. O'Mullane, and H. P. Summers, 2002, J. Phys. B **35**, 3729.
- Whiteford, A. D., N. R. Badnell, C. P. Ballance, M. G. O'Mullane, H. P. Summers, and A. L. Thomas, 2001, J. Phys. B **34**, 3179.
- Widing, K. G., J. G. Doyle, P. L. Dufton, and E. A. Kingston, 1982, Astrophys. J. **257**, 913.
- Widing, K. G., and G. D. Sandlin, 1968, Astrophys. J. **152**, 545.
- Wiese, W. L., J. Fuhr, and J. Deters, 1996, J. Phys. Chem. Ref. Data Monogr. **7**, 335.
- Wiese, W. L., M. W. Smith, and B. M. Glennon, 1966, Natl. Stand. Ref. Data Ser. (U.S., Natl. Bur. Stand.) NSRDS-NBS **4**, Vol. I.
- Wilson, S. M., T. K. McLaughlin, R. W. McCullough, and H. B. Gilbody, 1990a, J. Phys. B **23**, 1315.
- Wilson, S. M., T. K. McLaughlin, R. W. McCullough, and H. B. Gilbody, 1990b, J. Phys. B **23**, 2969.
- Woitke, O., N. Djuric, G. H. Dunn, M. E. Bannister, A. C. H. Smith, B. Wallbank, N. R. Badnell, and M. S. Pindzola, 1998, Phys. Rev. A **58**, 4512.
- Wojdowski, P. S., D. A. Liedahl, and M. Sako, 2001, Astrophys. J. **547**, 973.
- Wong, K. L., *et al.*, 1993, Phys. Rev. A **48**, 2850.
- Woodruff, P. R., M.-C. Hublet, and M. F. A. Harrison, 1978, J. Phys. B **11**, L305.
- Woods, D. T., J. M. Shull, and C. L. Sarazin, 1981, Astrophys. J. **249**, 399.
- Young, P. R., G. Del Zanna, E. Landi, K. P. Dere, H. E. Mason, and M. Landini, 2003, Astrophys. J., Suppl. Ser. **144**, 135.
- Younger, S., 1983, J. Quant. Spectrosc. Radiat. Transf. **29**, 67.
- Younger, S. M., 1980a, Phys. Rev. A **22**, 111.
- Younger, S. M., 1980b, Phys. Rev. A **22**, 1425.
- Younger, S. M., 1981a, Phys. Rev. A **23**, 1138.
- Younger, S. M., 1981b, Phys. Rev. A **24**, 1272.
- Younger, S. M., 1982a, Phys. Rev. A **25**, 3396.
- Younger, S. M., 1982b, Phys. Rev. A **26**, 3177.
- Zatsarinny, O., T. W. Gorczyca, J. Fu, K. T. Korista, N. R. Badnell, and D. W. Savin, 2006, Astron. Astrophys. **447**, 379.
- Zatsarinny, O., T. W. Gorczyca, K. T. Korista, N. R. Badnell, and D. W. Savin, 2003, Astron. Astrophys. **412**, 587.
- Zatsarinny, O., T. W. Gorczyca, K. T. Korista, N. R. Badnell, and D. W. Savin, 2004a, Astron. Astrophys. **426**, 699.
- Zatsarinny, O., T. W. Gorczyca, K. T. Korista, N. R. Badnell, and D. W. Savin, 2004b, Astron. Astrophys. **417**, 1173.
- Zatsarinny, O., T. W. Gorczyca, K. T. Korista, J. Fu, N. R. Badnell, W. Mitthumsiri, and D. W. Savin, 2005a, Astron. Astrophys. **440**, 1203.
- Zatsarinny, O., T. W. Gorczyca, K. T. Korista, J. Fu, N. R. Badnell, W. Mitthumsiri, and D. W. Savin, 2005b, Astron. Astrophys. **438**, 743.
- Zeijlmans van Emmichoven, P. A., M. E. Bannister, D. C. Gregory, C. C. Havener, R. A. Phaneuf, E. W. Bell, X. Q. Guo, J. S. Thompson, and M. Satake, 1993, Phys. Rev. A **47**, 2888.
- Zhang, H., 1996, Astron. Astrophys., Suppl. Ser. **119**, 523.
- Zhang, H., and D. Sampson, 1987, Astrophys. J., Suppl. Ser. **63**, 487.
- Zhang, H., and D. Sampson, 1989, At. Data Nucl. Data Tables **43**, 1.
- Zhang, H., *et al.*, 1989, At. Data Nucl. Data Tables **41**, 1.
- Zhang, H. L., M. Graziani, and A. K. Pradhan, 1994, Astron. Astrophys. **283**, 319.
- Zhang, H. L., and D. H. Sampson, 1992, At. Data Nucl. Data Tables **52**, 143.
- Zhang, H. L., and D. H. Sampson, 1994a, At. Data Nucl. Data Tables **56**, 41.
- Zhang, H. L., and D. H. Sampson, 1994b, At. Data Nucl. Data Tables **58**, 255.

- Zhang, H. L., and D. H. Sampson, 1996, At. Data Nucl. Data Tables **63**, 275.
- Zhang, H. L., D. H. Sampson, and C. J. Fontes, 1990, At. Data Nucl. Data Tables **44**, 31.
- Zhang, Y., C. B. Reddy, R. S. Smith, D. E. Golden, D. W. Mueller, and D. C. Gregory, 1991, Phys. Rev. A **44**, 4368.
- Ziegler, D. L., J. H. Newman, L. N. Goeller, K. A. Smith, and R. F. Stebbings, 1982, Planet. Space Sci. **30**, 1269.
- Zirin, H., 1988, *Astrophysics of the Sun* (Cambridge University Press, Cambridge), p. 440.
- Zong, W., R. Schuch, E. Lindroth, H. Gao, D. R. Dewitt, S. Asp, and H. Danared, 1997, Phys. Rev. A **56**, 386.
- Zygelman, B., P. C. Stancil, N. J. Clarke, and D. L. Cooper, 1997, Phys. Rev. A **56**, 457.